

## 2 鋼管継手の疲労試験

### 2.1 概 要

鋼管構造の疲労設計或は、研究を行う場合、疲労試験の成果を利用する必要が生ずることが多い。

本章は、この必要を満足させるため国内・外の鋼管継手の疲労試験の成果をなるべく多く紹介することを目的とする。

鋼管継手の疲労に関する研究は、日本以外では主にアメリカとヨーロッパにおいて行われており、本章においても3つに章を分けそれぞれの成果を紹介してある。

その内、アメリカの成果は、試験の種類と量が豊富であるばかりでなく技術的にも先覚的な役割を果たしている。

また、海洋鋼構造物の設計には API RP2A , AWS 等のアメリカの基準が多く用いられている。

従って、アメリカの成果については、試験結果の紹介の他 AWS , API RP2A および ASME の基準と試験結果との関係についても補足した。

試験結果を参照する際、荷重の繰り返し数 $N$ の定義に注意する必要がある。特にクラックの発生の定義 ( $N_c$  or  $N_i$ ) に関しては、日本、ヨーロッパおよびアメリカと違っており、アメリカにおいては、研究機関相互にも差がある。

疲労試験結果の蓄積については、WRC (Welding Research Council) においてその制度を確立しスタートしている。

この制度は、鋼管継手に限らず疲労の研究に有益であり、今後この制度の利用および協力について考えていく必要がある。

## 2.2 日 本

日本における鋼管継手の疲労強度に関する系統的な研究は、日本船用機器開発協会 FPC委員会（委員長 飯田國廣）において行われている。

この研究で12の疲労試験結果を示し、FEM 解析との比較を行っている。

その後、飯田他は国内で行われた他の疲労試験の成果を整理し直し合計139 の疲労試験データを表にしている。

ここでは、その成果を紹介する。

### (1) FPC 委員会での疲労試験 (IIW 1981, Doc.X111-1020-81, Doc. XV-497-81)

表 2.1に供試体の諸元と載荷方法を示す。

継手形式は T,TV の 2種類である。

供試体の材質は、JIS SM41Aで表 2.2に供試体の化学成分と機械的性質を示す。

疲労試験結果を表 2.3に示す。

クラックの発生寿命  $N_c$  の定義は表 2.3の注記に示すが実際に測定したクラックの長さを同表に示してある。

図 2.1に試験結果を横軸に  $N_c$  , 縦軸に最大歪振幅  $E_a$  をとり AWS-Xカーブと比較している。

この図からグラインダー仕上げした供試体は、as weldの供試体の2.6 倍の疲労強度があり、この溶接ビードの仕上げ状態を考慮しないで最大歪振幅だけで実構造の継手の疲労強度を AWS-Xカーブと対比し決定するのは妥当な方法とはいえないと述べている。

表 2. 1

Table 1; Dimensions of fatigue test specimens and loading mechanisms

Test Spec.	Dimensions (mm)								Weld toe is
	$D$	$d$	$T$	$t$	$L$	$g$	$\theta_1$ (deg)	$\theta_2$ (deg)	
TAW	609.6	323.8	20.5	12.7	4859.7	—	90.0	—	as-welded
TAG	do.	do.	do.	do.	do.	—	do.	—	grinder finished
TBW	do.	508.0	do.	20.5	do.	—	do.	—	as-welded
TBG	do.	do.	do.	do.	do.	—	do.	—	grinder finished
TY2	do.	406.4	19.0	16.0	4940.0	17.5	do.	45.0	as-welded
TY3	do.	do.	do.	do.	do.	119.1	do.	do.	do.

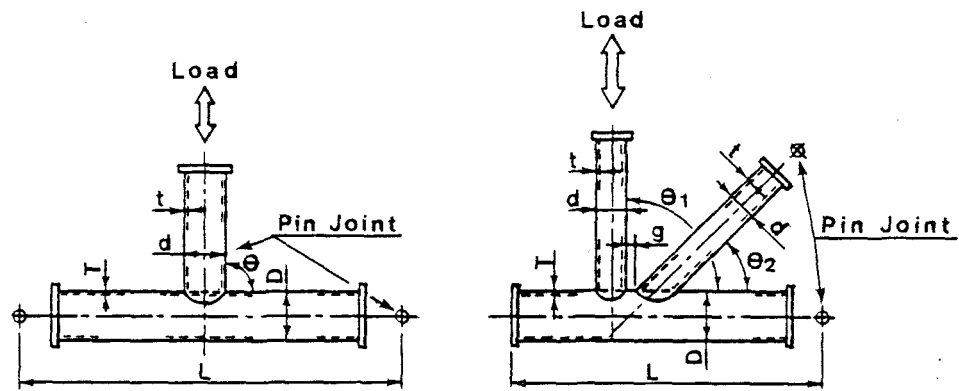


表 2. 2

Table 2; Chemical composition and mechanical properties of parent materials of fatigue specimens (from mill sheet)

Specimen	Chemical Composition (%)					Mechanical Properties		
	C	Si	Mn	P	S	Yield Stress (MN/m <sup>2</sup> )	Tensile Stress (MN/m <sup>2</sup> )	Elong. (%)
TA Chord	0.16	0.14	0.68	0.069	0.014	274.0	441.0	31.0
Brace	do.	0.15	0.69	0.016	0.050	255.0	do.	30.0
TB Chord	do.	0.14	0.68	0.069	0.014	274.0	do.	31.0
Brace	0.13	0.23	0.97	0.017	0.080	304.0	470.0	26.0
TY Chord	0.15	0.20	0.96	0.022	0.016	323.0	do.	32.0
Brace	0.14	0.18	0.62	0.026	0.013	314.0	441.0	31.0

表 2.3  
Table 3: Results of fatigue experiments

Test Spec.	Applied Load Amp. (kN)	Nominal Stress Amp. on Brace (MN/m <sup>2</sup> )	Crack Initiation Life, $N_c$	Failure Life, $N_f$	Measured Strain Amp. ( $\times 10^6$ )	Ditected Crack Length (mm)
TAW1	392.0	31.6	$3.80 \times 10^2$	$1.55 \times 10^4$	1610	2.0
TAW2	147.0	11.8	$2.55 \times 10^4$	$2.55 \times 10^5$	603	13.5
TAG1	490.0	39.5	$1.77 \times 10^3$	$1.20 \times 10^4$	3100	0.5
TAG2	343.0	27.6	$2.10 \times 10^4$	$1.50 \times 10^5$	1200	2.0
TBW1	588.0	18.7	$5.75 \times 10^3$	$4.20 \times 10^4$	1080	5.0
TBW2	784.0	25.0	$7.20 \times 10^2$	$1.50 \times 10^4$	1250	5.0
TBG1	931.0	29.7	$4.30 \times 10^3$	$1.90 \times 10^4$	1950	2.5
TBG2	588.0	18.7	$5.90 \times 10^4$	$2.74 \times 10^5$	960	—
TY21	do.	30.0	$2.81 \times 10^3$	$4.80 \times 10^4$	870	3.0
TY22	980.0	50.0	$2.30 \times 10^2$	$6.00 \times 10^3$	1900	7.0
TY31	588.0	30.0	$9.60 \times 10^2$	$1.70 \times 10^4$	1700	80.0
TY32	784.0	40.0	$2.03 \times 10^2$	$3.93 \times 10^3$	4260	7.0

$N_c$  : Visible crack initiation life; number of cycles to initiation of a surface crack of 5 to 20 mm long. This definition is available for the experiments by the authors.

$N_f$  : Fatigue failure life; number of cycles to 20% drop of the maximum load

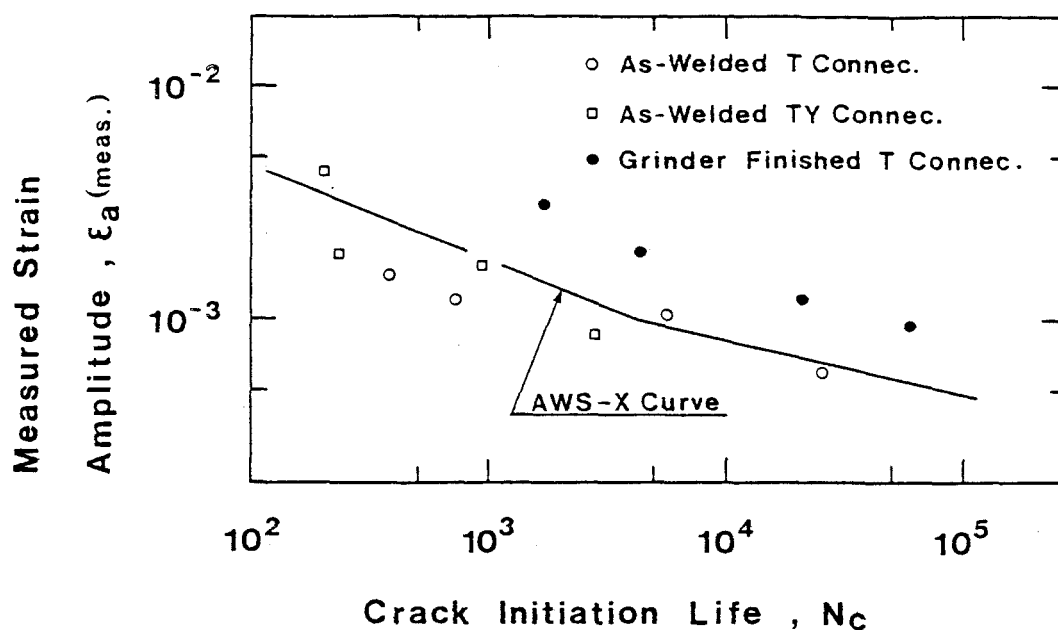


Figure 1; Measured maximum strain amplitude versus crack initiation life for tubular connections

図 2. 1

## (2) 国内の疲労試験の再整理

次頁以下に飯田他が行った国内の疲労試験の再整理の結果を示す。

同表のRef. No.は、下記の文献である。

6. Sawada, Y., Idogaki, S. and Sekita, K., "Static and fatigue tests on T-joints stiffened by an internal ring", OTC 3422, 1979.
7. Yamasaki, T., Takizawa, S. and Komatsu, M., "Static and fatigue tests on large-size tubular T-joints", OTC 3424, 1979.
8. Japan Ship Machinery Development Association, "Cyclic strain analysis and fatigue strength of tubular connections in offshore structures", Report of FPC Committee, 1976 - 1978.
25. Iida, K., Asano, K., Toyofuku, M. and Ishikawa, K., "A fatigue design procedure for offshore tubular connections", Second Intern. Sym. on Integrity of Offshore Structures, Glasgow, 1981.
28. Iwasaki, T., Katoh, A., Asano, K., Kawahara, M., "An analysis on applicability of fatigue data to design of offshore tubular joints", Journal of the Society of Naval Architects of Japan, Vol. 147, 1980 (in Japanese).

試験方法の詳細は、上記文献を参照して頂くものとし、ここでは割愛する。

表 2. 4

APPENDIX 1 TABLE OF RESULTS OF FATIGUE TESTS RE-ANALYZED

Type of Connc.	Spec. name	Weld toe is	Load ampli. (kW)	Dimensions (mm)				g (mm)	$\theta$ (deg.)	Experimental results			Ref. No.
				Dia.	Chord Thick.	Length	Brace Dia.			Thick.	Crack Initiation Life (Nc)	Failure Life (Nf)	
T	TAW1	A.W.	392.0	609.6	20.5	4856.0	323.8	12.7	90.0	$0.380 \times 10^3$	$0.155 \times 10^5$	$0.761 \times 10^{-2}$	25
T	TAW2	A.W.	147.0	609.6	20.5	4856.0	323.8	12.7	90.0	$0.255 \times 10^5$	$0.255 \times 10^6$	$0.630 \times 10^{-3}$	25
T	TBW1	A.W.	588.0	609.6	20.5	4856.0	508.0	20.5	90.0	$0.575 \times 10^4$	$0.420 \times 10^5$	$0.108 \times 10^{-2}$	25
T	TBW2	A.W.	784.0	609.6	20.5	4856.0	508.0	20.5	90.0	$0.720 \times 10^3$	$0.150 \times 10^5$	$0.125 \times 10^{-2}$	25
T	A1	A.W.	34.3	165.2	7.1	1000.0	165.2	7.1	90.0		$0.300 \times 10^7$	$0.460 \times 10^{-3}$	28
T	A2	A.W.	68.6	165.2	7.1	1000.0	165.2	7.1	90.0	$0.121 \times 10^6$	$0.275 \times 10^6$	$0.820 \times 10^{-3}$	28
T	A3	A.W.	93.1	165.2	7.1	1000.0	165.2	7.1	90.0	$0.170 \times 10^5$	$0.440 \times 10^5$	$0.131 \times 10^{-2}$	28
T	A4	A.W.	49.0	165.2	7.1	1000.0	165.2	7.1	90.0	$0.215 \times 10^6$	$0.282 \times 10^7$	$0.523 \times 10^{-3}$	28
T	B1	A.W.	44.1	165.2	5.5	1000.0	165.2	5.5	90.0	$0.620 \times 10^6$	$0.985 \times 10^6$	$0.670 \times 10^{-3}$	28
T	B2	A.W.	73.5	165.2	5.5	1000.0	165.2	5.5	90.0	$0.275 \times 10^5$	$0.507 \times 10^5$	$0.100 \times 10^{-2}$	28
T	B3	A.W.	34.3	165.2	5.5	1000.0	165.2	5.5	90.0	$0.372 \times 10^6$	$0.140 \times 10^7$	$0.556 \times 10^{-3}$	28
T	B4	A.W.	24.5	165.2	5.5	1000.0	165.2	5.5	90.0	$0.106 \times 10^7$	$0.393 \times 10^7$	$0.289 \times 10^{-3}$	28
T	C1	A.W.	24.5	165.2	5.5	1000.0	89.1	5.5	90.0	$0.390 \times 10^4$	$0.410 \times 10^5$	$0.964 \times 10^{-3}$	28
T	C2	A.W.	14.7	165.2	5.5	1000.0	89.1	5.5	90.0	$0.600 \times 10^4$	$0.300 \times 10^6$	$0.645 \times 10^{-3}$	28
T	C3	A.W.	19.6	165.2	5.5	1000.0	89.1	5.5	90.0	$0.150 \times 10^4$	$0.928 \times 10^5$	$0.813 \times 10^{-3}$	28
T	C4	A.W.	9.8	165.2	5.5	1000.0	89.1	5.5	90.0	$0.164 \times 10^6$	$0.938 \times 10^6$	$0.441 \times 10^{-3}$	28
T	D1	A.W.	24.5	165.2	5.5	1000.0	89.1	3.5	90.0	$0.310 \times 10^5$	$0.399 \times 10^5$	$0.129 \times 10^{-2}$	28
T	D2	A.W.	14.7	165.2	5.5	1000.0	89.1	3.5	90.0	$0.254 \times 10^6$	$0.941 \times 10^6$	$0.543 \times 10^{-3}$	28
T	D3	A.W.	19.6	165.2	5.5	1000.0	89.1	3.5	90.0	$0.147 \times 10^5$	$0.139 \times 10^6$	$0.632 \times 10^{-3}$	28
T	D4	A.W.	9.8	165.2	5.5	1000.0	89.1	3.5	90.0	$0.292 \times 10^6$	$0.138 \times 10^7$	$0.468 \times 10^{-3}$	28
T	E1	A.W.	24.5	165.2	5.5	1000.0	139.8	5.5	90.0	$0.179 \times 10^6$	$0.117 \times 10^7$	$0.587 \times 10^{-3}$	28
T	E2	A.W.	14.7	165.2	5.5	1000.0	139.8	5.5	90.0	$0.348 \times 10^7$	$0.880 \times 10^7$	$0.273 \times 10^{-3}$	28
T	E3	A.W.	44.1	165.2	5.5	1000.0	139.8	5.5	90.0	$0.200 \times 10^4$	$0.843 \times 10^5$	$0.881 \times 10^{-3}$	28
T	E4	A.W.	19.6	165.2	5.5	1000.0	139.8	5.5	90.0	$0.813 \times 10^6$		$0.318 \times 10^{-3}$	28

表 2.4 ( 続き )

Type of Connec.	Spec. name	Weld toe is	Load ampli. (kN)	Dimensions (mm)				g (mm)	$\theta$ (deg.)	Experimental results			Ref. No.
				Chord Thick.	Length	Brace Dia.	Thick.			Crack Initiation life (Nc)	Failure Life (Nf)	Strain amplitude	
T	NS1	A.W.	55.9	500.0	3000.0	200.0	6.4	6.4	90.0	$0.240 \times 10^5$	$0.160 \times 10^6$	$0.108 \times 10^{-2}$	8
T	NS2	A.W.	78.4	500.0	3000.0	200.0	6.4	6.4	90.0	$0.240 \times 10^4$	$0.750 \times 10^4$	$0.160 \times 10^{-2}$	8
T	NS3	A.W.	98.0	500.0	3000.0	200.0	6.4	6.4	90.0	$0.730 \times 10^3$	$0.220 \times 10^4$	$0.170 \times 10^{-2}$	8
T	T101	A.W.	182.3	500.0	2500.0	100.0	4.5	4.5	90.0	$0.150 \times 10^4$	$0.144 \times 10^5$	$0.102 \times 10^{-2}$	8
T	T102	A.W.	295.0	500.0	2500.0	100.0	4.5	4.5	90.0	$0.430 \times 10^3$	$0.400 \times 10^4$	$0.115 \times 10^{-2}$	8
T	T103	A.W.	279.3	500.0	2500.0	100.0	4.5	4.5	90.0	$0.290 \times 10^3$	$0.900 \times 10^3$	$0.198 \times 10^{-2}$	8
T	T201	A.W.	431.2	500.0	3000.0	200.0	6.4	6.4	90.0	$0.200 \times 10^3$	$0.800 \times 10^3$	$0.173 \times 10^{-2}$	8
T	T202	A.W.	186.2	500.0	3000.0	200.0	6.4	6.4	90.0	$0.700 \times 10^4$	$0.250 \times 10^5$	$0.925 \times 10^{-3}$	8
T	T203	A.W.	248.9	500.0	3000.0	200.0	6.4	6.4	90.0	$0.400 \times 10^3$	$0.100 \times 10^5$	$0.118 \times 10^{-2}$	8
T	T204	A.W.	156.8	500.0	3000.0	200.0	6.4	6.4	90.0	$0.160 \times 10^5$	$0.400 \times 10^6$	$0.625 \times 10^{-3}$	8
T	T251	A.W.	392.0	500.0	3000.0	250.0	6.4	6.4	90.0	$0.390 \times 10^3$	$0.700 \times 10^4$	$0.129 \times 10^{-2}$	8
T	T252	A.W.	303.8	500.0	3000.0	250.0	6.4	6.4	90.0	$0.130 \times 10^4$	$0.100 \times 10^5$	$0.110 \times 10^{-2}$	8
T	T253	A.W.	245.0	500.0	3000.0	250.0	6.4	6.4	90.0	$0.250 \times 10^4$	$0.250 \times 10^5$	$0.105 \times 10^{-2}$	8
T	T254	A.W.	156.8	500.0	3000.0	250.0	6.4	6.4	90.0	$0.290 \times 10^5$	$0.200 \times 10^6$	$0.650 \times 10^{-3}$	8
T	T351	A.W.	588.0	500.0	2500.0	350.0	6.4	6.4	90.0	$0.840 \times 10^3$	$0.900 \times 10^4$	$0.156 \times 10^{-2}$	8
T	T352	A.W.	774.0	500.0	2500.0	350.0	6.4	6.4	90.0	$0.130 \times 10^3$	$0.520 \times 10^4$	$0.243 \times 10^{-2}$	8
T	T353	A.W.	455.7	500.0	2550.0	350.0	6.4	6.4	90.0	$0.245 \times 10^4$	$0.130 \times 10^5$	$0.124 \times 10^{-2}$	8
T	T502	A.W.	1185.81	500.0	2500.0	500.0	6.4	6.4	90.0	$0.260 \times 10^4$	$0.400 \times 10^5$	$0.825 \times 10^{-3}$	8
K	K1	A.W.	1470.01	812.8	8594.0	812.8	11.1	-272.0	37.0	$0.320 \times 10^4$	$0.230 \times 10^5$	$0.145 \times 10^{-2}$	8
K	K2	A.W.	1470.01	812.8	8594.0	812.8	11.1	-272.0	37.0	$0.320 \times 10^4$	$0.560 \times 10^5$	$0.103 \times 10^{-2}$	8
K	K3	A.W.	1470.01	812.8	8594.0	812.8	11.1	-272.0	37.0	$0.210 \times 10^4$	$0.240 \times 10^6$	$0.111 \times 10^{-2}$	8
K	8K2	A.W.	343.0	179.0	1400.0	76.2	7.0	70.2	45.0	$0.500 \times 10^2$	$0.560 \times 10^3$	$0.365 \times 10^{-2}$	8
K	8K3	A.W.	294.0	179.0	1400.0	76.2	7.0	70.2	45.0	$0.180 \times 10^3$	$0.200 \times 10^4$	$0.245 \times 10^{-2}$	8
K	8K4	A.W.	225.4	179.0	1400.0	76.2	7.0	70.2	45.0	$0.290 \times 10^3$	$0.450 \times 10^4$	$0.220 \times 10^{-2}$	8

表 2.4 ( 続き )

Type of Connec.	Spec. name	Weld toe is	Load (kN)	Dimensions (mm)				Experimental results				Ref. No.	
				Chord Thick.	Length	Brace Dia.	Thick.	9 (mm)	$\theta$ (deg.)	Crack initiation Life (Nc)	Failure Life (NF)		Strain amplitude
K	8K5	A.W.	142.1	179.0	1400.0	76.2	7.0	70.2	45.0	$0.582 \times 10^4$	$0.115 \times 10^5$	$0.120 \times 10^{-2}$	8
K	8K6	A.W.	93.1	179.0	1400.0	76.2	7.0	70.2	45.0	$0.104 \times 10^5$	$0.300 \times 10^5$	$0.100 \times 10^{-2}$	8
K	8K7	A.W.	58.8	179.0	1400.0	76.2	7.0	70.2	45.0	$0.105 \times 10^6$		$0.590 \times 10^{-3}$	8
K	8K8	A.W.	19.6	179.0	1400.0	76.2	7.0	70.2	45.0	$0.107 \times 10^7$		$0.330 \times 10^{-3}$	8
K	8K9	A.W.	73.5	179.0	1400.0	76.2	7.0	70.2	45.0	$0.145 \times 10^5$		$0.540 \times 10^{-3}$	8
K	8K10	A.W.	465.5	179.0	1400.0	76.2	13.0	70.2	45.0	$0.100 \times 10^2$	$0.770 \times 10^2$	$0.538 \times 10^{-2}$	8
K	8K11	A.W.	215.6	179.0	1400.0	76.2	13.0	70.2	45.0	$0.280 \times 10^3$	$0.100 \times 10^4$	$0.245 \times 10^{-2}$	8
K	IHA1	A.W.	58.8	165.2	1200.0	76.3	4.0	57.3	45.0	$0.370 \times 10^3$		$0.249 \times 10^{-2}$	8
K	IHA2	A.W.	39.2	165.2	1200.0	76.3	4.0	57.3	45.0	$0.790 \times 10^3$		$0.200 \times 10^{-2}$	8
K	IHA4	A.W.	98.0	165.2	1200.0	76.3	4.0	57.3	45.0	$0.210 \times 10^2$		$0.730 \times 10^{-2}$	8
K	IHA5	A.W.	78.4	165.2	1200.0	76.3	4.0	57.3	45.0	$0.150 \times 10^3$		$0.258 \times 10^{-2}$	8
K	IHA6	A.W.	19.6	165.2	1200.0	76.3	4.0	57.3	45.0	$0.601 \times 10^6$		$0.525 \times 10^{-3}$	8
K	IHB1	A.W.	176.4	165.2	1200.0	76.3	4.0	-25.3	45.0	$0.110 \times 10^3$		$0.300 \times 10^{-2}$	8
K	IHB4	A.W.	34.3	165.2	1200.0	76.3	4.0	-25.3	45.0	$0.102 \times 10^7$		$0.250 \times 10^{-3}$	8
K	IHB5	A.W.	58.8	165.2	1200.0	76.3	4.0	-25.3	45.0	$0.370 \times 10^5$		$0.500 \times 10^{-3}$	8
K	IHB6	A.W.	98.0	165.2	1200.0	76.3	4.0	-25.3	45.0	$0.300 \times 10^4$		$0.120 \times 10^{-2}$	8
K	IHC1	A.W.	98.0	165.2	1200.0	76.3	4.0	2.1	45.0	$0.488 \times 10^3$		$0.350 \times 10^{-2}$	8
K	IHC2	A.W.	68.6	165.2	1200.0	76.3	4.0	2.1	45.0	$0.126 \times 10^4$		$0.138 \times 10^{-2}$	8
K	IHC3	A.W.	39.2	165.2	1200.0	76.3	4.0	2.1	45.0	$0.680 \times 10^5$		$0.670 \times 10^{-3}$	8
K	IHC5	A.W.	156.8	165.2	1200.0	76.3	4.0	2.1	45.0	$0.230 \times 10^2$		$0.373 \times 10^{-2}$	8
K	IHC6	A.W.	49.0	165.2	1200.0	76.3	4.0	2.1	45.0	$0.172 \times 10^5$		$0.800 \times 10^{-3}$	8
TY	TY11	A.W.	588.0	609.6	4940.0	406.4	16.0	-168.0	90.0	$0.215 \times 10^6$	$0.120 \times 10^7$	$0.365 \times 10^{-3}$	8
TY	TY12	A.W.	1176.0	609.6	4940.0	406.4	16.0	-168.0	90.0	$0.255 \times 10^5$	$0.150 \times 10^6$	$0.810 \times 10^{-3}$	8
TY	TY21	A.W.	588.0	609.6	4940.0	406.4	16.0	17.7	90.0	$0.281 \times 10^4$	$0.480 \times 10^6$	$0.870 \times 10^{-3}$	8



表 2.4 ( 続き )

Type of Conneec.	Spec. name	Weld toe is	Load ampli. (kN)	Dimensions (mm)				Experimental results					
				Chord Thick.	Length	Brace Dia.	Thick.	g (mm)	$\theta$ (deg.)	Crack initiation life (Nc)	Failure Life (Nf)	Strain amplitude	Ref. No.
TY	TY22	A.W.	980.0	609.6	4940.0	406.4	16.0	17.7	90.0	$0.231 \times 10^3$	$0.600 \times 10^4$	$0.190 \times 10^{-2}$	8
TY	TY31	A.W.	588.0	609.6	4940.0	406.4	16.0	118.9	90.0	$0.960 \times 10^3$	$0.170 \times 10^5$	$0.170 \times 10^{-2}$	8
TY	TY32	A.W.	784.0	609.6	4940.0	406.4	16.0	118.9	90.0	$0.203 \times 10^3$	$0.393 \times 10^4$	$0.426 \times 10^{-2}$	8
TY	IA2	A.W.	39.2	165.2	1100.0	76.3	4.2	57.3	90.0	$0.622 \times 10^3$		$0.120 \times 10^{-2}$	8
TY	IA3	A.W.	9.8	165.2	1100.0	76.3	4.2	57.3	90.0	$0.959 \times 10^6$		$0.425 \times 10^{-3}$	8
TY	IA4	A.W.	70.5	165.2	1100.0	76.3	4.2	57.3	90.0	$0.200 \times 10^2$		$0.410 \times 10^{-2}$	8
TY	IA5	A.W.	19.6	165.2	1100.0	76.3	4.2	57.3	90.0	$0.400 \times 10^5$		$0.500 \times 10^{-3}$	8
TY	IB2	A.W.	58.8	165.2	1100.0	76.3	4.2	-25.3	90.0	$0.269 \times 10^5$		$0.100 \times 10^{-2}$	8
TY	IB3	A.W.	107.8	165.2	1100.0	76.3	4.2	-25.3	90.0	$0.120 \times 10^4$		$0.160 \times 10^{-2}$	8
TY	IB4	A.W.	34.3	165.2	1100.0	76.3	4.2	-25.3	90.0	$0.145 \times 10^7$		$0.920 \times 10^{-3}$	8
TY	IB5	A.W.	196.0	165.2	1100.0	76.3	4.2	-25.3	90.0	$0.340 \times 10^2$		$0.105 \times 10^{-1}$	8
TY	2C2	A.W.	39.2	165.2	1100.0	101.6	4.2	42.5	90.0	$0.965 \times 10^4$		$0.800 \times 10^{-3}$	8
TY	2C4	A.W.	137.2	165.2	1100.0	101.6	4.2	42.5	90.0	$0.150 \times 10^2$		$0.910 \times 10^{-2}$	8
TY	2C5	A.W.	68.6	165.2	1100.0	101.6	4.2	42.5	90.0	$0.440 \times 10^3$		$0.330 \times 10^{-2}$	8
TY	2D2	A.W.	225.4	165.2	1100.0	101.6	4.2	-40.0	90.0	$0.700 \times 10^2$		$0.835 \times 10^{-2}$	8
TY	2D3	A.W.	35.3	165.2	1100.0	101.6	4.2	-40.0	90.0	$0.200 \times 10^7$		$0.680 \times 10^{-3}$	8
TY	2D4	A.W.	176.4	165.2	1100.0	101.6	4.2	-40.0	90.0	$0.110 \times 10^3$		$0.390 \times 10^{-2}$	8
TY	2D5	A.W.	117.6	165.2	1100.0	101.6	4.2	-40.0	90.0	$0.640 \times 10^4$		$0.138 \times 10^{-2}$	8
T	KS1	G.F.	98.0	641.8	3300.0	256.0	12.2		90.0	$0.107 \times 10^6$	$0.774 \times 10^6$	$0.752 \times 10^{-3}$	7
T	KS2	G.F.	196.0	642.1	3300.0	255.8	12.2		90.0	$0.599 \times 10^4$	$0.879 \times 10^5$	$0.153 \times 10^{-2}$	7
T	KS3	G.F.	294.0	641.6	3300.0	257.3	12.1		90.0	$0.284 \times 10^4$	$0.253 \times 10^5$	$0.319 \times 10^{-2}$	7
T	KS4	G.F.	58.8	641.4	3300.0	255.3	12.2		90.0	$0.154 \times 10^7$	$0.500 \times 10^7$	$0.443 \times 10^{-3}$	7
T	KS5	G.F.	245.0	642.0	3300.0	255.8	12.3		90.0	$0.219 \times 10^4$	$0.798 \times 10^5$	$0.208 \times 10^{-2}$	7
T	KS6	G.F.	147.0	641.5	3300.0	256.0	12.0		90.0	$0.776 \times 10^5$	$0.842 \times 10^6$	$0.997 \times 10^{-3}$	7

表 2.4 ( 続き )

Type of Connec. Spec. name	Weld toe is	Load ampli. (kN)	Dimensions (mm)				Experimental results				Ref. No.	
			Chord Thick.	Length	Brace Dia.	g Thick.	$\theta$ (deg.)	Crack initiation life (Nc)	Failure Life (Nf)	Strain amplitude		
T	KS7	G.F.	98.0	641.5	3300.0	255.8	12.2	90.0	$0.534 \times 10^6$	$0.460 \times 10^7$	$0.840 \times 10^{-3}$	7
T	KS8	G.F.	245.0	643.6	3300.0	256.3	13.0	90.0	$0.547 \times 10^4$	$0.139 \times 10^6$	$0.154 \times 10^{-2}$	7
T	KS9	G.F.	196.0	643.5	3300.0	256.0	13.0	90.0	$0.280 \times 10^5$	$0.226 \times 10^6$	$0.128 \times 10^{-2}$	7
T	KS10	G.F.	98.0	643.9	3300.0	256.0	12.9	90.0	$0.846 \times 10^6$	$0.250 \times 10^7$	$0.575 \times 10^{-3}$	7
T	CC20	G.F.	196.0	500.0	3000.0	200.0	6.4	90.0	$0.140 \times 10^5$	$0.540 \times 10^5$	$0.223 \times 10^{-2}$	8
T	CC30	G.F.	294.0	500.0	3000.0	200.0	6.4	90.0	$0.110 \times 10^4$	$0.460 \times 10^4$	$0.422 \times 10^{-2}$	8
T	CC40	G.F.	392.0	500.0	3000.0	200.0	6.4	90.0	$0.390 \times 10^3$	$0.100 \times 10^4$	$0.848 \times 10^{-2}$	8
T	CV20	G.F.	196.0	500.0	3000.0	200.0	6.4	90.0	$0.670 \times 10^3$	$0.800 \times 10^4$	$0.251 \times 10^{-2}$	8
T	CV30	G.F.	294.0	500.0	3000.0	200.0	6.4	90.0	$0.110 \times 10^3$	$0.100 \times 10^4$	$0.394 \times 10^{-2}$	8
T	CV40	G.F.	392.0	500.0	3000.0	200.0	6.4	90.0	$0.190 \times 10^2$	$0.120 \times 10^3$	$0.941 \times 10^{-2}$	8
T	FL20	G.F.	196.0	500.0	3000.0	200.0	6.4	90.0	$0.650 \times 10^3$	$0.800 \times 10^4$	$0.228 \times 10^{-2}$	8
T	FL30	G.F.	294.0	500.0	3000.0	200.0	6.4	90.0	$0.180 \times 10^3$	$0.120 \times 10^4$	$0.380 \times 10^{-2}$	8
T	FL40	G.F.	392.0	500.0	3000.0	200.0	6.4	90.0	$0.500 \times 10^2$	$0.190 \times 10^3$	$0.100 \times 10^{-1}$	8
K	8K1T	T.D.	392.0	179.0	1400.0	76.3	13.0	45.0	$0.510 \times 10^4$		$0.485 \times 10^{-2}$	8
K	8K3T	T.D.	147.0	179.0	1400.0	76.3	13.0	45.0	$0.167 \times 10^6$		$0.175 \times 10^{-2}$	8
K	8K4T	T.D.	254.8	179.0	1400.0	76.3	13.0	45.0	$0.104 \times 10^5$		$0.318 \times 10^{-2}$	8
K	8K5T	T.D.	196.0	179.0	1400.0	76.3	13.0	45.0	$0.379 \times 10^5$		$0.270 \times 10^{-2}$	8
K	8K6T	T.D.	313.6	179.0	1400.0	76.3	13.0	45.0	$0.360 \times 10^4$		$0.335 \times 10^{-2}$	8
K	8K7T	T.D.	931.0	179.0	1400.0	76.3	13.0	4.50			$0.980 \times 10^{-3}$	8
K	8K8T	T.D.	490.0	179.0	1400.0	76.3	13.0	45.0	$0.310 \times 10^3$		$0.510 \times 10^{-2}$	8
K	8K9T	T.D.	490.0	179.0	1400.0	76.3	13.0	45.0	$0.560 \times 10^3$		$0.200 \times 10^{-2}$	8
T	TAG1	G.F.	490.0	609.6	4856.0	323.8	12.7	90.0	$0.177 \times 10^4$	$0.120 \times 10^5$	$0.310 \times 10^{-2}$	25
T	TAG2	G.F.	343.0	609.6	4856.0	323.8	12.7	90.0	$0.210 \times 10^5$	$0.150 \times 10^6$	$0.120 \times 10^{-2}$	25
T	TBG1	G.F.	931.0	609.6	4856.0	508.0	20.5	90.0	$0.430 \times 10^4$	$0.190 \times 10^5$	$0.195 \times 10^{-2}$	25

表 2.4 ( 続き )

Type of Spec. Connec. name	Weld toe is	Load ampli. (kN)	Dimensions (mm)				Chord Thick.	g (mm)	$\theta$ (deg.)	Experimental results				Ref. No.
			Dia.	Length	Dia.	Brace Thick.				Crack initiation life (Nc)	Failure Life (Nf)	Strain amplitude		
T TBG2	G.F.	588.0	609.6	4856.0	508.0	20.5	20.5	90.0	$0.590 \times 10^5$	$0.274 \times 10^6$	$0.960 \times 10^{-3}$	25		
T NSC1	G.F.	98.0	711.2	3600.0	318.5	6.9	6.9	90.0	$0.150 \times 10^4$	$0.250 \times 10^4$	$0.250 \times 10^{-2}$	6		
T NSC2	G.F.	196.0	711.2	3600.0	318.5	6.9	6.9	90.0	$0.900 \times 10^3$	$0.150 \times 10^3$	$0.500 \times 10^{-2}$	6		
T NSC3	G.F.	49.0	711.2	3600.0	318.5	6.9	6.9	90.0	$0.200 \times 10^6$	$0.310 \times 10^6$	$0.120 \times 10^{-2}$	6		
T NSC4	G.F.	294.0	711.2	3600.0	318.5	6.9	6.9	90.0	$0.440 \times 10^5$	$0.350 \times 10^5$	$0.160 \times 10^{-2}$	6		
T NSC5	G.F.	392.0	711.2	3600.0	318.5	6.9	6.9	90.0	$0.900 \times 10^4$	$0.180 \times 10^5$	$0.230 \times 10^{-2}$	6		
T NSC6	G.F.	196.0	711.2	3600.0	318.5	6.9	6.9	90.0	$0.250 \times 10^6$	$0.110 \times 10^{-2}$		6		

Remarks

A.W. : Welded toe is left as-welded.

G.F. : Welded toe is finished by grinder.

T.D. : Welded toe is finished by TIG.

g : Clear space distance between the two braces measured on the crown of the chord.

(g takes a negative value when the braces overlap.)

$\theta$  : Angle of intersection between chord and brace to which load is applied.

Strain amplitude : Measured maximum strain amplitude.

### (3) 試験結果の評価

疲労試験の結果はすべて  $N_c$  (Crack Initiation Life) で整理されている。

図 2.2にT継手, 図 2.3に TY, およびK継手について試験結果を図示する。両図の縦軸は, 荷重振巾と JSSC または黒羽の計算式による耐荷力との比である。

両図には, as weld とグラインダー仕上げ, Mild steelと80k に鋼とに区分して試験結果をプロットしてある。

この2つの図から溶接ビームの仕上げ状態は疲労強度に大きな差があり, グラインダー仕上げした供試体の疲労強度は as weld の供試体の約2倍であるとなっている。

図 2.3には, Mild steel の TY, K継手の50%残存確率曲線と80k 鋼のK継手の50%残存確率曲線を示しているが, 80k 鋼の試験結果は Mild steelに比べて疲労強度が低いことがわかる。

図 2.4に縦軸に歪振巾を採り, 試験結果をプロットし AWS-Xカーブと対比している。

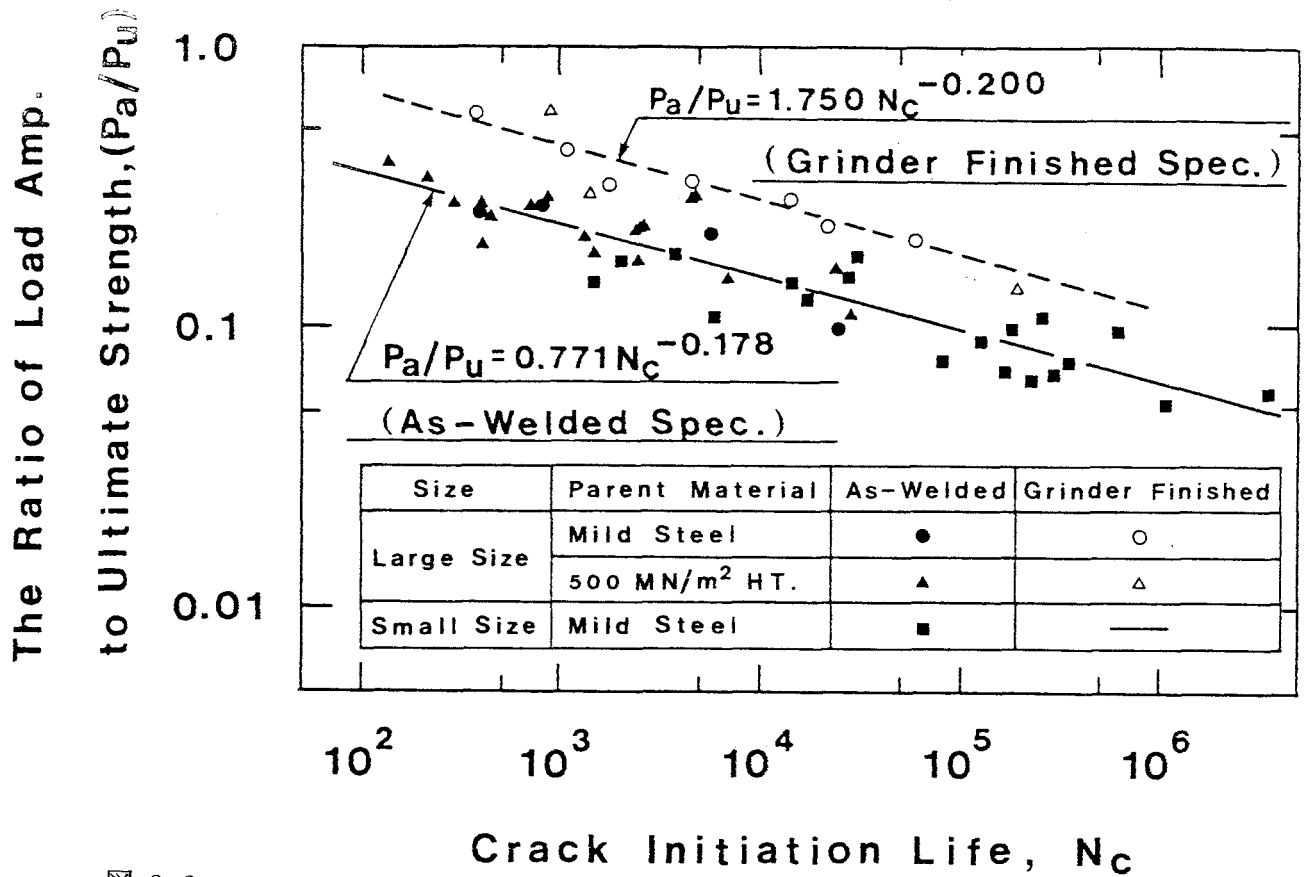
この歪振巾は, 溶接止端部から 2mm~5mm 離れた点で測定した値である。

同図から AWS-Xカーブは sa weld の試験結果のほぼ中央にあり, グラインダー仕上げの試験結果の下限に近いことが分かる。

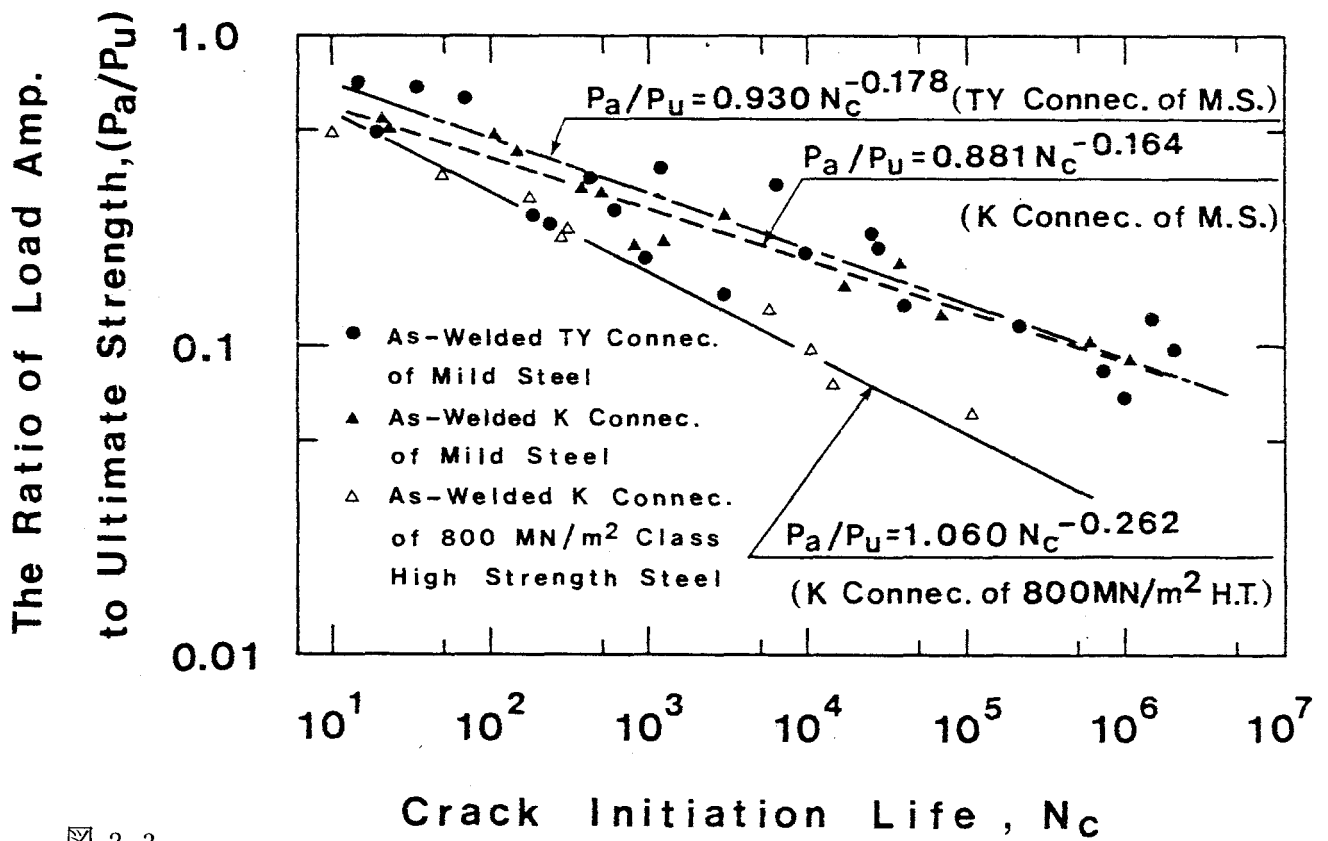
図 2.5に図 2.4と同じ試験結果を用い, 支管に働く平均弾性歪に応力集中係数を掛けた実弾性歪と  $N_c$  の関係でプロットしたものである。

同図に AWS-Xカーブも示しているが, as weld での97.7%残存確率曲線は AWS-Xカーブを下廻っている。

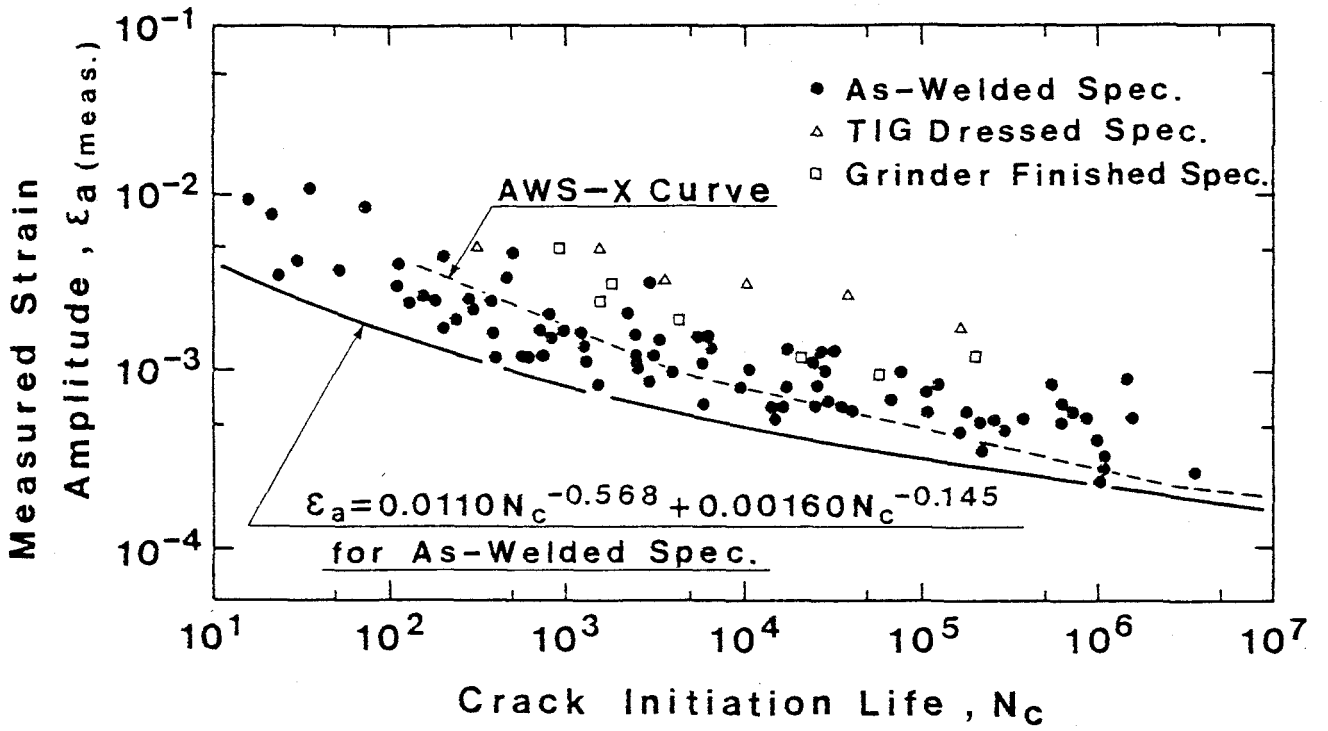
本文献ではこれらの結果を基に Hot Spot Strain を比較的簡便に求める方法を提案し, その設計法による設計疲労曲線を示しているが, ここでは割愛する。



2.2  
Figure 5; Normalized load amplitude versus crack initiation life for tubular T-connections

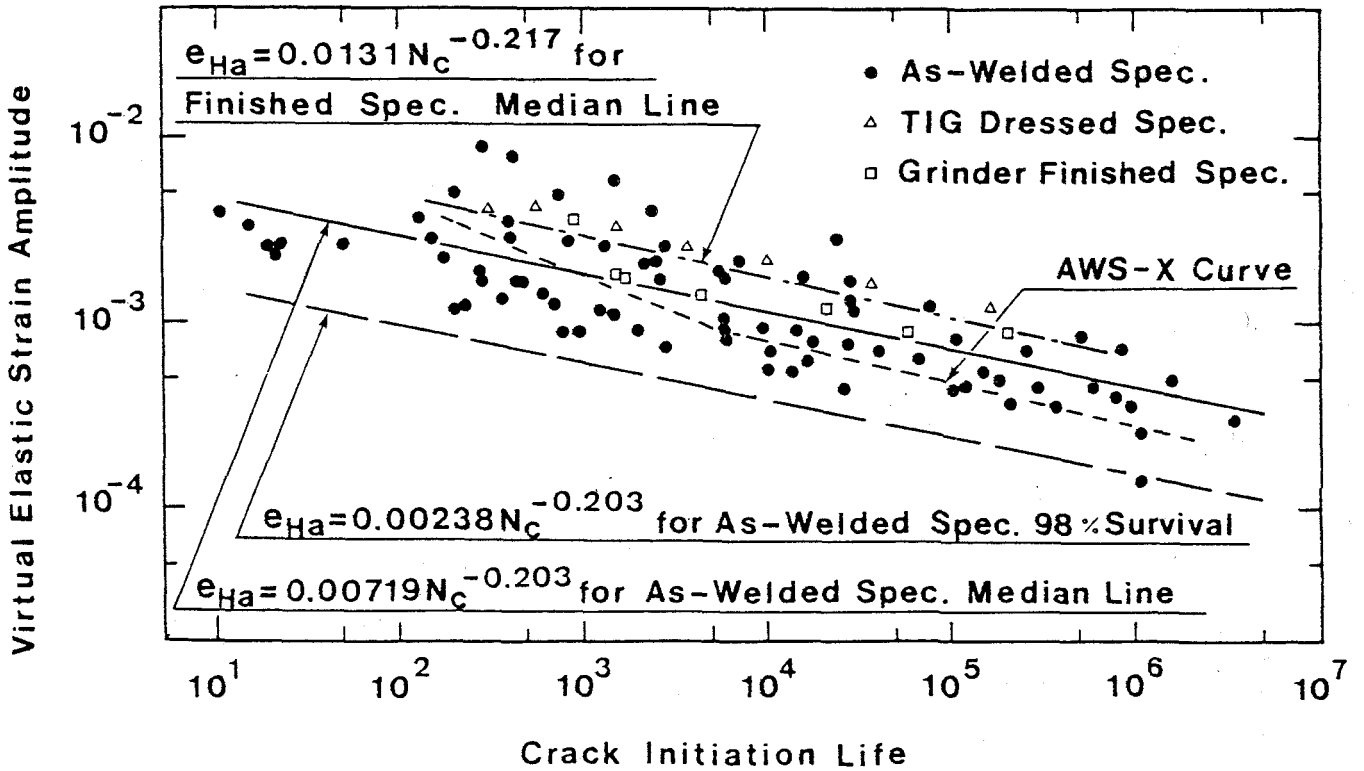


2.3  
Figure 6; Normalized load amplitude versus crack initiation life for tubular TY and K-connections



2.4

Figure 7; Measured hotspot strain amplitude versus crack initiation life for tubular connections



2.5

Figure 8; Virtual elastic strain amplitude versus crack initiation life for tubular connections

## REFERENCES

1. American Welding Society, "AWS Structural Welding Code 1972, Section 10 Design of new tubular structures", 1972.
2. Iida, K., Sakurai, H. and Hayashi, S., "Fatigue strength of welded tubular K-joints of 800 N/mm<sup>2</sup> class high strength steel", IIW Doc. XIII-872-78, 1978.
3. Iida, K., "Notch effects in low cycle fatigue of steels", Selected Papers from the Journal of the Society of Naval Architects of Japan, vol. 11, 1973.
4. Yoshida, K., Inui, T. and Iida, K., "Behavior analysis and crack initiation prediction of tubular T-connections", OTC 2854, 1977.
5. Iwasaki, T., Kawahara, M. and Asano, K., "Fatigue crack growth behavior in welded tubular joints in T, TY and K", OTC 3423, 1979.
6. Sawada, Y., Idogaki, S. and Sekita, K., "Static and fatigue tests on T-joints stiffened by an internal ring", OTC 3422, 1979.
7. Yamasaki, T., Takizawa, S. and Komatsu, M., "Static and fatigue tests on large-size tubular T-joints", OTC 3424, 1979.
8. Japan Ship Machinery Development Association, "Cyclic strain analysis and fatigue strength of tubular connections in offshore structures", Report of FPC Committee, 1976 - 1978.
9. American Petroleum Institute, "Recommended practice for planning, designing, and constructing fixed offshore platforms", API RP 2A 11th edition, 1980.
10. Department of Energy, "Offshore installations: Guidance on design and construction", 1977.
11. Det Norske Veritas, "Rules for the construction and classification of mobile offshore units", 1980.
12. Kuang, J.R., Potvin, A.B. and Leick, R.D., "Stress concentration in tubular joints", OTC 2205, 1975.
13. Beale, L.A. and Toprac, A.A., "Analysis of in-plane T, Y and K welded tubular connections", WRC Bulletin 125, 1967.
14. Visser, W., "On the structural design of tubular joints", OTC 2117, 1974.
15. Rever, J.B. Jr., "Ultimate strength design of tubular joints", OTC 1664, 1972.
16. Mitsui, N., "An experimental study on local stresses in and total strength of steel tubular connections", Dissertation to Osaka University for the degree of doctor of engineering, 1973 (in Japanese).
17. Akiyama, N., Yazima, M., Akiyama, H. and Ohtake, A., "Experimental study on strength

- of joints in steel tubular structures”, Society of Steel Construction of Japan, Vol. 10, No.102, 1974 (in Japanese).
18. Kanatani, H., “Experimental study of welded tubular connections, (Pts. 1, 2 and 3)”, Trans. of the Architectural Institute of Japan, No.108 - No.110, 1965 (in Japanese).
  19. Washio, K., Togo, T. and Mitsui, Y., “Experimental study on local failure of chords in tubular truss joints, (Pts. 1, 2 and 3)”, Trans. of the Architectural Institute of Japan, No.138 - No.140, 1967 (in Japanese).
  20. Kurobane, Y., “Ultimate strength formulae for simple tubular joints”, IIW Doc. XV-385-76, 1976.
  21. Kondo, K., “Application examples of optimization program”, Seminar on Optimum Design and Optimization Technique, Society of Steel Construction of Japan, 1980 (in Japanese).
  22. Iida, K. and Kho, Y., “A method for calculation of fatigue strength reduction factor”, 1974 Symp. on Mech. Behavior of Materials, Kyoto, 1974.
  23. American Society of Mechanical Engineers, “Criteria on the ASME boiler and pressure vessel code for design by analysis in section III Div.1”, 1972.
  24. Asano, K., Iwasaki, T., Tsuruta, Y., Ishikawa, K. and Kamesaki, K., “Stress analysis of the fillet weld toe by three dimensional photoelasticity and its application to fatigue strength estimation”, Proceedings of the Japan Society for Photoelasticity, No.1, 1079 (in Japanese).
  25. Iida, K., Asano, K., Toyofuku, M, and Ishikawa, K., “A fatigue design procedure for offshore tubular connections”, Second Intern. Sym. on Integrity of Offshore Structures, Glasgow, 1981.
  26. Iida, K. and Fujii, E., “Low cycle fatigue strength of steels and welds in relation to static tensile properties”, IIW Doc. XIII-816-77, 1977.
  27. Iida, K., “Comparison of fatigue strengths of steels under deflection controlled bending and strain controlled axial load cycling”, Second Intern. Conf. on Mech. Behavior of Materials, Boston, 1976.
  28. Iwasaki, T., Katoh, A., Asano, K., Kawahara, M., “An analysis on applicability of fatigue data to design of offshore tubular joints”, Journal of the Society of Naval Architects of Japan, Vol. 147, 1980 (in Japanese).
  29. Nishida, M., “Stress concentration”, Morikita Publ. Co., 1967.



## 2.3 アメリカ合衆国

海底油田の開発に関連しアメリカ合衆国は、海洋構造の開発が最も進んでおり、鋼管継手の疲労強度に関しても先覚的な役割を果たしている。

当然、鋼管継手の疲労試験研究も膨大な数になるものと予想され、これらの試験データを集約することは非常に困難である。

一方、海洋構造物を設計する場合、多くは API RP2A 或は AWS を用いる。

従って、この2つの規準の基礎となるデータを紹介することは、国内の設計技師あるいは研究者にとって有益となると考えられる。

これに関し WRC (Welding Research Council) bulletin256 (1980.1) において、E. C. Rodabaugh がAWS D1.1-1975, API RP2A-1978の2つの規準と試験データの間係を紹介しているので、ここでは上記文献の鋼管継手の疲労試験データの部分を紹介する。

### (1) K継手

#### 1) 供試体

供試体の諸元を表 2.5に、供試体に使用した材料の鋼種と機械的特性を表 2.6に示す。

供試体の溶接法の詳細については不明である。ただし、余熱、後熱、応力除去はしていない。

また、溶接部の欠陥の有無、補修の有無についても不明である。

表 2. 5

Table 2—Dimensional Parameters, K-Joints Used in Fatigue Tests

Ref. No.	Test Specimens	Chord D, in.	$r = D/2T$	$\beta = d/D$	$\gamma = t/T$	$\theta_h$ , deg.	$\theta_d$ , deg.	Gap $\delta$					
5	A	12.75	10.2	0.44	0.41	90	35	-0.116					
	B		11.3						0.46				
	C		11.3						0.33				
	D		19.3						0.57				
6	E1	12.75	11.3	0.44	0.33	90	35	-0.241					
	E2		11.3						0.33				
	E3		19.3						0.57				
	E4, E5		19.3						0.57				
7	F	12.75	19.3	0.44	0.57	90	35	-0.399					
8	B1, 2, 3	8.625	23.4	0.41	1.12	90	45	0.42					
	B4, 5, 6												
	B7, 8, 9												
	C1, 2, 3		22.9						0.44	1.00			0.027
	C4, 5, 6												-0.023
	C7, 8, 9												-0.257
9	F15	4.00	15.4	0.42	0.97	60	60	0.20					
	K15		7.51						18.9	0.40	0.63		0.278
10	1, 2, 3	5.50	17.9	0.44	0.82	90	35	0.214					
	4, 5		16.6						0.44	0.76		0.179	
	6, 7, 8		18.0						0.55	0.82		0.214	
	9		16.0						0.55	0.73		0.179	
	10, 11, 12		17.9						0.64	0.82		0.214	
	13		16.4						0.64	0.73		0.179	
	14, 15, 16		17.7						0.44	0.81		0.079	
	17		16.4						0.44	0.75		-0.214	
	18, 19, 20		17.7						0.44	0.81		-0.214	
	21		16.4						0.44	0.75		-0.344	
	22, 23, 24, 25		16.4						0.55	0.75		0.214	
11	41/48G	6.50	18.1	0.46	0.89	45	45	0.347					
	61, 62, 63		13.5						0.67				
	71, 73, 74		11.6						0.57				
12	JPG	6.50	18.1	0.46	0.89	45	45	0.847					
	JGM		18.1						0.89			-0.154	
13	1/12	41.5	13.8	0.43	0.33	84.29	42.71	0.102					
14	13, 14	41.5	13.8	0.43	0.33	84.29	42.71	0.102					
15	SW-1	20.0	20.0	0.54	0.50	45	45	0.240					

表 2. 6

Table 3—Materials, K-Joints Used in Fatigue Tests

Ref. No.	Test Specimens	Material	Measured Tensile Properties					
			$F_y$ , ksi		$F_u$ , ksi		El., %	
			Chord	Brace	Chord	Brace	Chord	Brace
5	All	API 5LGr. B	—	—	—	—	—	—
6	All	↓	—	—	—	—	—	—
7	All		—	—	—	—	—	—
8	B		53.1	31.7	71.2	54.2	25	35
"	C	52.9	72.5	72.8	92.0	25	15	
9	F15	a	57.4	61.4	69.5	67.7	26	27
"	K15	a	46.1	—	64.6	—	37	—
10	All	JIS STK-41	47/54	—	57/71	—	31/38	—
11	T-4.5	b	—	34.7	76.5	50.2	—	44
	T-6.0	b	54.6	—	71.7	—	31	—
	T-7.1	b	49.6	—	68.8	—	35	—
12	All	STK-41	50.5	58.9	64.0	72.7	36	29
13	1/12	—	—	—	—	—	—	—
14	13, 14	c	50.0	—	77.5	—	37	—
15	SW-1	ASTM A441	—	—	—	—	—	—

(a) Chord: JIS STK-41 (~ASTM A36)

(b) Brace: JIS STK-50 (~ASTM A441)

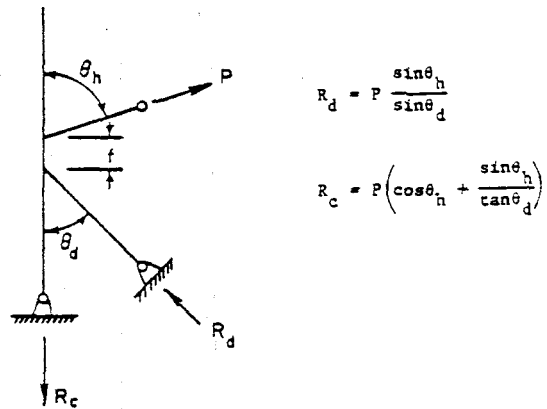
(c) Chord: STK-41  
Brace: STPG-38

(d) Chemical Composition: C-0.20, Mn-1.08, Si-0.21, Al-0.03 percent

## 2) 試験方法

図 2.6 に荷重載荷概要を示す。ただし Ref.11,12 は図 2.7, 図 2.8 に示す。

図 2.6 で  $f > 0$  であるが  $f > 0$ ,  $f < 0$  の両方の場合がある。



Ref. No.	$\theta_h$ deg.	$\theta_d$ deg.	$R_d/P$	$R_c/P$	Loading Rate, cpm
5 (a)	90	35	1.743	1.428	—
6 (a)	90	35	1.743	1.428	15
7	90	35	1.743	1.428	30
8 (b)	90	45	1.414	1.000	200
9	60	60	1.000	1.000	—
10	60	60	1.000	1.000	180/1500
13 (c)	84.29	42.71	1.467	1.078	—
14 (c)	84.29	42.71	1.467	1.078	—
15	45	45	1.000	1.414	—

(a) Refs. 5 and 6 do not indicate which end of the chord was pinned.

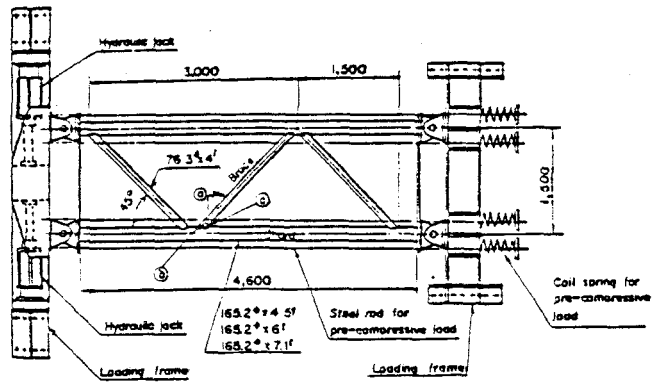
(b) For Ref. 8, series B, the pinned end of the chord is at the top, free end at the bottom.

(c) Load was applied to chord.

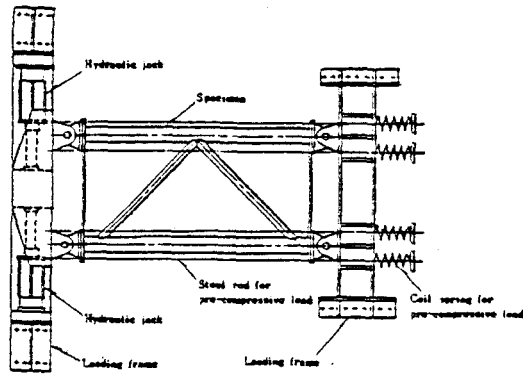
Fig. 1—Loadings on K-Joints in fatigue tests

図 2.6

また、試験上の特殊条件は、表 2.7 の脚注 (a) ~ (o) 参照されたい。



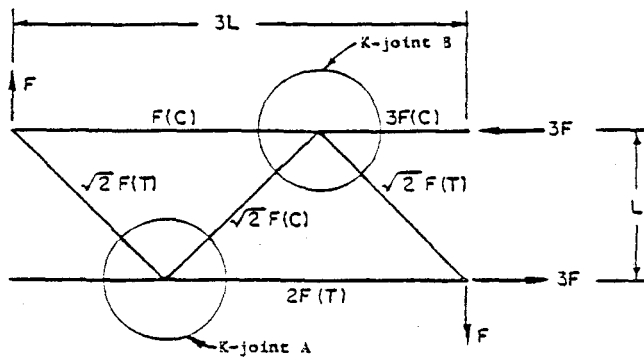
(a) Loading Arrangement, Ref. 11



(b) Loading Arrangement, Ref. 12

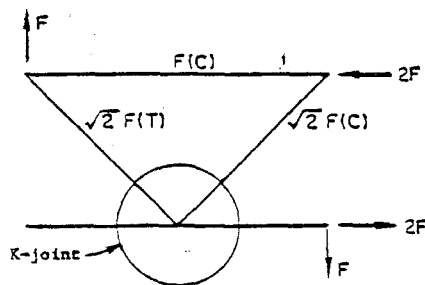
Fig. 2—Loading arrangements, K-Joint fatigue tests, Refs. 11 and 12

☒ 2. 7



(a) Reference 11

(C) ≡ compression  
(T) ≡ tension



(b) Reference 12

Fig. 3—internal loads, trusses used in Refs. 11 and 12 fatigue tests of K-joints

☒ 2. 8

### 3) 試験結果

表 2.7に試験結果を示すが $N_i$  (number of cycles to crack initiation) の定義は文献により相違しており表 2.8に表示する。

また、 $N_f$  (number of cycles to failure) の定義も明確ではないが、写真と説明文から主管から支管が完全に離れるかあるいはあと少しの繰返し荷重で主管、支管が完全に分離する回数であると考えられる。

表 2.9に破壊位置の一覧を示す。この表からすべての試験でクラックの発生位置は溶接止端部外表面であることが明らかである

クラックは溶着金属中ではなく主管、支管の母材中を進展している。

表 2.8

Table 4—Definitions of Crack Initiation

Ref. No.	Test Specimens	Definition of Crack Initiation
5	All	$N_i$ represents "the number of stress cycles to visible crack initiation".
6	E	"During these tests the strains on a couple of gages were recorded continuously for a limited number of cycles every 100 cycles. The results were studied for any changes in strain level and magnitude, which would indicate a crack development and a change in the local load transfer. In addition to this record, the specimens were further inspected visually after removal from the water every 500 cycles".
7	F	Not defined
8	B,C	Apparently (per Fig. 4.17 of Ref. 8) a crack in the outside surface about 2" long.
9	F15 1-11	"Cracks were observed, through a magnifying glass, on the white-washed surfaces of the specimens".
10	F15 12-16	"A low-power microscope was used for crack detection. Finer cracks could be detected by the microscope than those which were detected by magnifying glass".
10	J4	"Fatigue cracks were observed on the surfaces of the as-welded specimens through a magnifying glass. Liquid penetrant was sprayed on the surfaces of the specimens. The penetrant bubbled out from the cracks under the action of pulsating loads, which facilitated the detection of cracks. The chord was filled with surfactant solution. Leakage of the solution demonstrated a formation of a crack that penetrated through the chord wall." (Ref. 10 does not indicate whether the tabulated values of "cycles-to-crack initiation" represent surface cracks or leakage cracks.)
11	—	Does not give cycles-to-crack initiation
12	—	Does not give cycles-to-crack initiation
13	L1-12	"Observations were made through a 10 power magnifying glass. The term 'crack initiation' refers to the first visual observation of a crack."
14	L13, I4	Visual. Figure shows locations and sizes of several separated "initial" cracks.
15	SW-1	"Crack initiation is noted at 7100 cycles". Ref. 15, Fig. 26, indicates no crack at 6500 cycles, about 1.5" long crack at 7100 cycles.

表 2.7

Table 1—Summary of Axial Load Fatigue Test Data on K-Joints

Ref. No.	Ident.	D, in.	d, in. <sup>a</sup>	T, in.	t, in. <sup>b</sup>	$\theta_h^c$ , deg.	$\theta_d^c$ , deg.	Gap, in. <sup>d</sup>	$S_y$ , ksi <sup>e</sup>			Cycles <sup>f</sup>		
									Max.	Min.	Range	$N_1$	$N_2$	
5	A1	12.75	5.563	0.625	0.258	90	35	1.474	(No entries under these columns indicate: R = -1)			23.2	14,500	34,600
	2			"	"				18.6	49,000	94,900			
	B1			0.562	0.258				23.2	6,400	22,600			
	2			"	"				23.2	7,500	19,000			
	3			"	"				18.6	35,000	106,000			
	4			"	"				14.0	150,000	218,000			
	C1 <sup>h</sup>			0.188 <sup>g</sup>	"				31.6	9,900	9,900			
	2			"	"				25.2	16,100	27,700			
	3			"	"				19.0	27,500	75,900			
	4			"	"				15.8	67,000	85,600			
	5			"	"				12.6	382,000	—			
	D1 <sup>h</sup>			0.330	"				31.6	60	450			
	2 <sup>i</sup>			"	"				31.6	1,400	6,300			
	3 <sup>i</sup>			"	"				31.6	1,200	6,800			
	6 <sup>j</sup>			E1 <sup>h</sup>	0.562				0.188	1.474	31.6	9,900	9,900	
				2	"				"	-3.078	31.6	7,000	7,500	
3 <sup>h</sup>		0.330	"	1.474	31.6	60	450							
4		"	"	-3.078	31.6	4,000	4,000							
5		"	"	"	31.6	3,000	3,000							
7	F1	0.330	0.188	-5.089	31.6	1,800	3,020							
	2	"	"	"	31.6	3,130	6,000							
8	B1	8.625	3.500	0.184	0.206	90	45	2.088	8.50	1.67	6.83	4,480	12,100	
	2			"	"				6.22	1.67	4.55	83,000	130,000	
	3			"	"				3.95	1.67	2.28	1.08E6	1.55E6	
	4			"	"				0.088	8.50	1.67	6.83	27,000	65,000
	5			"	"				6.22	1.67	4.55	77,400	100,000	
	6			"	"				3.95	1.67	2.28	1.86E6	>2.2E6	
	7			"	"				-1.912	8.50	1.67	6.83	82,700	135,000
	8			"	"				6.62	1.67	4.55	448,000	823,000	
	9			"	"				3.95	1.67	2.29	>2.0E6	>2.0E6	
8	C1	8.625	3.750	0.188	0.188	90	45	1.786	-11.65	-2.65	9.00	3,010	20,430	
	2			"	"				-8.5	-1.67	6.83	20,300	30,800	
	3			"	"				-3.95	-1.67	2.28	1.32E6	>2E6	
	4			"	"				-0.214	-16.0	-2.65	13.75	7,100	33,500
	5			"	"				-11.65	-2.65	9.00	219,000	239,000	
	6			"	"				-6.22	-1.67	4.55	1.49E6	>2.1E6	
	7			"	"				-2.214	-20.95	-2.65	18.30	15,700	35,300
	8			"	"				-16.40	-2.65	13.75	31,900	70,000	
	9			"	"				-1.05	-2.65	9.00	2.00E6	>2.0E6	
9	F15-1	4.00	1.68	0.133	0.126	60	60	0.80	27.6	4.16	23.4	150	5,700	
	2			0.136	"				29.4	4.41	25.0	1/2	1,100	
	3			0.136	"				31.2	4.70	26.5	1/2	993	
	4			0.130	"				29.4	4.41	25.0	5	2,030	
	5			0.129	"				31.2	4.70	26.5	1/2	163	
	6			0.119	"				27.6	4.16	23.4	1/2	6	
	7			0.134	"				25.1	3.76	21.3	1,270	5,620	
	8			0.128	"				25.1	3.76	21.3	6,700	15,600	
	9			0.121	"				27.6	4.16	23.4	1/2	95	
	10			0.120	"				27.6	4.16	23.4	79	297	
	11			0.136	"				25.1	3.76	21.3	>7,380	>7,380	
	12			0.126	"				25.1	3.76	21.3	1/2	286	
	13			0.127	"				23.3	3.50	19.8	1/2	4,960	
	14			0.127	"				21.5	3.23	18.3	1/2	7,080	
	15			0.130	"				25.1	3.76	21.3	1/2	2,260	
	16			0.128	"				21.5	3.23	18.3	1/2	10,200	
K15-1	7.51	3.00	0.199	0.126	60	60	1.34	26.4	3.95	22.5	1/2	6,550		

表 2.7 ( 続 き )

Table 1 (Cont.)—Summary of Axial Load Fatigue Test Data on K-Joints

Ref. No.	Iden.	D, in.	d, <sup>a</sup> in.	T, in.	t, <sup>b</sup> in.	$\theta_h^c$ , deg.	$\theta_d^c$ , deg.	Cap, <sup>d</sup> in.	$S_b$ , ksi <sup>e</sup>			Cycles <sup>f</sup>									
									Max.	Min.	Range	$N_i$	$N_f$								
10	J4-1	5.50	2.40	0.155	0.126	60.	60.	1.18	14.7	50,000	55,800										
	2			0.154				5.88				1.96E6	2.38E6								
	3			0.154				7.84				219,000	479,000								
	4			0.168				20.6				19,000	24,600								
	5			0.165				16.2				10,300	175,000								
	6			3.00				0.153				1.18	5.04	4.29E6	5.21E6						
	7			0.153				8.14				120,000	299,000								
	8			0.155				10.9				56,000	79,100								
	9			0.172				20.2				3,900	11,300								
	10			3.52				0.156				1.180	5.91	1.41E6	1.92E6						
	11			0.154				7.22				347,000	924,000								
	12			0.154				12.1				45,200	128,000								
	13			0.172				14.4				28,600	52,500								
	14			2.40				0.156				0.433	15.7	71,300	107,000						
	15			0.155				8.33				6.98E6	7.32E6								
	16			0.154				11.8				280,000	496,000								
	17			0.168				28.4				3,000	5,800								
	18			0.155				-1.18				23.5	100,000	129,800							
	19			0.155				23.5				174,000	178,000								
	20			0.154				14.7				1.52E6	2.96E6								
	21			0.168				27.9				9,500	16,100								
	22			3.00				0.172				-1.89	27.9	14,500	23,900						
	23			0.167				20.9				78,000	137,900								
	24			0.166				15.1				505,000	1.04E6								
	25			0.166				13.6				1.16E6	5.06E6								
	26			2.40				0.174				1.18	13.7	97,000	132,000						
	27			0.174				7.35				551,000	970,000								
	28			0.174				9.31				796,000	1.12E6								
11 <sup>k</sup>	J-41	6.50	3.00	0.18	0.16	45.	45.	2.257	11.2	—	70,000										
	42			6.5				—				>2E6									
	43			9.0				—				>2E6									
	45			17.8				—				9,000									
	46			13.4				—				50,000									
	47			11.2				—				110,000									
	42G <sup>2</sup>			17.8				—				40,000									
	43G <sup>2</sup>			10.2				—				450,000									
	48G			11.0				—				850,000									
	61			0.42				10.2				—	950,000								
	62			15.4				—				110,000									
	63			12.2				—				520,000									
	71			0.28				21.4				—	90,000								
	73			17.8				—				350,000									
	74			15.4				—				1.4E6									
	12 <sup>m</sup>			JPG-1				—				—	0.18	—	—	—	5.51	11.2	—	18,000	
2		8.8	—	95,000																	
3		6.6	—	390,000																	
4		4.4	—	820,000																	
JGM-1		—	—	—	—	—	—		-1.00	17.6	—		340,000								
2									16.2								—				235,000
3									14.0								—				88,000
4									14.0								—				160,000
5									9.6								—				1.4E6

表 2.7 ( 続 き )

Table 1 (Cont.)—Summary of Axial Load Fatigue Test Data on K-Joints

Ref. No.	Iden.	D, in.	d, <sup>a</sup> in.	t, in.	t, <sup>b</sup> in.	$\theta_h$ , <sup>c</sup> deg.	$\theta_d$ , <sup>c</sup> deg.	Gap, <sup>d</sup> in.	$S_b$ , ksi <sup>e</sup>			Cycles <sup>f</sup>	
									Max.	Min.	Range	$N_i$	$N_f$
13 <sup>a</sup>	L1	41.5	18.0	1.50	0.500 <sup>g</sup>	84.29	42.71	4.24			38.0	1,200	8,960
	2											590	6,900
	3											1,200	10,600
	4											3,400	9,790
	5											730	12,700
	6											430	9,030
	7											900	4,070
	8											250	6,550
	9											470	4,000
	10											700	5,150
	11											1,640	9,730
	12											700	8,000
14 <sup>a</sup>	13										30.0	1,140	32,550
	14										50.0	250	3,175
15	SW-1	20.	10.75	0.50	0.25	45	45	4.797	21.8	-7.27	29.1	7,100	12,400

(a) d is the diameter of both braces

(b) t is the wall thickness of the brace with  $\theta = \theta_d$ . Unless otherwise noted, the wall thickness of the brace with  $\theta = \theta_h$  is the same.

(c)  $\theta_h$  = larger of the two angles between braces and chord.  
 $\theta_d$  = smaller of the two angles between braces and chord.

(d) Gap between braces, see Nomenclature illustration.

(e)  $S_b$  is the nominal stress,  $P/[t\pi(d-t)]$ , in the brace with  $\theta = \theta_h$ . The nominal stress in the brace with  $\theta = \theta_d$  is given by:

$$S_b(\theta = \theta_d) = S_b(\sin\theta_h/\sin\theta_d)[t(d-t)]/[t_d(d-t_d)], \text{ where } t_d \text{ is the}$$

wall thickness of the brace with  $\theta = \theta_d$ .

(f)  $N_i$  = cycles to crack initiation,  $N_f$  = cycles to failure

(g) The wall thickness of the brace with  $\theta = \theta_d$  is given as 0.258".

(h) From the number of cycles, it appears that C1 is a duplicate of E1, D1 is a duplicate of E3. However, the cited references indicate that the wall thickness of the brace with  $\theta = \theta_d$  is 0.258 for C1 and D1 whereas that wall thickness is given as 0.188 for E1 through E3.

(i) The chord tubes of specimens D2 and D3 were filled with cement grout.

(j) A constant compressive load of 140,000 lb was maintained on the chord during the fatigue tests. During the fatigue tests the specimens were submerged in a salt water (3.5% NaCl) solution.

(k) A constant compressive stress of 7.0 ksi for specimens J-41 through J-48G, 5.3 ksi for specimens J-61, -62, and -63, 4.9 ksi for specimens J-71, -73, and -74, was maintained on the chord during the fatigue tests.

(l) Specimens J-42 and J-43 were first tested in an as-welded condition to  $2 \times 10^6$  load cycles, at which no fatigue cracks were found, and were subsequently tested as J-42G and J-43G at a higher stress after grinding welds to a concave profile. Specimen J-48G welds were ground to a concave profile prior to fatigue testing.

(m) A constant compressive stress of 7.1 ksi was maintained on the chord during the fatigue tests.

(n) These specimens are different from other specimens in that:

(1) there was a 36" "pile" inside the chord; the pile was 36" O.D. x 0.375" wall. The annular space between the chord and pile contained a cement grout material.

(2) there was another K-joint, of the same size, located 90° around the chord from the loaded K-joint.

(3) the specimens were described as:

Properly fabricated	L1, L2, L3, L4
Repaired	L5, L6, L13, L14
Defective in fabrication	L7, L8, L9, L10
Actual Structure	L11, L12

(o) The wall thickness of the brace with  $\theta = \theta_d$  was 0.625".



表 2.9 Table 5—Failure Locations, K-Joint Fatigue Tests

Ref. No.	Series	Description of Failure Locations
5	All	At toe of welds. About 50% of the cracks were in the chord wall, 50% in the brace wall. All specimens except B-4 and C-3 failed around the brace with $\theta=90^\circ$ ; B-4 and C-3 failed around the brace with $\theta=35^\circ$ .
6	E1	Toe of weld in brace wall, around brace with $\theta=90^\circ$
	E2	Toe of weld in brace wall, brace with $\theta=35^\circ$ (Final form of failure not apparent from Reference)
	E3	Toe of weld in chord wall, around brace with $\theta=90^\circ$
	E4, E5	Toe of weld between the (overlapping) braces, in the wall of the brace with $\theta=35^\circ$ .
7	F1, F2	"Crack in diagonal member" (Presumably in weld at brace with $\theta=35^\circ$ .)
8	B1, 2, 3	Toe of weld in chord wall, around brace with $\theta=90^\circ$
	B4-9	Toe of weld in chord wall, started around brace with $\theta=90^\circ$ but propagated around both braces.
8	C1-9	Similar to B-series.
9	F15	"Fatigue cracks were usually found on the chord surface along the toes of the brace-to-chord welds". First cracks and failures occurred around tension-loaded brace.
10	All	"The joints with extended braces ( $gap > 0$ ) developed the first crack at the toes of the brace-to-chord welds, on the crown where the two welds between the braces and the chord approached. The cracks extended first along the weld toes and then also into the chord wall"  "In the joints with overlapping braces, the first cracks usually appeared at the points where the three welds met. Final failures were mostly governed by a separation of a brace from the joint."  Judging from photographs of typical failures, cracks in joints with $gap > 0$ were in the chord wall; cracks in joints with $gap < 0$ were through the brace wall.
11	J	Toe of weld in chord wall. Crack started at crown, progressed around brace.
12	JPG	(Joints with $g > 0$ .) Same as 11
	JPM	(Joints with $g < 0$ .) At toe of weld between the braces, in brace wall.
13	L1/12	"The initial cracks were often preceded by a series of short cracks which within 10 to 20 cycles would grow into a single crack. In general, these cracks were observed as surface cracks in the chord walls along the welds."  "The cyclic loading was normally terminated after the development of a significant tearing of the branch wall."
14	L13	Photographs indicate numerous cracks at toes of welds and through the welds. The major crack was at the toe of the fillet weld in the chord wall around the brace with $\theta=84.29^\circ$ . Some cracks started at the toe of the weld, then turned parallel to the chord wall surface under the weld; termed "Lamellar tears" by Ref. 14. Weld roots were poor but only minor cracks at weld roots occurred.
14	L14	Photographs indicate that the major crack was at the toe of the fillet weld in the brace wall, around the brace with $\theta=84.29^\circ$ .
14 & 13	L1/14	Ref. 14 states that Specimen L13 failed by cracking through the "can" (chord), and "This was the only failure of this type observed in the total of 14 specimens tested." Presumably the other 13 specimens failed by cracking through a brace. Ref. 14 indicates that "cause of failure" was "Diag. Tearing" for all except L5 and L10, "Horiz. Fracture" for L5, "Horiz. Tearing" for L10. "Diag." presumably refers to the brace with $\theta=42.71^\circ$ , "Horiz." to the brace with $\theta=84.29^\circ$ .
15	SW-1	Crack initiated at toe of fillet weld in chord at the point of nearest approach of the two braces and grew normal to the chord surface and around the brace.

4) 試験結果の評価

i)  $N_f$  vs  $V_p$  (range of punching shear stress)

試験結果をAWS D1.1-75 と対比したのが図 2.9である。

同図で (1), (2) の直線はギャップある場合とオーバーラップの場合の試験結果の平均で, 下端の2点鎖線はAWS K-curve を示しており, 試験結果の分布を対数正規分布と仮定し26 (97.7 %) 残存確率として求めたものである。

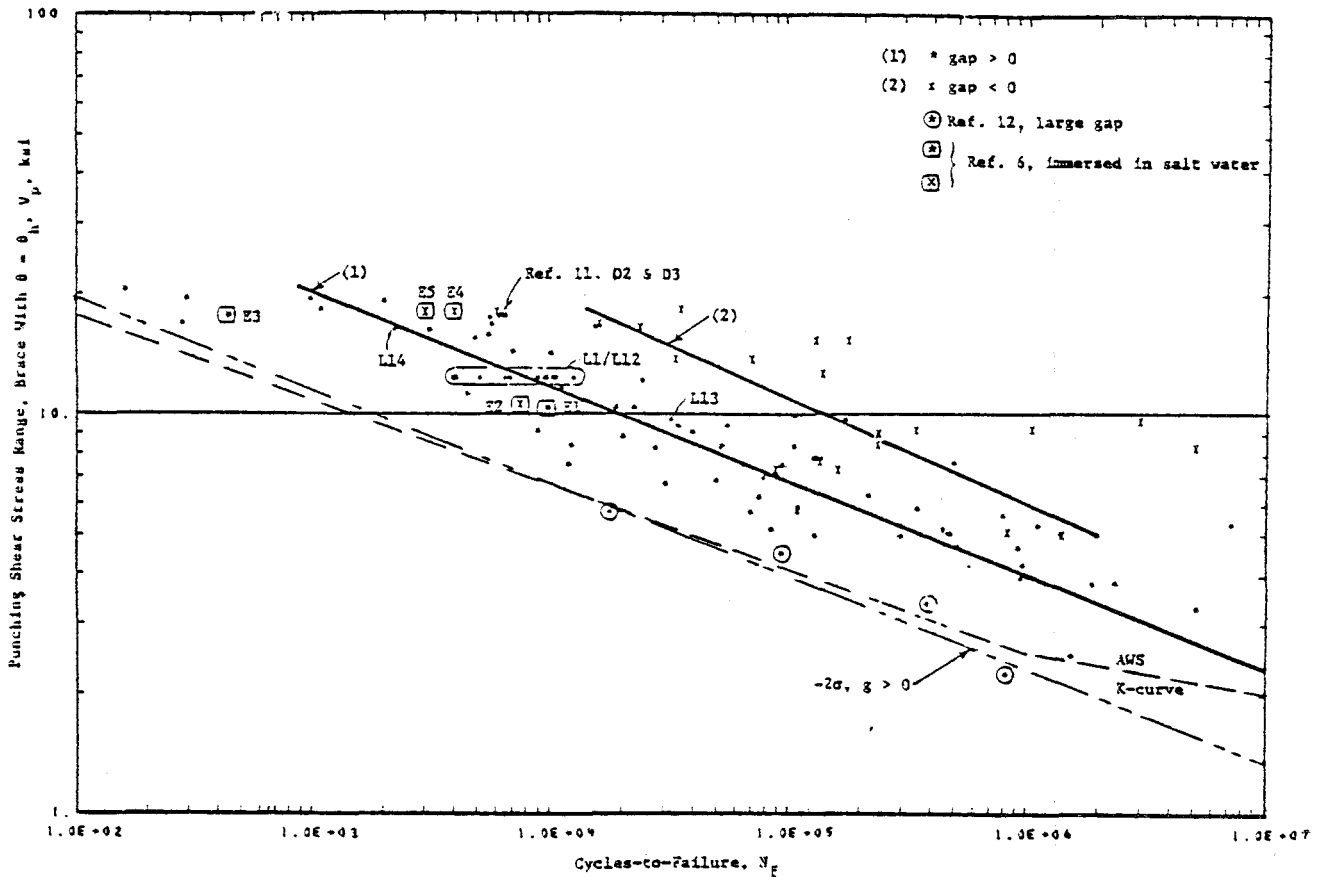


Fig. 4—Comparison of  $V_p$  vs  $N_f$  with AWS K-Curve

図 2.9

また, 試験結果の分布を最小二乗法で曲線で示すと図 2.10, 図 2.11 のようになる。

図 2.10 は2次, 図 2.11 は3次式で求めたものである。

図 2.12 は供試体の“寸法効果”を示すもので, Small は 7.51 in  $\phi$  (19cm) 以下, Larger は 12.75 in  $\phi$  (32cm) 以上の場合である。

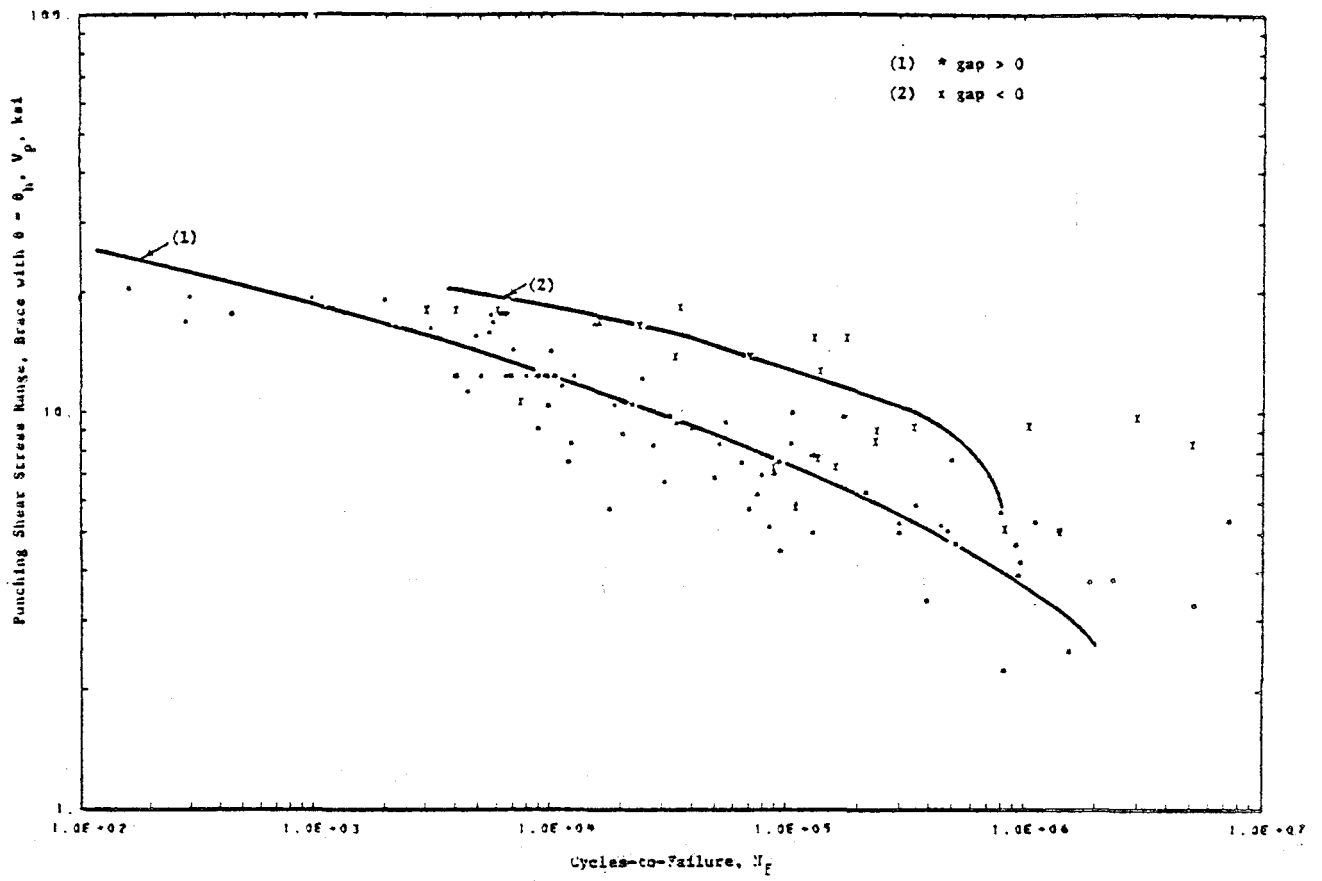


Fig. 5—Least squares fit using Eq. (6), K-joints  $\boxtimes$  2.10

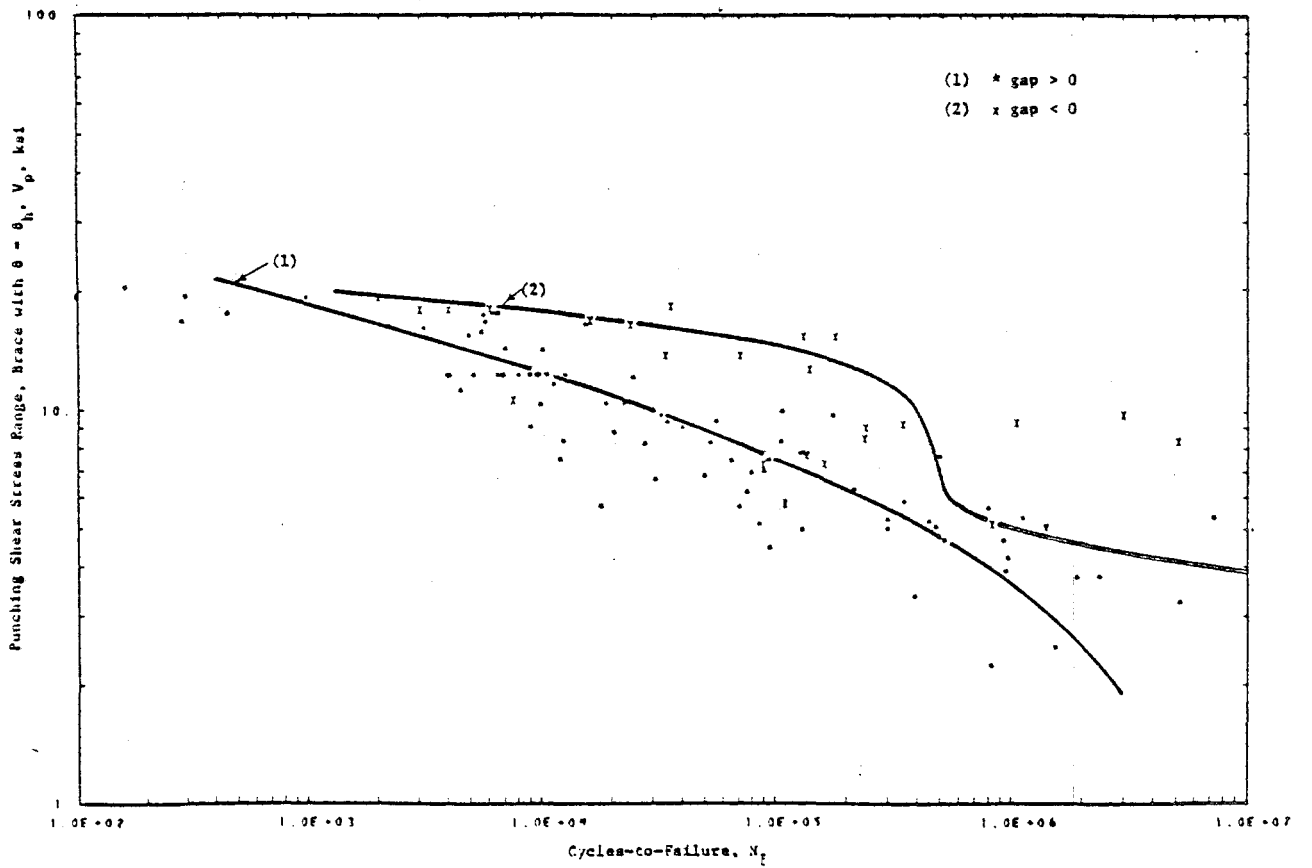


Fig. 6—Least squares fit using Eq. (7), K-joints  $\boxtimes$  2.11

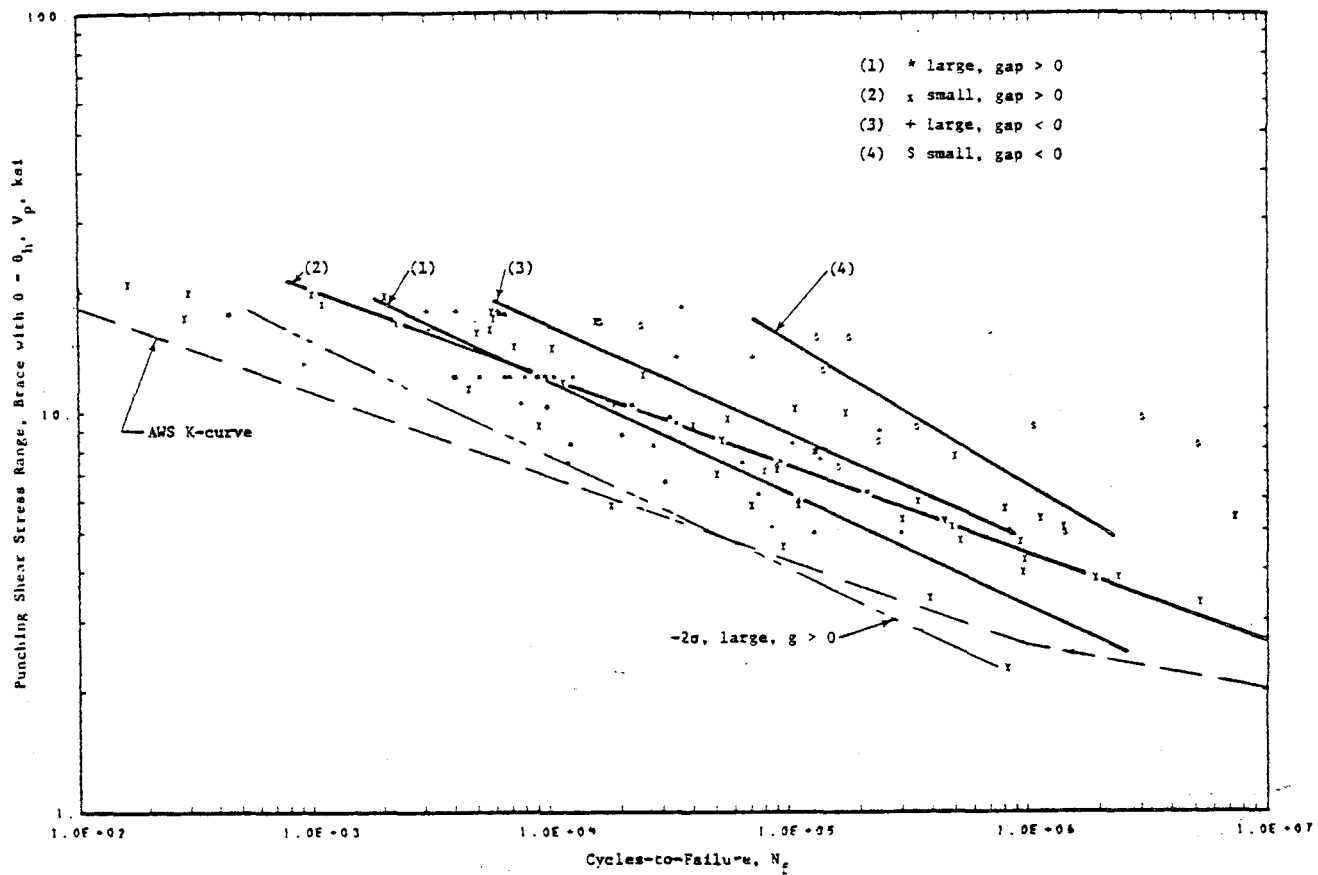


Fig. 7— $V_p$  vs  $N_f$  tests divided into four groups X 2. 1. 2

ii) Ni vs Vp

図 2.13 に Ni (cycles-to-crack initiation) と Vp (Punching shear stress) との関係を示す。

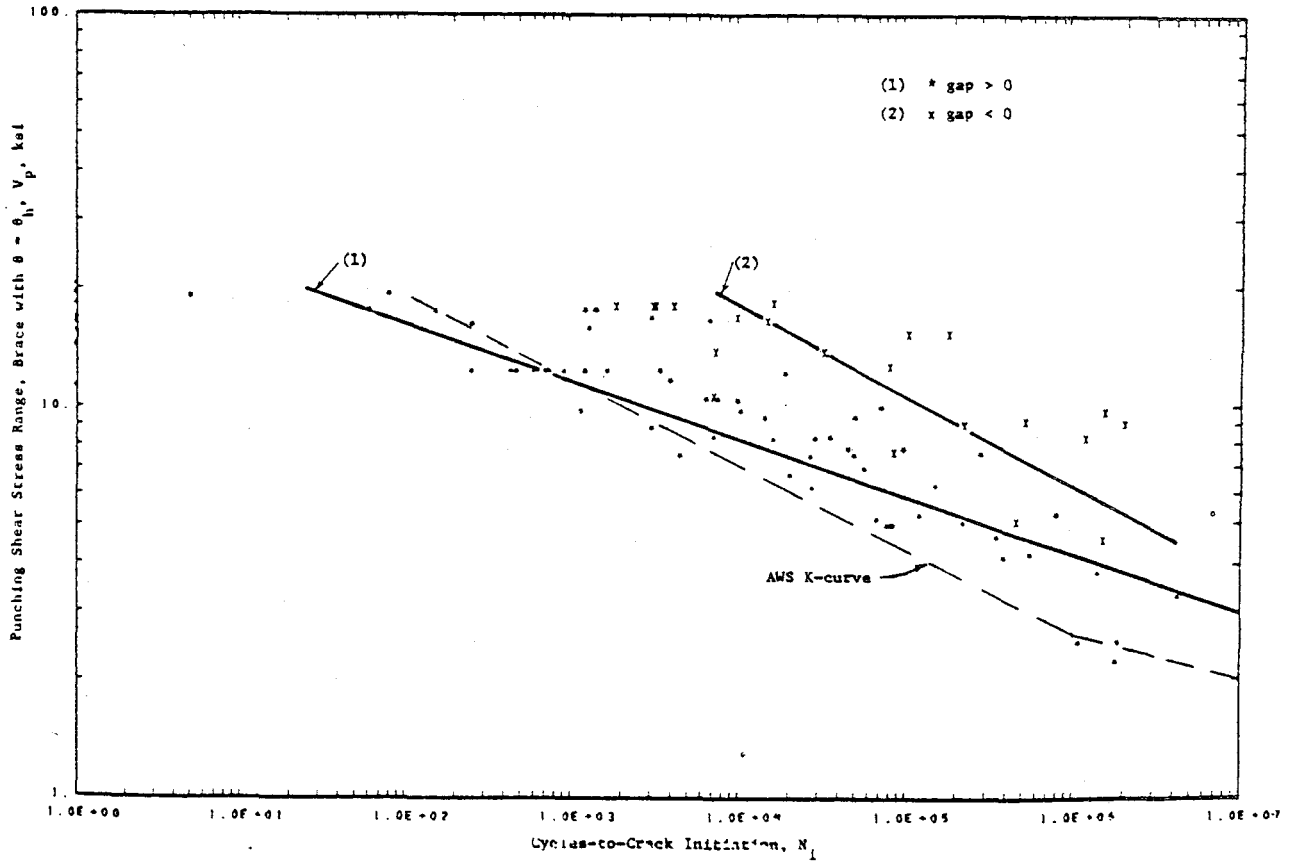


Fig. 8—Comparison of  $V_p$  vs  $N_i$  (crack initiation) with AWS K-curve

図 2.13

表 2.8に  $N_i$  (Crack initiation) の定義を示した。この定義の相異が図 2.13 の試験結果のバラツキが大きな原因であると述べている。

この表から言えることは、ギャップのある継手 ( $g > 0$ ) ではAWS-Kcurveで許される $N_i$ ,  $V_p$  は50%の信頼度しかないということである。

しかし、オーバーラップ継手 ( $g < 0$ ) では、AWS-Kcurveで許される $N_i$ ,  $V_p$  で2%しか微少クラックは発生しないことになる。

iii)  $N_f$  vs  $S_b / f_a'$

API RP2A, Par. 2.22Cで規定されている許容静荷重との関係を図示する。

$S_b$ はブレースの標準応力範囲,  $f_a'$ はAPI RP2Aに規定されている, ブレースの静的許容標準軸応力である。

図 2.14 に  $S_b / f_a'$  と  $N_f$  の関係をプロットしたもので, 図 2.15 では gapがあるK継手で供試体が大きい場合 (管径 32 cm以上) と小さい場合 (管径 19 cm以下) を示している。

表 2.10 に図 2.14, 図 2.15 に示した直線の諸定数を示す。

表 2.10

Table 6—Summary of Correlation Equations, Fatigue Tests of K-Joints

Cycles	Stress	No. of Tests	Group	C	n	$\sigma$	Fig.
$N_f$	$V_p$	90	g>0	3.53E8	-4.25875	0.5220	3-4
		24	g<0	9.09E8	-3.80503	0.6203	
$N_f$	$V_p$	37	large, g>0	5.52E7	-3.51534	0.2982	3-7
		53	small, g>0	6.10E8	-4.46538	0.6167	
		11	large, g<0	3.31E8	-3.72464	0.4397	
		13	small, g<0	1.57E8	-2.75313	0.5722	
$N_f$	$V_p$	76	g>0	1.31E10	-6.71939	1.0190	3-8
		21	g<0	2.13E9	-4.26589	0.6275	
$N_f$	$S_b / f_a'$	90	g>0	1.26E5	-4.25868	0.5436	3-9
		24	g<0	9.82E5	-3.52741	0.6510	
$N_f$	$S_b / f_a'$	37	large, g>0	6.48E4	-3.33191	0.3392	3-10
		53	small, g>0	1.69E5	-4.53614	0.6138	
$N_f$	$1S_b$	37	large, g>0	1.26E11	-3.33182	0.2995	3-11
			small, g>0	1.16E14	-4.94877	0.5688	

表 2.10 での記号は以下の通りである。

C, n : 最少二乗法で求めた直線の定数

$\sigma$  : 標準偏差

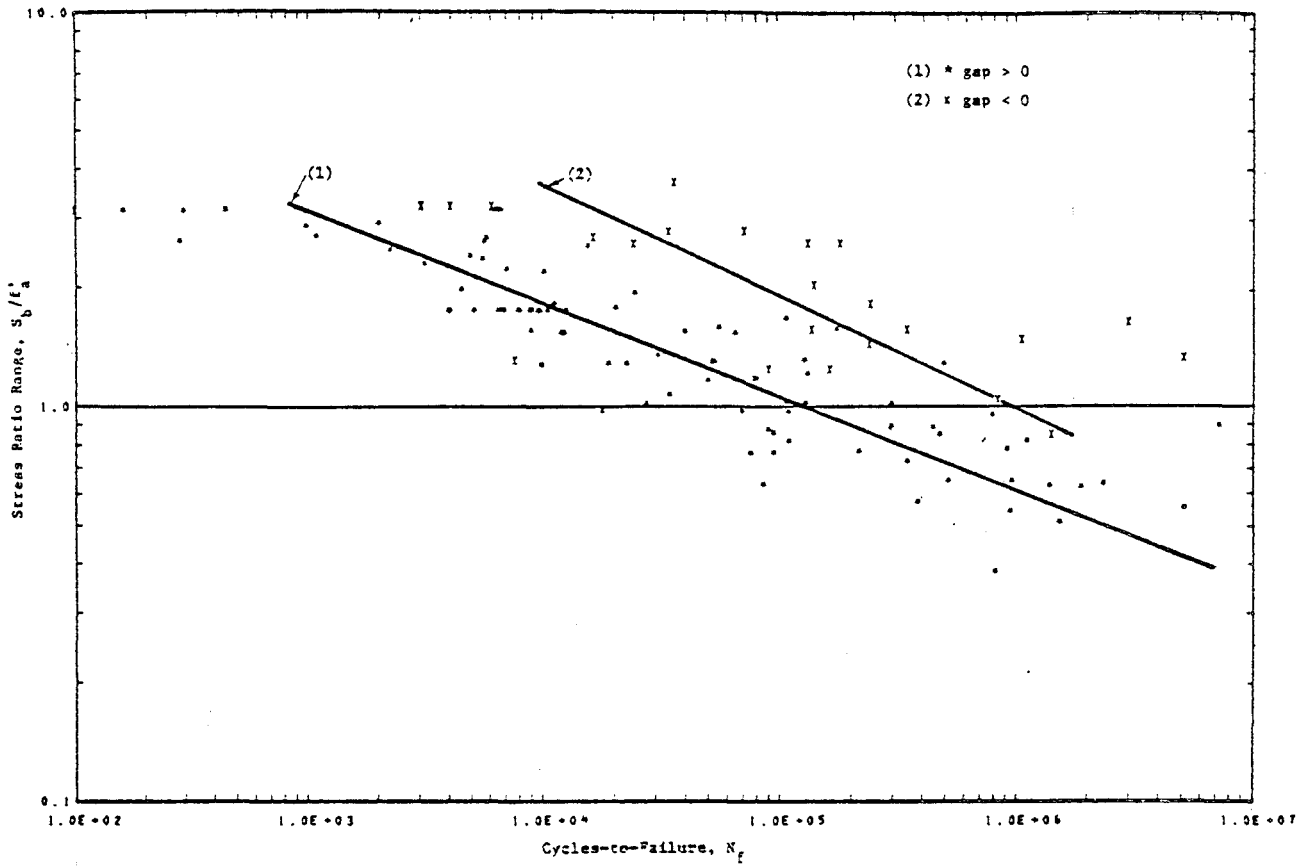


Fig. 9—Evaluation of K-joints as function of stress ratio,  $S_b/f_a$ , overlapping (Gap < 0) and non-overlapping (Gap > 0)  
 ☒ 2. 14

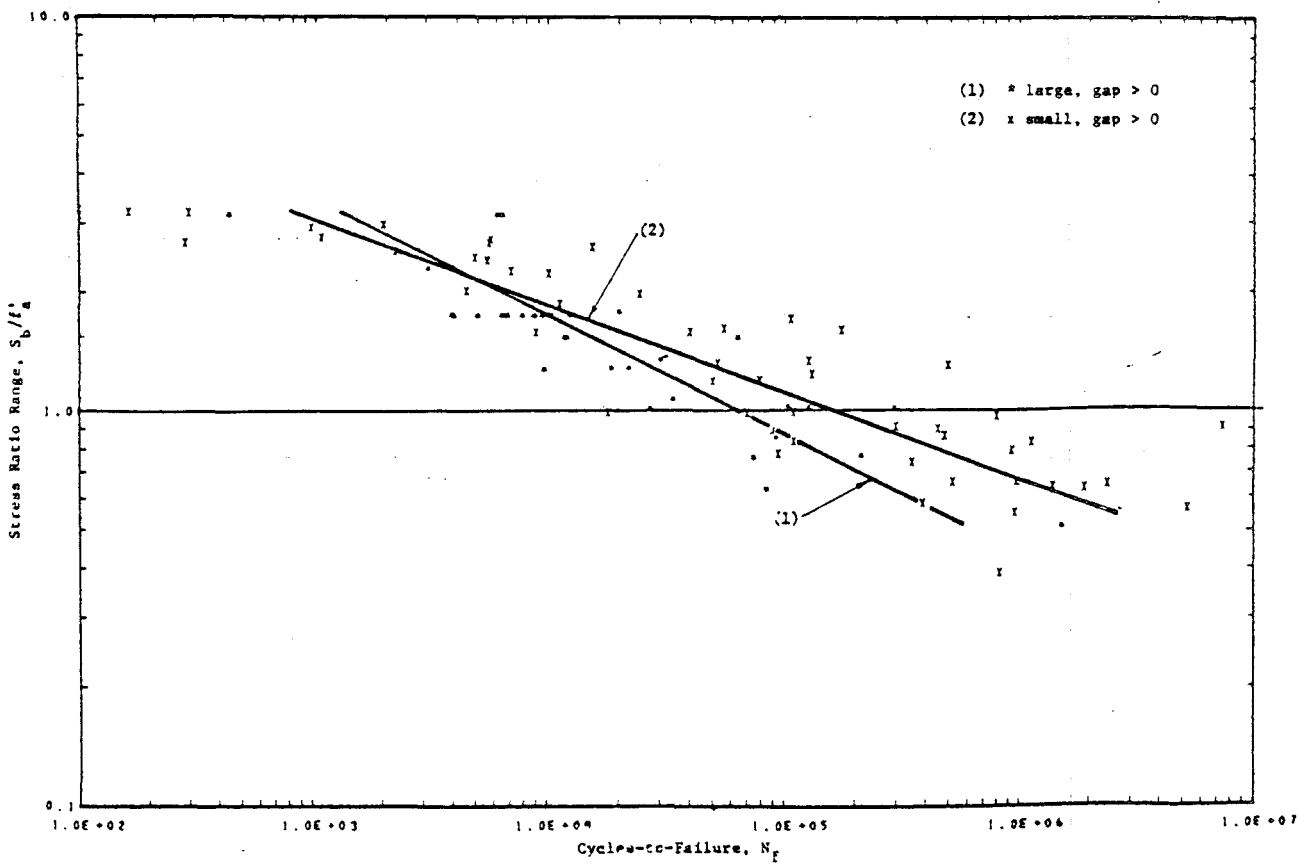


Fig. 10—Evaluation of K-joints as function of stress ratio,  $S_b/f_a$ , all non-overlapping but divided into large and small test specimens  
 ☒ 2. 15

iv) Nf vs iSb

“hot spot stresses” と試験結果との関係を示す。

まず、Kuang 他により開発されMaddoxにより修正された応力集中係数算定式を表 2.11 に示す。

また、疲労試験においてK継手に用いた応力集中係数を表 2.12 に示す。

図 2.16 に表 2.12 に示すMaddox/Kangの式で求めた最大応力集中係数 (maximum S. C. F.)  $i$  に  $S_b$  (ブレースの標準応力範囲) を掛けた “hot spot stresses” と Nf との関係を図示する。

同図にAWS-X-Curve も示してあるが、このAWS-X-Curve に対しては、Nfが大きくなるとAWS-X-Curve は控え目であるが、Nfが小さくなると控え目ではないことが分かる。

この理由は、弾性的に計算した応力範囲より “hot spot stresses” が高い領域では歪の範囲が大きいためであると述べている。

そのため、この領域では弾塑性状態と考える必要がある。

ASME Code, para, NB-3228.3, 原子力プラント部品の設計で簡便な弾塑性解析法の規定があり、図 2.17 にこの方法で計算した曲線、試験結果とAWS X-Curve の比較を示す。

同図からAWS X-Curve はASME failure curveと平行となっていることが分る。



表 2.11

Table 7—Kuang/Maddox<sup>18</sup> Equations for Stress Concentration Factors (S.C.F.)<sup>(a)</sup>

$$S.C.F. = C(2\gamma)^{n_1} \beta^{n_2} \tau^{n_3} (D/L)^{n_4} (g/D)^{n_5} (\sin\theta)^{n_6}$$

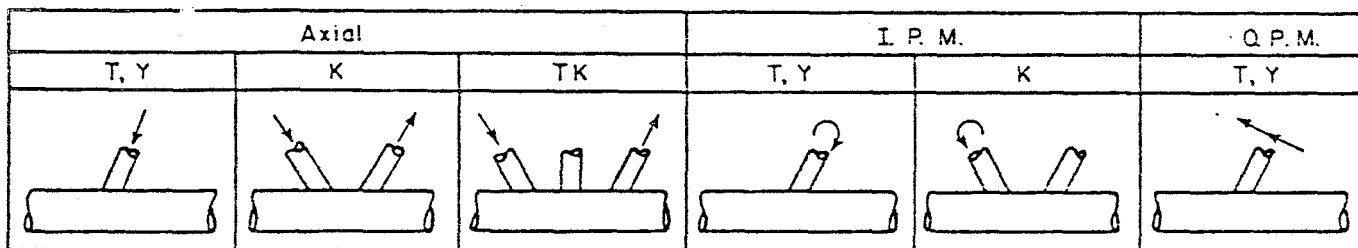
Joint Type	Part <sup>b</sup>	Load <sup>c</sup>	C	n <sub>1</sub>	n <sub>2</sub>	n <sub>3</sub>	n <sub>4</sub>	n <sub>5</sub> <sup>f</sup>	n <sub>6</sub>	Special Limit
T,Y	Chord	Axial	1.177	0.808	d	1.333	-0.057	0	1.694	---
T,Y	Brace	↓	2.784	0.55	e	1.000	-0.12	0	1.94	---
K	Chord	↓	0.949	0.666	-0.059	1.104	0	0.067	1.521	30° < θ < 90°
K	Brace	↓	0.825	0.157	-0.441	0.560	0	0.058	g	30° < θ < 90°
TK	Chord	↓	1.26	0.54	0.12	1.068	0	0	1.00	---
↓	D-Brace	↓	5.65	0.1	-0.36	0.68	0	0.126	0.5	θ < 45°
↓	D-Brace	↓	12.88	0.1	-0.36	0.68	0	0.126	2.88	θ > 45°
↓	N-Brace	↓	4.491	0.123	-0.396	0.672	0	0.159	2.267	---
T,Y	Chord	I.P.M.	0.463	0.6	-0.04	0.86	0	0	0.57	---
T,Y	Brace	↓	1.109	0.23	-0.38	0.38	0	0	0.21	---
K	Chord	↓	1.40	0.38	0.06	0.94	0	0	0.9	---
K	Brace	↓	2.827	0	-0.35	0.35	0	0	0.5	---
T,Y	Chord	O.P.M.	0.465	1.014	0.787	0.889	0	0	1.557	β < 0.55
↓	Chord	↓	0.199	1.014	-0.619	0.889	0	0	1.557	β > 0.55
↓	Brace	↓	0.803	0.852	0.801	0.543	0	0	2.033	β < 0.55
↓	Brace	↓	0.420	0.852	-0.281	0.543	0	0	2.033	β > 0.55

(a) The limits of applicability are stated to be:

$$8.3 < \gamma < 33; 0.3 < \beta < 0.8; 0.2 < \tau < 0.8; 0.01 < g/D < 1.0; 0.05 < D/L < 0.3; 0 < \theta < 90^\circ$$

(b) Part in which stress occurs. For TK joints, D-brace = diagonal brace, N-brace = normal brace

(c) Load:



(d) Replace  $\beta^{n_2}$  with  $EXP(-1.2\beta^3)$

(e) Replace  $\beta^{n_2}$  with  $EXP(-1.35\beta^3)$

(f) For TK joints,  $g = g_1 + g_2$ , where  $g_1$  = gap between one diagonal brace and the normal brace,  $g_2$  = gap between the other diagonal brace and the normal brace.

(g) Replace  $(\sin \theta)^{n_6}$  with  $EXP(1.448 \sin \theta)$

表 2. 1 2

Table 8—Stress Concentration Factors<sup>(a)</sup> for K-Joints Used in Fatigue Tests

Ref. No.	Test Specimens	Chord		Brace	
		$\theta = \theta_h$	$\theta = \theta_d$	$\theta = \theta_h$	$\theta = \theta_d$
5	A	2.42	1.81	4.37*	4.11
	B	2.92	2.18	4.71*	4.43
	C	2.06	1.54	3.95*	3.71
7	D	5.28	3.96	5.78*	5.44
	E1	2.06	1.54	3.95*	3.71
6	E3	5.28	3.96	5.78*	5.44
8	B1, 2, 3	13.37*	11.16	9.38	8.68
	B4, 5, 6	10.81*	9.02	7.80	7.22
7	C1, 2, 3	11.49*	9.59	8.44	7.81
9	F15	6.80*	6.80*	6.48	6.48
9	K15	4.86	4.86	5.37*	5.37*
10	1, 2, 3	6.19*	6.19*	5.94	5.94
	4, 5	5.36	5.36	5.58*	5.58*
	6, 7, 8	6.25*	6.25*	5.44	5.44
	9	5.02*	5.02*	4.95	4.95
	10, 11, 12	6.05*	6.05*	5.02	5.02
	13	4.97*	4.97*	4.61	4.61
	14, 15, 16	5.97*	5.97*	5.61	5.61
17	5.02	5.02	5.29*	5.29*	
11	26, 27, 28	5.04	5.04	5.47*	5.47*
	41/48G	5.23*	5.23*	4.99	4.99
	61, 62, 63	3.14	3.14	4.06*	4.06*
71, 73, 74	2.33	2.33	3.60*	3.60*	
12	JPG	5.55*	5.55*	5.26	5.26
13	L/12	2.30	2.42	4.02	4.22*
14	13,14	2.30	2.42	4.02	4.22*
15	SW-T	2.87	2.87	3.37*	3.37*

(a) These stress concentrations are calculated from the equations shown in Table 7. However, they are adjusted for the brace with  $\theta = \theta_d$  so that the hot spot stress range is always the tabulated S.C.F. times the nominal stress range in the brace with  $\theta = \theta_h$ .

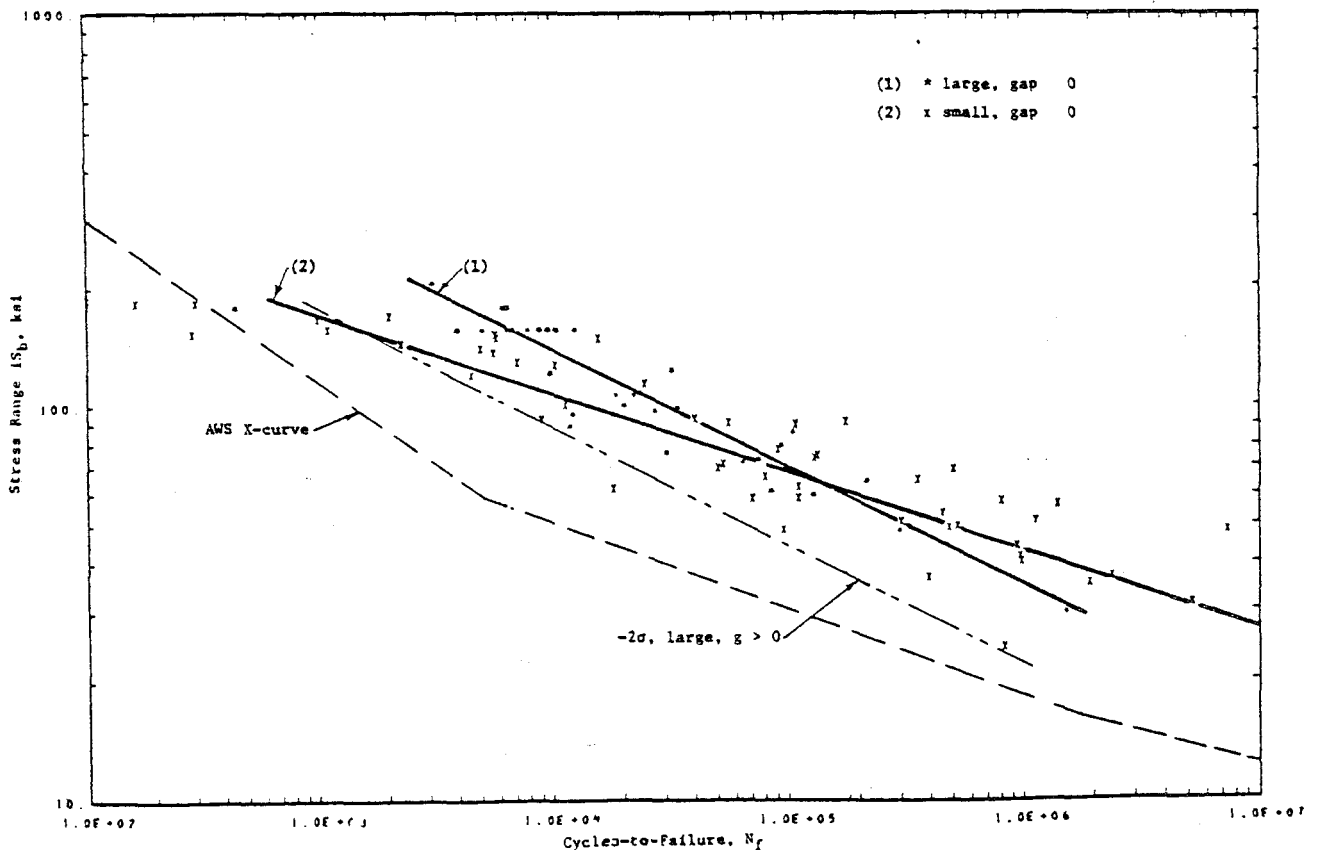


Fig. 11—Comparison of calculated hot spot stresses,  $iS_b$ , with AWS X-curve, K-joints

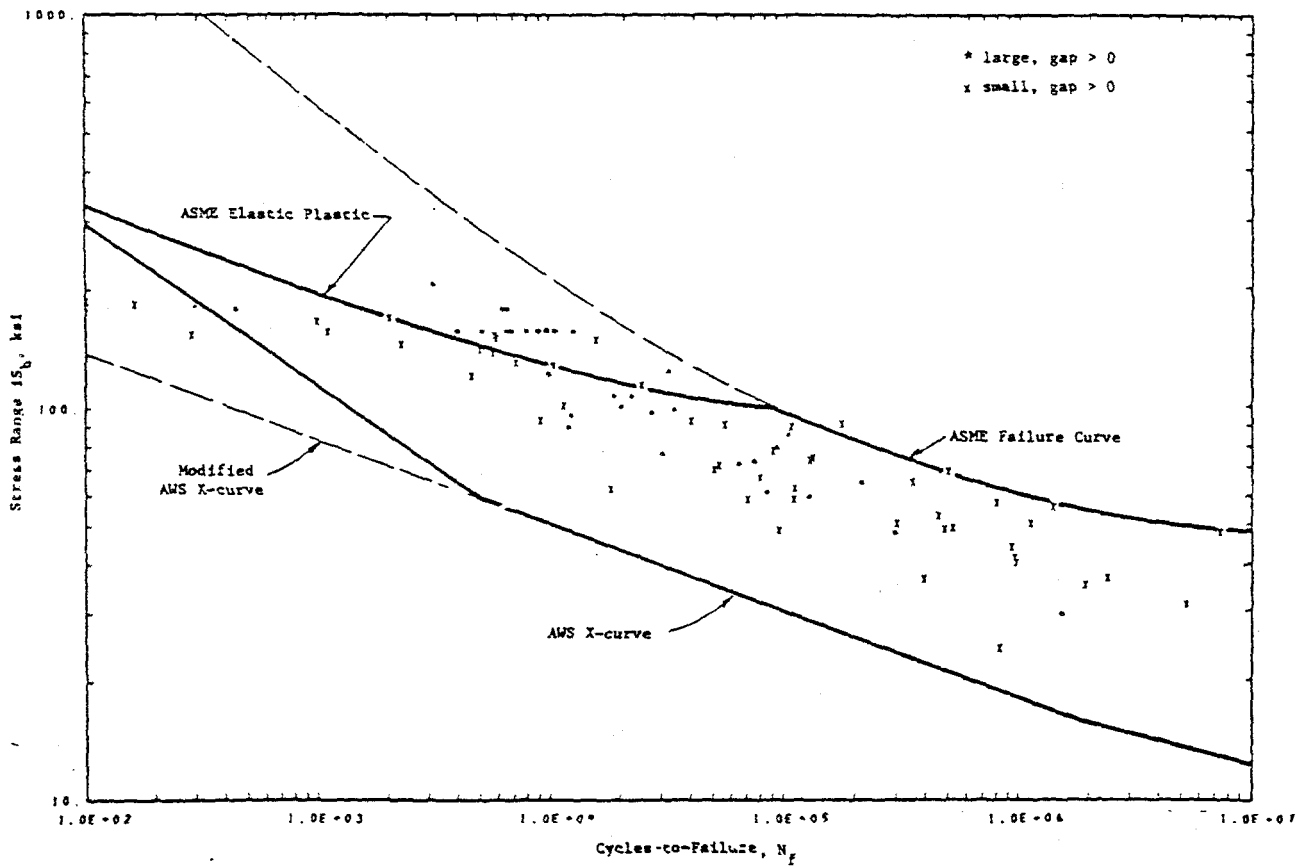


Fig. 13—Comparison of calculated hot spot stresses,  $1S_b$ , with ASME fatigue evaluation method, K-joints X 2. 17

(2) T 継 手

1) 供 試 体

供試体の緒元、寸法パラメータを表 2.13 に示す。

供試体に使用した材料の鋼種および引張試験結果を表 2.14 に示す。

供試体は、予熱、後熱または応力除去はしていない。また、試験前にはクラックの有無の検査はしていない。

表 2.13

Table 10—Dimensional Parameters, T-Joints Used in Fatigue Tests

Ref. No.	Test Specimens	D, in.	$\gamma = D/2T$	$\beta = d/D$	$\tau = c/T$	L/D	$v,^a$ in.
18	SA	2.25	24.5	0.23	0.76	4.0	0.134
	SB		24.5	0.44	1.02	4.0	0.094
	SC		24.5	0.67	1.20	4.0	0.092
	SD		24.5	0.89	1.09	4.0	0.056
	SE		14.6	0.44	0.61	4.0	0.103
19	MG	4.5	10.7	0.53	0.90	4.0	0.33
8	F	8.61	22.8	0.44	1.02	4.1	0.291
	N	8.625	21.3	0.43	0.97	4.1	—
	T	8.625	22.2	0.44	0.97	4.1	5/16
20	L	19.68	19.7	0.40	0.50	5.4	—
15	SW	20.0	20.0	0.54	0.50	3.0	—

(a)  $v$  is the length of the weld leg measured from the outside surface of the brace to the toe of the weld at the chord surface.

表 2.14

Table 11—Materials, T-Joints Used in Fatigue Tests

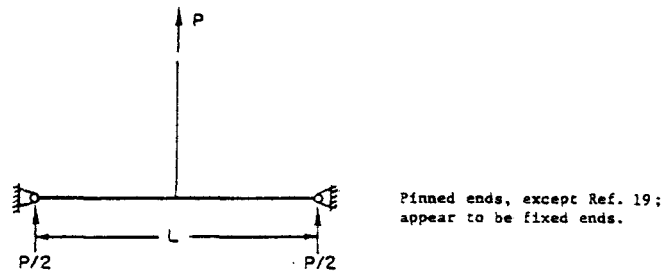
Ref. No.	Test Specimens	Material	Measured Tensile Properties					
			$F_y, \text{ ksi}$		$F_u, \text{ ksi}$		El., %	
			Chord	Brace	Chord	Brace	Chord	Brace
18	All	—	37/49	45/58	47/55	51/61	44/62	31/50
19	MG	BS 4360, Gr. 43C	40/50		62/72		20/34	
8	F	API 5L	63.5	63.0	71.5	79.6	19	17
	N	Gr. B	60.0	63.0	71.0	79.6	18	17
	T	—	50.5	88.0	62.0	101.0	27	16
20	L	—	—	—	—	—	—	—
15 <sup>a</sup>	SW-1	(a)	—	—	—	—	—	—

(a) ASTM A-36 for chord, ASTM A53 Grade B for brace.

2) 試験方法

図 2.18 にすべての試験の荷重載荷要領を示す。

この試験では、主管に曲げ応力が発生し、この曲げ応力と支管の標準軸応力の比も図 2.18 に示す。



Ref. No.	Specimens	L, in.	$f_b/S_b^a$	Loading Rate, cpm
18	SA	9.0	0.683	1800
	SB, SBP		1.841	
	SC		3.266	
	SD		4.007	
	SE		1.147	
19	MG	18.0	1.023	900
8	F	35.0	1.833	—
	N		1.733	—
	T		1.738	200
20	L	107. <sup>b</sup>	1.136	—
15	SW-1	60.	0.849	—

(a)  $f_b$  = nominal bending stress at center of chord =  $PL/4Z$ , for all except Ref. 19

$$Z = (\pi/32)(D^4 - D_1^4)/D$$

$$D_1 = D - 2T$$

$$f_b/S_b = 8LD(d-c)t/(D^4 - D_1^4); \text{ for Ref. 19, use 4 instead of 8}$$

(b) Length between pins was somewhat longer: perhaps 15% longer judging by scaling of drawing.

Fig. 14—Loadings on T-joints in fatigue tests

図 2.18

すべての試験は荷重制御である。これは実際の海洋構造物の継手に対しては、クラック進展速度は過大評価で、破壊にいたる繰返し数に対し過少評価となる。

(3) 試験結果

表 2.15 に試験結果を示す。クラック発生の定義は引用文献毎に表 2.16 に示す。

表 2.16

Table 12—Definitions of "Crack Initiation," T-Joint Fatigue Tests

Ref. No.	Test Specimens	Definition of "Crack Initiation"
18	All	Chord filled with kerosene, kerosene leakage
19	MG	Chord pressurized with air at 20 psi. Air leakage caused pressure drop (of some unscated amount) which shut down test.
8	F	Visual, magnifying glass
	N	Not scated
	T	"Inspection"
20 <sup>d</sup>	L	"Crack started at the hot spot attains about 20 mm."
15	SW-1	"Crack noted on first inspection"

(a) Ref. 20 also gives values of  $N^*$ , where  $N^*$  is the "number of cycles when the strain amplitude starts to drop at the measured point closest to the hot spot." These cycles are 600, 3100, 12,000, and 70,000 for specimens L-1, L-2, L-3, and L-4, respectively.

破壊の定義についてはK・継手と同様である。表 2.17 に破壊位置を示す。

表 2.17

Table 13—Failure Locations, T-Joint Fatigue Tests

Ref. No.	Test Specimens	Description of Failure Locations
18	All	"The fatigue cracks in most specimens initiated at the points of stress concentration near the toe of the welds at the center section of the chord. In general, there exist two points of peak stress concentration in each T-joint, 180° apart. The first crack was found at either one of these points. As the number of cycles increased, the second crack developed at the other point of stress concentration. Most of the cracks propagated along the toe of the welds. When the first and second cracks extended to a certain length, a portion of the chord wall at the crown was suddenly torn." (Failure is defined as complete separation of chord from brace.)
19	MG	None given except by the sentence: "Some of the initial tests were restarted after recording the cycles to the first through-crack and attempts were made to measure the length of the crack as it grew around the weld toe toward the crown."
8	75N	None given.
	T	"The fatigue cracks in all T-joints initiated at the point of stress concentration $S_0$ ." The location of $S_0$ is not identified.
20	L	None given.
15	SW-1	Photographs indicate cracks initiated at toe of weld in chord wall, propagated around the brace until, at final failure, the chord wall was severed all around.



i)  $N_f$  vs  $V_p$  or  $V_p'$

図 2.19 に  $N_f$  と  $V_p$  (Punching shear Stress Range) との関係を図示する。

同図で small は、主管の直径が 4.5in (11.43cm) 以下、large は主管の直径が 8.625 in (22cm) 以上の供試体を示す。

表 2.18 に図 2.19 に示した 2 つの直線の係数を示す。

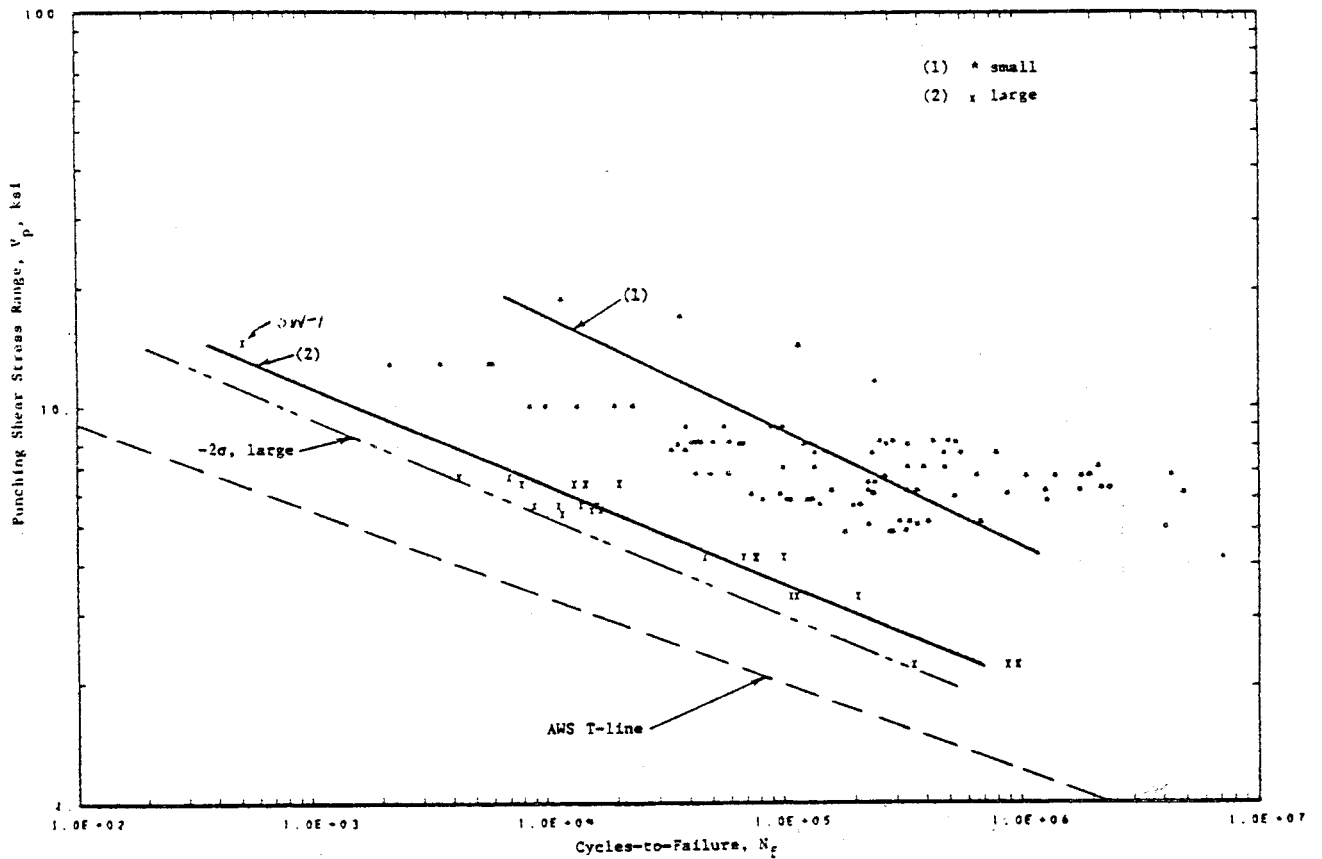


Fig. 15—Comparison of  $V_p$  vs  $N_f$  with AWS T-line

図 2.19

$V_p$  の値は、API Fig 2.22-1 により求めたものである。

図 2.19 で small と large に大きな差が生じているのは、1 つには表 2.15 に示す供試体のパラメータによるもの以外に  $V_p$  の計算方法にもある。

API の規定によれば、パンチングシャーの面積は  $\pi (d - t) T$  であるが実際は最小  $\pi d T$  と考えられる。

また、破壊の発生位置は溶接止端部であることから、パンチングシャー面積は  $\pi (d + 2w) T$  に近い値と考えられる。ここで  $W$  は表 2.15 に示した値で隅肉溶接の脚長である。したがって、小さな試験体ほど実質的なパンチングシャー面積が増加して



いるからである。

この溶接ビード部の面積を考慮したパンチングシヤー応力  $V_p'$  を用いて試験結果をプロットした結果を図 2.20 に示す。

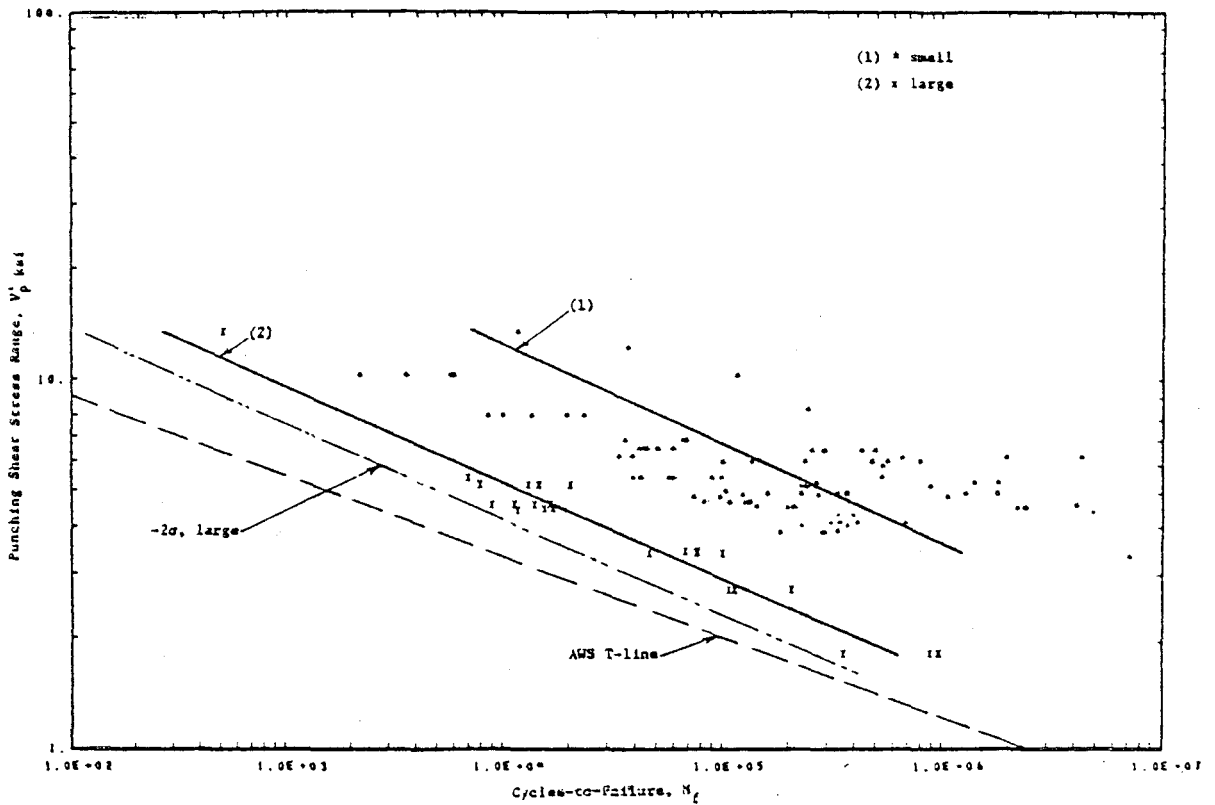


Fig. 16—Comparison of  $V_p'$  (shear area at weld toe) versus  $N_f$  with AWS T-line

図 2.20

表 2.18

Table 14—Summary of Correlation Equations, Fatigue Tests of T-Joints

Cycles	Stress	No. of Tests	Group	c	n	$\sigma$	Fig.
$N_f$	$V_p$	98	small	1.70E8	-3.44186	0.5474	15
		24	large	1.65E7	-4.00810	0.1701	
$N_f$	$V_p'$	98	small	1.12E8	-3.69246	0.5366	16
		24	large	6.06E6	-3.86319	0.1807	
$N_i$	$V_p$	94	small	3.95E7	-3.01787	0.6226	17
		25	large	1.15E7	-4.27409	0.2506	
$N_f$	$V_p$	26	SB, R = -1	1.39E10	-5.89641	0.2831	18
		24	SB, R ≠ -1	2.71E8	-4.28608	0.1682	
$N_f$	$S_b/f_a'$	98	small	7.44E5	-4.56297	0.3696	19
		24	large	2.32E4	-4.13690	0.1640	
$N_f$	$1S_b$	98	small	1.04E14	-3.94736	0.3809	20
		24	large	2.36E13	-4.30998	0.1644	

図 2.20 で small と large との差は図 2.19 より少なくなっているが、まだ大きな差がある。

この原因は主管と枝管のスムーズな形状変化、残留応力、溶接の輪廓、アンダーカットや施工中のトウクラックや材料等であると考えられる。

しかし、AWS T-Line は large グループの 26 (97.7%非破壊確率) 線よりかなり低い側に位置しており、図 2.12 において AWS K-Line は large グループの  $-2\sigma$  線とほぼ一致していることと対比して、AWS T-Line は K-Line より安全側に定められた設計線図といえる。

## ii) $N_i$ vs $V_p$

$N_i$  (クラックの発生) の定義は表 2.16 に示したが、大部分はかなり大きなクラックを定義している。

図 2.21 に  $N_i$  と  $V_p$  との関係を示す。

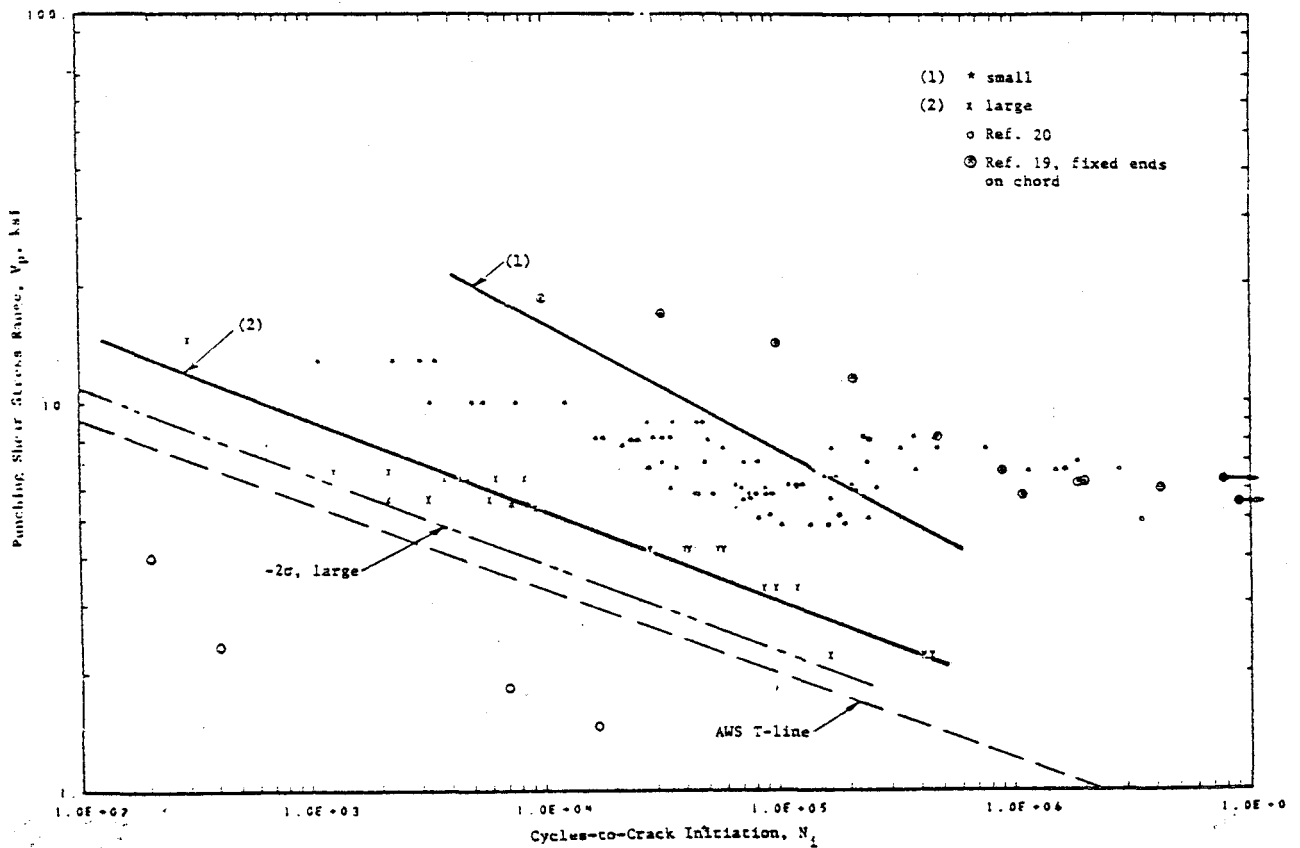


Fig. 17—Comparison of  $V_p$  vs  $N_i$  (crack initiation) with AWS T-line

図 2.21

図 2.21 の AWS T-Lineはクラック発生に関しても安全側であることを示している。  
 また、同図でも small と large の差はかなり大きい。

iii) 応力比の効果

図 2.22 に Ref 18 の SB シリーズにおいて  $R = S_b(\min) / S_b(\max) = -1$   
 と  $R \neq -1$  の 2 つに分け試験データをプロットする。

$R = -1$  は完全両振り荷重であることを示す。

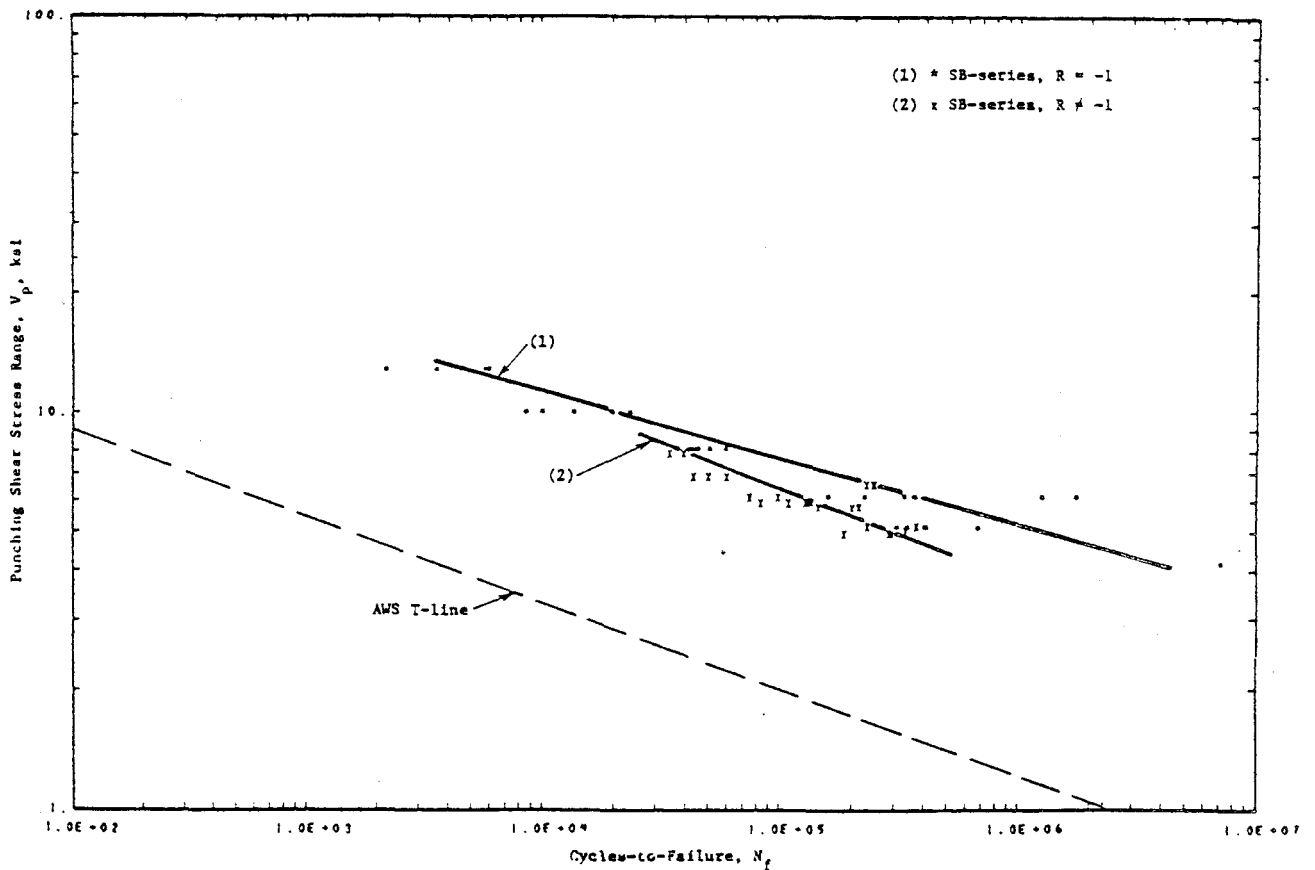


Fig. 18—Indication of stress ratio effect

図 2.22

同図から  $R \neq -1$  の場合、若干、疲労寿命が短くなる傾向があることが分かる。しかし  $R \neq -1$  と  $R = -1$  との差は少ない。

iv)  $N_f$  vs  $S_b/f_a$

$S_b$ はT継手の項で説明したように API RP2A , Par 2.22c に規定されている静的許容荷重である。

図 2.23 は  $S_b/f_a$  と  $N_f$ の関係で試験結果をプロットしたものである。

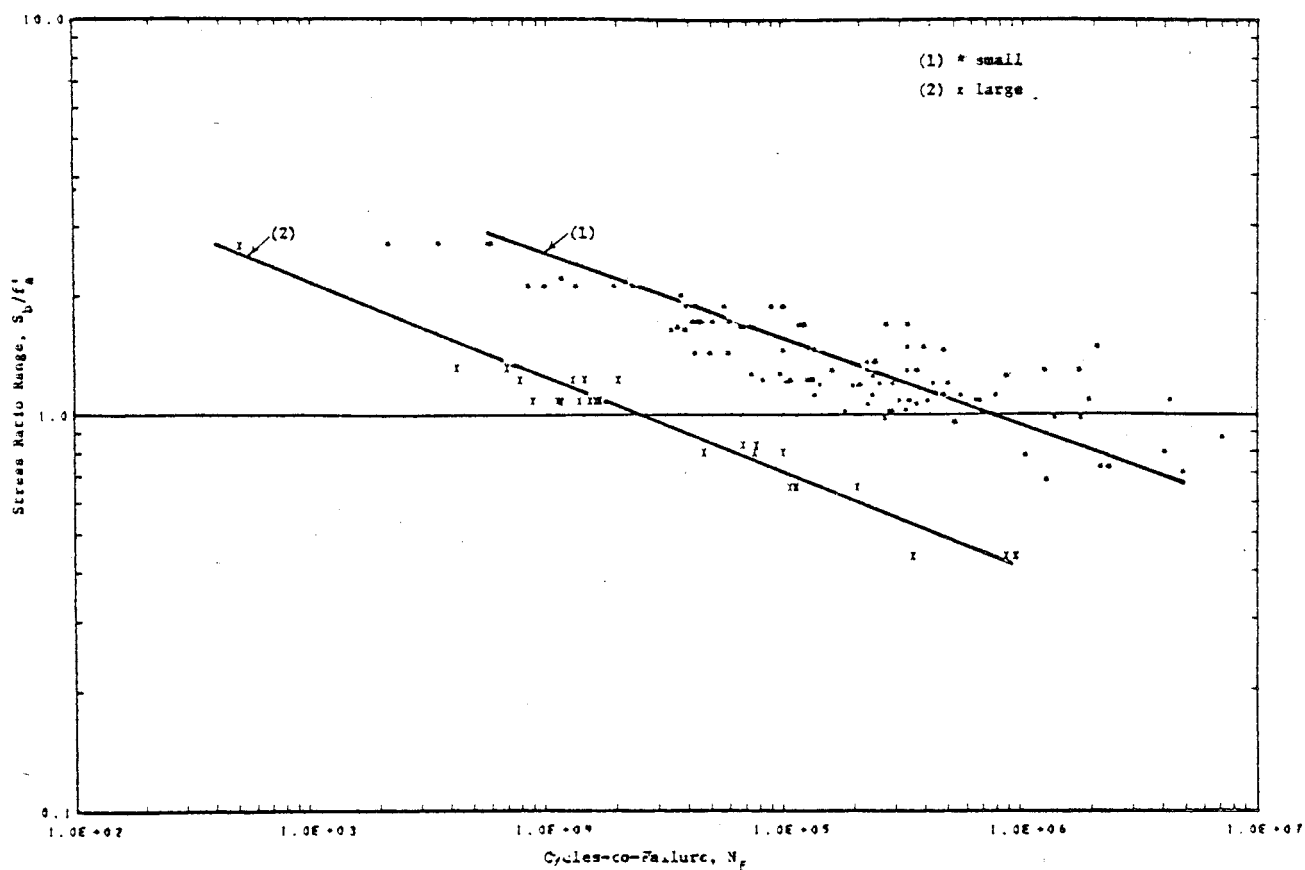


Fig. 19—Evaluation of T-joints as function of stress ratio,  $S_b/f_a$

図 2.23

図 2.23 の直線の定数は表 2.18 に示すが、 $N_f$  vs  $V_p$  と  $N_f$  vs  $(S_b/f_a)$  との標準偏差  $\sigma$  を比較し、 $N_f$  vs  $(S_b/f_a)$  の方が小さく試験結果のバラツキが小さいことが分る。

v)  $N_f$  vs  $iS_b$

ここでは試験結果を“hot spot stresses”で評価す。

応力集中係数は、K継手と同様表 2.11 に示したKuang / Maddoxの式を用いる。

T継手の応力集中係数を表 2.19 に示す。

図 2.24 に“hot spot stresses”  $iS_b$  と  $N_f$  との関係で試験結果をプロットする。

表 2.19

Table 15—Stress Concentration Factors<sup>(a)</sup> for T-Joints  
Used in Fatigue Tests

Ref. No.	Test Specimens	S.C.F.	
		Chord	Brace
18	SA	20.2	20.9*
	SB	27.3*	25.4
	SC	26.3*	22.4
	SD	14.2*	11.8
	SE	9.08	11.4*
19	MG	11.1	13.1*
8	F	25.8*	24.4
	N	22.9*	22.4
	T	23.8*	23.0
20	L	9.27	11.8*
15	SW	8.13	9.80*

(a) These stress concentration factors are calculated from the equations in Table 7. The hot spot stress range is equal to the tabulated S.C.F. times the nominal stress range in the brace.

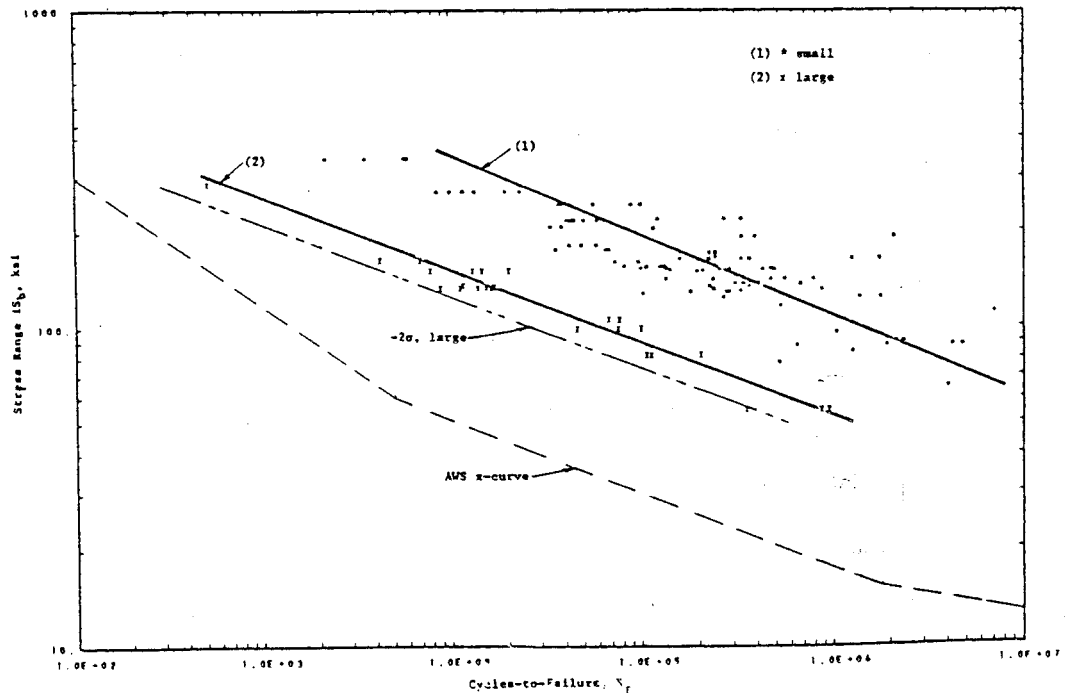


Fig. 20—Comparison of calculated hot spot stresses,  $iS_b$ , with AWS X-curve, T-joints

図 2.24

図2.25に応力範囲とNfの関係を示す。

Small と large との差は大きく Kuang / Maddoxの応力集中係数はその差を説明することはできないことが分かる。

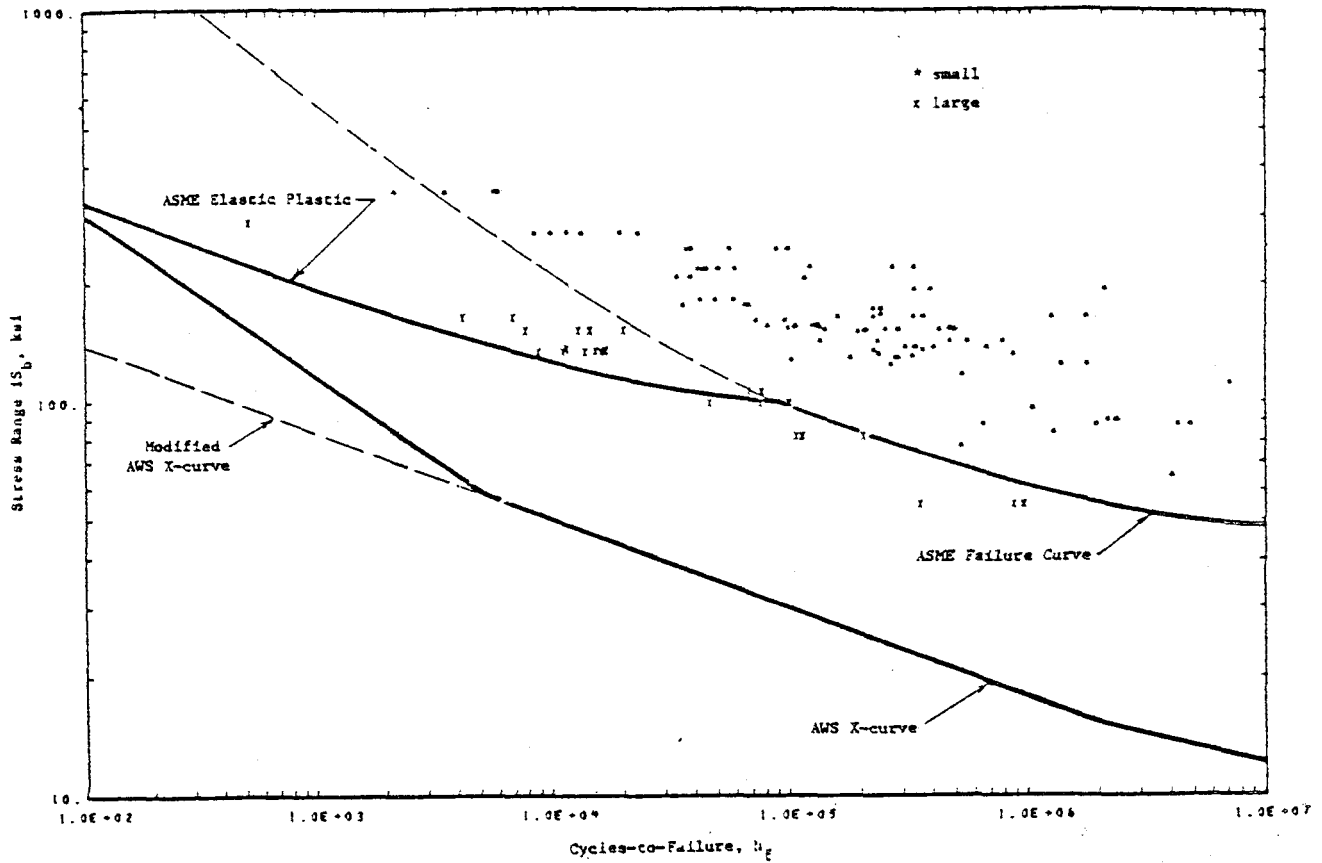


Fig. 21—Comparison of calculated hot spot stresses,  $iS_b$ , with ASME fatigue evaluation method, T-joints

図2.25

図2.24, 図2.25から Kuang / Maddoxの応力集中係数は安全側であることを示している。

## References

1. American Welding Society, Section 10 of D1.1-1975, "Design of New Tubular Structures."
2. American Petroleum Institute, API RP2A, 7th Ed., Jan. 1976 "Recommended Practice for Planning, Designing, and Constructing Fixed Offshore Platforms."
3. American Society of Mechanical Engineers, Boiler and Pressure Vessel Code, Section III—Div. 1, Nuclear Power Plant Components, 1977 Ed.
4. American National Standard Code for Pressure Piping, ANSI B31.3-1976, "Chemical Plant and Petroleum Refinery Piping."
5. Mukhopadhyay, A., Itoh, Y., and Bouwkamp, J. G., "Fatigue Behavior of Tubular Joints in Offshore Structures," Seventh Annual Offshore Technology Conference, May 1975, OTC Paper No. 2207.
6. Bouwkamp, J. G., "Tubular Joints Under Slow-Cycle Alternating Loads," Proceedings of the International Symposium on the Effects of Repeated Loading of Materials and Structures, International Union of Testing and Research Labs for Materials and Structures, RILEM, Mexico City, Vol. VI, pp. 1-31 (Sept. 15-17, 1966).
7. Toprac, A. A., "Review of Research, Tubular Connections Investigations in U.S.A., Static, Fatigue, Analysis," Austin, Texas (May 1969).
8. Toprac, A. A. and Louis, B. G., "The Fatigue Behavior of Tubular Connections," Structures Fatigue Research Laboratory, Department of Civil Engineering, The University of Texas, S. F. R. L. Tech. Rpt. P550-13, Austin, Texas, (May 1970).
9. Kurobane, Y., Makino, Y., and Sagawa, M., "Low Cycle Fatigue Research on Tubular K-joints," Memoirs of the Faculty of Engineering, Kumamoto University, Kumamoto, Japan, Vol. XVI, No. 2, May 1970.
10. Kurobane, Y. and Konomi, M., "Fatigue Strength of Tubular K-Joints," IIW Doc. XV-340-73, Feb. 1973.
11. Maeda, T., Uchino, K., and Sakurai, H., "Experimental Study on the Fatigue Strength of Welded Tubular K-Joints," July 1969, IIW Doc. No. XV-269-69.
12. Uchino, K., Sakurai, H., and Sugiyama, S., "Experimental Study on the Fatigue of Welded Tubular K-Joints, 2nd Report Influences of the Joint Eccentricity on the Fatigue Strength," Sept. 1973, IIW Doc. No. XV-344-73 and XIII-690-73.
13. Bouwkamp, J. G., Offshore Development Engineering, Inc., "Cyclic Loading of Full-Size Tubular Joints," presented at the Eighth Annual Offshore Technology Conference, Houston, Texas (May 3-6, 1976) Preprint No. OTC 2605.
14. Peterson, M. L., "Fatigue Tests of Two Full-Scale K-Joints for Off-shore Structures," CONOCO Research Report No. 106-3-4-1-73, Nov. 1973. (Confidential—not releasable by Battelle).
15. Grigory, S. C., "A Study to Develop a Design Procedure for Analysis of Plastic Fatigue Life of Tubular Joints on Offshore Structures," Shell Development Co., Houston, Texas, Final Report on SwRI Project No. 30-1882 (May 23, 1969).
16. Kuang, J. G., Potvin, A. B., and Leick, R. D., "Stress Concentration in Tubular Joints," Seventh Annual Offshore Technology Conference, 1975, OTC Paper No. 2205. A private communication from N. R. Maddox to E. C. Rodabaugh, March 15, 1977, states seven of the formulas presented in Table 2 of OTC 2205 have been modified. The modified equations are contained in Table 7 herein.
17. Criteria of the ASME Boiler and Pressure Vessel Code for Design by Analysis in Sections III and VIII—Division 2, 1969, Published by the American Society of Mechanical Engineers, 345 E. 47th St., New York, NY 10017.
18. Kurobane, Y., Natorajan, M., and Toprac, A. A., "Fatigue Tests of Tubular T-Joints," Nov. 1967, Structures Fatigue Research Laboratory, Univ. of Texas, Austin, Texas.
19. Martin, T. and McGregor, J., National Engineering Laboratory, Scotland, "An Investigation into the Stress Distribution and Fatigue Strength of a Welded Tubular T-Joint," Ninth Annual Offshore Technology Conference May 1977, OTC Paper No. 2856.
20. Yoshida, K., Inui, T., and Iida, K., "Behavior Analysis and Crack Initiation Prediction of Tubular T-Connections," Ninth Annual Offshore Technology Conference, May 1977, OTC Paper No. 2854.
21. Bouwkamp, J. G., Univ. of California, "Behavior of Tubular Gusset-Plate Joints," presented at the Fifth Annual Offshore Technology Conference, Houston, Texas (April 29-May 2, 1973) Preprint No. OTC 1821.
22. Markl, A. R. C., "Fatigue Tests of Piping Components," Trans. ASME, 1952.
23. Maeda, T., Uchino, K., and Sakurai, H., "Experimental Study on the Fatigue Strength of Welded Tubular T- and X-Joints," IIW Doc. XV-270-69, July 1969.
24. Maeda, T., Uchino, K., and Sakurai, H., "Experimental Study of the Fatigue Strength of Welded Tubular X-joints With and Without Stiffener Rings," Supplement to IIW Document XV-270-69, July 1970.
25. Matoba, M., Teramoto, S., Kawasaki, T., and Kaminokado, S., "Fatigue Strength of Welded Tubular Joints With Various Stiffeners in Offshore Structures," IIW Doc. XIII-687-73A (1974).

## 2.4 ヨーロッパ

### (1) 概 説

鋼管継手の疲労強度について広範囲でしかも系統的な研究がECSC (European Coal and Steel Community) で行われている。ここではその成果を紹介する。

この研究は、英国のOffshore steel Research Project として行われ鋼管継手に関する多くの研究プログラムが含まれている。

また、この研究はオランダ、イタリア、フランスおよびノルウェーとの協力の下に行われている。

ドイツで行われた研究成果も紹介してあるが、これは上記の共同研究とは別である。

図 2.26 に供試体の形状とサイズと国別の範囲を示す。

供試体に使用した鋼材はEuronorm 25-75, Fe 510 DD の鋼板または相当品である。

また、実験結果を統一的に整理するため以下に示す 4 段階に破壊のレベルに分け報告するようにしている。

N<sub>1</sub> : 15% reduction in strain-gauge measurements

N<sub>2</sub> : first crack observation

N<sub>3</sub> : crack through chord wall

N<sub>4</sub> : end of test

試験結果の表にはN<sub>2</sub>, N<sub>3</sub> と N<sub>4</sub> が示してある。

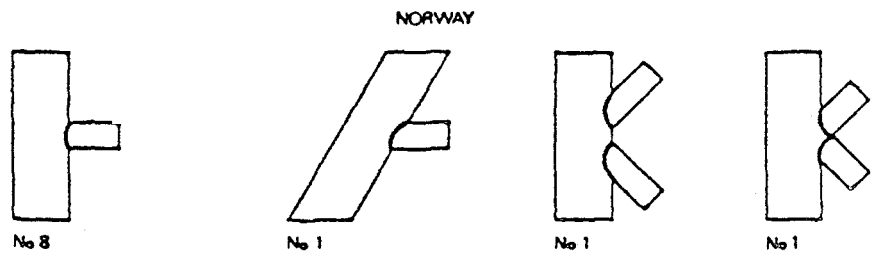
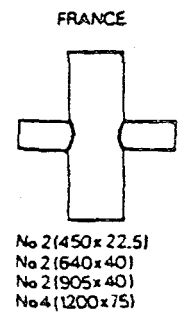
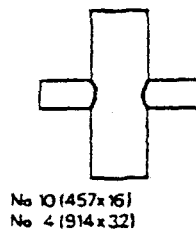
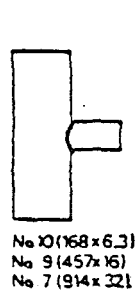
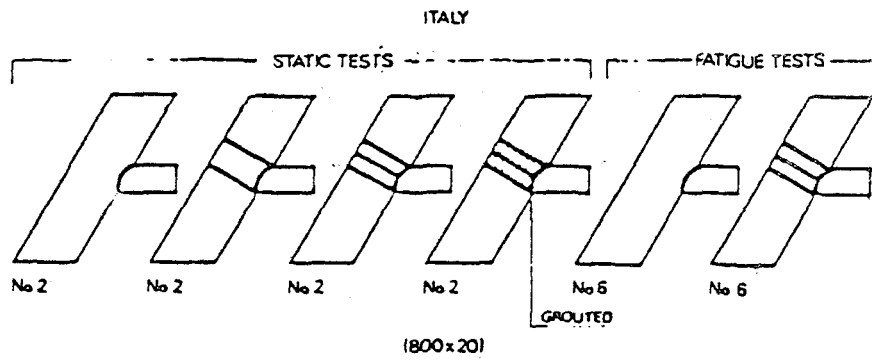
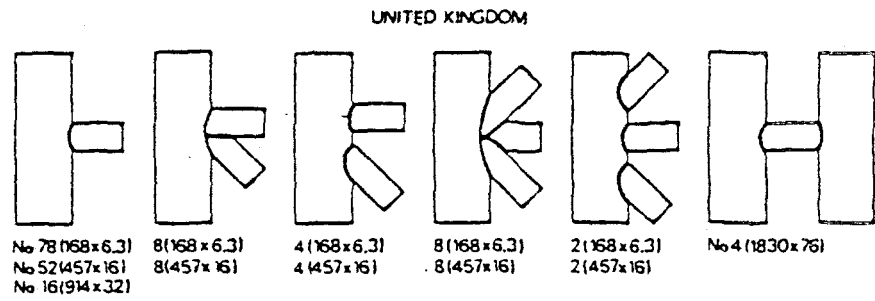
また、最大局部応力範囲 (maximum local stress range) は、図 2.27 に示すように A, B 点の測定結果から外挿法で求めている。

また、図 2.27 には A.W.S, B.S.I. のhot spot stress の定義も合わせて示す。

表 2.20 ~ 表 2.24 に各国の試験概要を示す。



Fig. 1 - Types of nodes tested



(508x16)

☒ 2. 2 6

Definition of hot-spot stress

A.W.S. - Total range of worst hot-spot stress or strain on the outside surface of intersecting members at the toe of the weld joining them - measured after shakedown in model or prototype connection or calculated with best available theory.

B.S.I. - For each configuration where stress concentration is involved, the magnitude of hot-spot stress or strain should be determined accurately by measurements on models or full-scale assemblies or photo-elastic investigation. The stress ranges used should be those which are as near as possible to the connection without being influenced by the weld profile.

Experimentale determination of SNCF

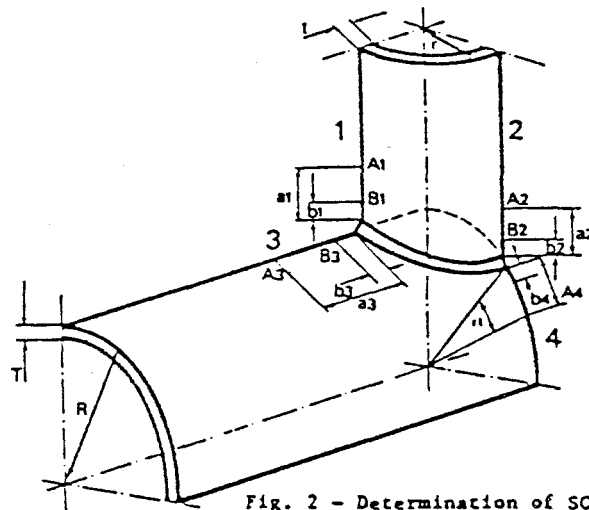


Fig. 2 - Determination of SCF (SNCF)

SNCF is obtained extrapolating linearly to the weldtoe, measurements of strain gauges located in points A and B.

$$a_1 = a_2 = 0.65 \sqrt{rt}$$

$$a_3 = 0.4 \sqrt[4]{(rt) (RT)}$$

$$\alpha = 5^\circ$$

$$b_1 = b_2 = b_3 = b_4 = 0.2 \sqrt{rt} \quad \text{but not less than 4 mm}$$

図 2.27 最大局部応力 ( hot Spot stress ) の定義

表 2.20

Table 1 - United Kingdom

SPECIMEN	D - I	$\beta$	$\bar{z}$	TYPE	R	TEST	
						FREQUENCY Hz	LOADING
17/1-2-4	168-6.3	1	1	T	-1	5410	AX
17/2-12	168-6.3	1	1	T	-1	5410	AX + Comp.
17/6-7-8	168-6.3	1	1	T	-1	10415	IPB
17/9-10-11	168-6.3	1	1	T	-1	10415	IPB + Comp.
18/1-5-7-8-9-12-15	168-6.3	1	0.71	T	-1	5410	AX
18/2-11	168-6.3	1	0.71	T	-1	5410	AX + Comp.
18/4-6-10-13-14-16	168-6.3	1	0.71	T	-1	10415	IPB
19/1-2-3	168-6.3	0.53	0.86	T	-1	5410	AX
19/4-5	168-6.3	0.53	0.86	T	-1	5410	AX + Comp.
19/11-12-13	168-6.3	0.53	0.86	T	-1	10415	IPB
20/4-10-11	168-6.3	0.53	0.51	T	-1	5410	AX
20/1-8	168-6.3	0.53	0.51	T	-1	5410	AX + Comp.
20/2-5-6	168-6.3	0.53	0.51	T	-1	10415	IPB
37/3-5-9	457-16	1	1	T	-1	2	AX
37/1-7-13	457-16	1	1	T	-1	24.4	IPB
37/8-10-12	457-16	1	1	T	-1	24.4	IPB + Comp.
38/4-5-8	457-16	1	0.55	T	-1	2	AX
38/1-7	457-16	1	0.55	T	-1	24.4	AX + Comp.
38/2-3-6	457-16	1	0.55	T	-1	24.4	IPB
39/4-5	457-16	0.25	0.39	T	-1	44.6	AX
39/6-7	457-16	0.25	0.39	T	-1	44.6	AX + Comp.
39/1-2-3	457-16	0.25	0.39	T	-1	44.6	IPB
40/12	457-16	0.25	0.28	T	-1	44.6	AX
40/3-4-5	457-16	0.25	0.28	T	-1	44.6	IPB
E1/B-C	914-32	0.5	1	T	-1	24.4	AX
E1/A-D	914-32	0.5	1	T	-1	24.4	IPB
E2/B-C	914-32	0.5	0.275	T	-1	24.4	AX
E2/A-D	914-32	0.5	0.275	T	-1	24.4	IPB
F1/A-B	914-32	0.24	0.5	T	-1	24.4	AX
F1/C-D	914-32	0.24	0.5	T	-1	24.4	IPB
F2/C-D	914-32	0.24	0.25	T	-1	24.4	AX
F2/A-B	914-32	0.24	0.25	T	-1	24.4	IPB
H 20	1830-76	0.5	0.5	H	-1	1	AX
H 21	1830-76	0.5	0.5	H	-1	3	IPB
H 22	1830-76	0.25	0.25	H	-1	1	AX
H 23	1830-76	0.25	0.25	H	-1	3	IPB

AX = Axial load in brace  
 IPB = In plane bending of brace  
 Comp. = Compressive load in chord

表 2. 2 1

Table 2 - Holland

SPECIMEN	D - T	$\beta$	$\bar{z}$	TYPE	R	TEST	
						FREQUENCY Hz	LOADING
1-2-3	168- 6.3	0.5	0.5	T	0	10	Axial load in brace
4 (1)	457-16	0.5	0.5	T	0	0.2	" " " "
5-6-7-9	457-16	0.5	0.5	T	0	4	" " " "
8	457-16	0.5	0.5	T	0	5	" " " "
10 (1)	457-16	0.5	0.5	T	-1	0.2	" " " "
11	457-16	0.25	0.39	T	-1	8	" " " "
12	457-16	0.25	0.39	T	-1	5	" " " "
13-15	914-32	0.5	0.5	T	0	2.8	" " " "
14	914-32	0.5	0.5	T	0	1.5	" " " "
16-17 (1)	914-32	0.5	0.5	T	0	0.2	" " " "
18-19-(2)	168- 6.3	0.5	0.5	T	0	10	" " " "
20 (2)	914-32	0.5	0.5	T	0	2.5	" " " "
21 (2)	914-32	0.5	0.5	T	0	4	" " " "
22-23 (3)	168- 6.3	0.5	0.5	T	0	10	" " " "
24-25-26	168- 6.3	0.5	0.5	T	0	10	In plane bending
28	457-16	1	1	X	-1	1.3	Axial load in brace
27-29	457-16	1	1	X	-1	2	" " " "
30-33	457-16	1	0.5	X	-1	2	" " " "
37-38	457-16	1	0.5	X	-1	3	" " " "
31-32 (4)	457-16	1	0.5	X	-1	-	" " " "
34	914-32	0.5	0.5	X	0	8	" " " "
35	914-32	0.5	0.5	X	0	3	" " " "
36 (5)	457-16	1	0.5	X	-1	3	" " " "
39 (2)	914-32	0.5	0.5	X	0	6	" " " "
40 (2)	914-32	0.5	0.5	X	0	3	" " " "

- (1) Seawater test
- (2) One additional unloaded brace
- (3) Two additional unloaded braces
- (4) Random test
- (5) Axial load in chord

表 2. 2 2

Table 3 - Italy

SPECIMEN	TEST					
	D - T	800 - 20	TYPE	FREQUENCY Hz	LOADING	REMARKS
		0.46				
		1				
III A	Y	Static test		Axial tension in brace	Unstiffened node	
II A	Y	" "		" compression in brace	" "	
I B	Y	" "		" tension in brace	2 internal stiffeners	
IV B	Y	" "		" compression in brace	" " "	
IV A	Y	" "		" tension in brace	3 " "	
III B	Y	" "		" compression in brace	" " "	
I A	Y	" "		" tension in brace	3 int. stiffeners + concrete	
II B	Y	" "		" compression in brace	" " " "	
II E - IV C	Y	0.5		High axial load in brace	Unstiffened nodes	
I D - III D	Y	0.5		Medium axial load in brace	" "	
II C - IV D	Y	0.5		Low axial load in brace	" "	
III E - IV E	Y	0.5		High axial load in brace	3 internal stiffeners	
II D - III C	Y	0.5		Medium axial load in brace	" " "	
I C - I E	Y	0.5		Low axial load in brace	" " "	

R = -1

The angle between chord and brace is 60°

表 2.23

Table 4 - France

SPECIMEN	O - T	$\beta$	$\bar{z}$	TYPE	R	TEST	LOADING
						FREQUENCY Hz	
A	473-22.8	0.72	0.94	X	0.10	3	Axial load in brace
B	682-41.6	0.50	0.54	X	0.10		" " " "
D	949-41.6	0.72	1.00	X	0.10	~1	" " " "
C	1280-77	0.27	0.29	X	0.10		" " " "
E	1280-75	0.53	0.53	X	0.10		" " " "
A'	472-22.3	0.72	0.99	X	0.10	~0.4	In plane bending
B'	685-40	0.50	0.50	X	0.10		" " "
D'	947-44	0.72	1.00	X	0.10		" " "
C'	1275-75	0.27	0.30	X	0.10		" " "
E'	1273-75.7	0.54	0.57	X	0.10	0.5	" " "

O = chord external diameter  
T = chord thickness

表 2.24

Table 5 - Norway

SPECIMEN		$\beta$	$\bar{z}$	TYPE	R	TEST	LOADING	REMARKS
O - T	508-16					FREQ. Hz		
1-3-5-6		0.5	0.8	T	-1	3	Axial in brace	
2-4		0.5	0.75	T	-1	3.2	" " "	
1/79		0.5	0.8	T	-1	1.8	" " "	
2/79		0.8	0.8	K	-1	-	" " "	Not overlapping
3/79		0.8	0.8	K	-1	2.8	" " "	Overlapping
A-B		0.5	0.8	T	-1	1	" " "	Seawater tests

試験を実施した研究機関を国別に表 2.25 に示す。

表 2.25 国別研究機関

United Kingdom	<ul style="list-style-type: none"><li>○ Welding Institute</li><li>○ National Engineering Laboratory</li></ul>
Holland	<ul style="list-style-type: none"><li>○ Stevin Laboratory of Delft Univesity</li><li>○ Institute TNO for Building Materials and Building Structures (IBBC-TNO)</li></ul>
Italy	<ul style="list-style-type: none"><li>○ Italiano Navale and Marine Militare</li></ul>
France	<ul style="list-style-type: none"><li>○ IRSID</li></ul>
Norway	<ul style="list-style-type: none"><li>○ Norske Veritas Laboratory</li></ul>

## (2) 試験結果

各国の試験結果を表 2.16 ～表 2.30 に示す。

また、図 2.28 ～図 2.32 に試験結果を図示する。

図の縦軸はひずみ ( $\mu\text{mm}/\text{mm}$ ) で横軸は荷重の繰返し数であり、実験値は $N_2$  (first crack observation) から $N_3$  (through wall crack) までを横線で示している。

表 2.26

Table 6 - United Kingdom

SPECIMEN NUMBER	LOAD RANGE Kn	NOMINAL STRAIN RANGE	STRAIN CONCENTRATION FACTOR	LOCAL STRAIN RANGE	$\epsilon_2$	$\epsilon_j$	$\epsilon_k$	FAILED MEMBER
17/6	38	672	1.93	1300	$1.12 \times 10^5$	$4.9 \times 10^6$	$9.97 \times 10^6$	C
17/7	25	466	1.93	900	$1.08 \times 10^6$	$2.1 \times 10^6$	$5.16 \times 10^6$	C
17/8	21	388	1.93	750	$3.7 \times 10^6$		$6.39 \times 10^6$	C
17/9	38	670		1300	$9.8 \times 10^6$	$1.43 \times 10^6$	$1.55 \times 10^6$	C
17/10	25	460		900			$2.0 \times 10^7$	U
17/10(R)	42	770		1500	$1.0 \times 10^6$	$1.46 \times 10^6$	$1.75 \times 10^6$	C
17/11	42			1500	$1.2 \times 10^6$	$1.48 \times 10^6$	$1.85 \times 10^6$	C
18/4	36	880	1.4	1232	$6.0 \times 10^5$	$8.9 \times 10^5$	$1.97 \times 10^6$	C
18/6	20	480	1.4	672			$6.1 \times 10^6$	U
18/6(R)	33	805	1.4	1130	$7.0 \times 10^5$	$1.0 \times 10^6$	$1.86 \times 10^6$	BAC
18/10	38	930	1.4	1300	$1.3 \times 10^6$	$2.04 \times 10^6$	$2.51 \times 10^6$	C
18/13	56	1450	1.4	2000	$6.99 \times 10^4$	$2.22 \times 10^5$	$2.65 \times 10^6$	C
18/14	42	1071	1.4	1500	$2.99 \times 10^5$	$6.6 \times 10^5$	$1.1 \times 10^6$	C
18/16	26	667	1.4	934	$5.8 \times 10^5$		$8.6 \times 10^6$	C
19/11	8.9	669		1000	$7.52 \times 10^5$	$8.2 \times 10^5$	$1.07 \times 10^6$	C
19/12	6.8	525	1.43	750	$1.57 \times 10^6$	$1.89 \times 10^6$	$2.53 \times 10^6$	C
19/13	12	1050		1500		$3.62 \times 10^5$	$4.19 \times 10^6$	C
20/2	12.8	1390	1.15	1600	$2.9 \times 10^5$	$3.37 \times 10^5$	$3.93 \times 10^6$	C
	6.3	695	1.15	800			$2.0 \times 10^7$	U
20/5	8	882	1.15	1000	$1.85 \times 10^5$	$5.18 \times 10^5$	$6.5 \times 10^5$	B
20/6	4.6	522	1.15	600	$8.23 \times 10^5$	$1.0 \times 10^7$	$1.04 \times 10^7$	B
17/1	114	185	5	933	$7.98 \times 10^5$	$1.53 \times 10^6$	$2.06 \times 10^6$	C
17/3	86	140	5	700	$2.7 \times 10^6$	$5.2 \times 10^6$	$5.8 \times 10^6$	C
17/4	174	280	5	1400	$4.59 \times 10^4$	$1.85 \times 10^5$	$2.0 \times 10^6$	C
17/2	144		6.3		$5.4 \times 10^4$	$3.24 \times 10^5$	$3.73 \times 10^5$	C
	84		6.3				$2.0 \times 10^7$	U
17/12	114		6.3		$3.83 \times 10^5$	$8.39 \times 10^5$	$1.17 \times 10^6$	C
18/1	180	416		1330	$1.26 \times 10^5$	$4.9 \times 10^5$	$5.42 \times 10^5$	C

表 2. 26 (続き)

Table 6 (following) - United Kingdom

SPECIMEN NUMBER	LOAD RANGE K <sub>n</sub>	NOMINAL STRAIN RANGE	STRAIN CONCENTRATION FACTOR	LOCAL STRAIN RANGE	N <sub>2</sub>	N <sub>3</sub>	N <sub>4</sub>	FAILED MEMBER
18/5	108	244		717			2.0 x 10 <sup>7</sup>	U
18/5(R)	180	418		1330	1.0 x 10 <sup>6</sup>	1.4 x 10 <sup>6</sup>	1.64 x 10 <sup>6</sup>	C
18/7	124	294		940			5.4 x 10 <sup>6</sup>	B
18/8	90	208	3.2	665			1.5 x 10 <sup>7</sup>	U
18/8(R)	210	486		1555	2.08 x 10 <sup>6</sup>	3.87 x 10 <sup>6</sup>	4.22 x 10 <sup>6</sup>	C
18/9	200	462		1480		2.2 x 10 <sup>6</sup>	2.7 x 10 <sup>6</sup>	C
18/12	230	532		1702	4.6 x 10 <sup>6</sup>	2.17 x 10 <sup>6</sup>	2.36 x 10 <sup>6</sup>	C
18/15	140	334		1070	2.1 x 10 <sup>6</sup>	4.15 x 10 <sup>6</sup>	5.43 x 10 <sup>6</sup>	C
18/2	124	286	3.65	1043			20.00 x 10 <sup>6</sup>	U
18/11	140	323	3.65	1181	4.87 x 10 <sup>6</sup>	1.0 x 10 <sup>6</sup>	1.49 x 10 <sup>6</sup>	C
20/4	67	360	4.16	1500	4.2 x 10 <sup>6</sup>	2.35 x 10 <sup>5</sup>	3.56 x 10 <sup>5</sup>	C
	27	144	4.16	600			2.0 x 10 <sup>7</sup>	U
20/10	45	240	4.16	1000				
20/11	66	360	4.16	1500	2.25 x 10 <sup>5</sup>		4.0 x 10 <sup>5</sup>	o
20/8	66			1500	2.76 x 10 <sup>5</sup>	4.5 x 10 <sup>5</sup>	7.8 x 10 <sup>5</sup>	C
20/1	45			1000			2.0 x 10 <sup>7</sup>	U
20/1(R)	66			1000	2.36 x 10 <sup>6</sup>	2.7 x 10 <sup>6</sup>	2.9 x 10 <sup>6</sup>	C
37/1	230	477		1275	7.9 x 10 <sup>6</sup>	2.9 x 10 <sup>6</sup>	5.0 x 10 <sup>6</sup>	C
37/7	110	231	2.67	817	2.27 x 10 <sup>6</sup>	10.01 x 10 <sup>6</sup>	1.44 x 10 <sup>7</sup>	C
37/13	140	294		785	3.27 x 10 <sup>5</sup>	7.29 x 10 <sup>6</sup>	1.44 x 10 <sup>6</sup>	C
37/8	230	477		1275	5.1 x 10 <sup>6</sup>	1.2 x 10 <sup>6</sup>	1.53 x 10 <sup>6</sup>	C
37/10	140	294		785	6.06 x 10 <sup>6</sup>	3.79 x 10 <sup>6</sup>	6.18 x 10 <sup>6</sup>	C
38/2	134	405		750			3.0 x 10 <sup>6</sup>	B
38/3	181	540	1.85	1000	4.09 x 10 <sup>6</sup>	6.1 x 10 <sup>6</sup>	1.7 x 10 <sup>6</sup>	C
38/6	115	351		650	1.0 x 10 <sup>6</sup>	1.8 x 10 <sup>6</sup>	5.22 x 10 <sup>6</sup>	C
40/3(R)	16.8				9.15 x 10 <sup>6</sup>	9.7 x 10 <sup>6</sup>	1.1 x 10 <sup>6</sup>	B
40/3	5.6						2.0 x 10 <sup>7</sup>	U



表 2.26 ( 続き )  
Table 6 ( following ) - United Kingdom

SPECIMEN NUMBER	LOAD RANGE $K_n$	NOMINAL STRAIN RANGE	STRAIN CONCENTRATION FACTOR	LOCAL STRAIN RANGE	$\epsilon_2$	$\epsilon_3$	$\epsilon_4$	FAILED MEMBER
E1A	42	80	4.12	330	$2.19 \times 10^5$	$21.0 \times 10^5$	$26.19 \times 10^5$	C
E1D	59	114		470	$1.11 \times 10^5$	$3.46 \times 10^5$	$4.9 \times 10^5$	C
E2A(R)	87.5	462		1050	$9.5 \times 10^4$	$5.3 \times 10^5$	$9.0 \times 10^5$	C
E2A	37.5	198		450			$2.0 \times 10^7$	U
E2D	63.5	352	2.27	800	$1.20 \times 10^5$	$2.23 \times 10^5$	$3.32 \times 10^5$	C
37/3	1000	192	7.0	1344	$6.2 \times 10^4$	$1.44 \times 10^5$	$1.53 \times 10^5$	C
37/5	560	110	7.0	770	$5.9 \times 10^5$	$1.0 \times 10^6$	$1.5 \times 10^6$	C
37/9	350	70	7.0	500	$2.39 \times 10^5$	$6.95 \times 10^5$	$8.73 \times 10^5$	C
38/4	723	200		750		$5.25 \times 10^5$	$6.78 \times 10^5$	C
38/1	723		2.47	750	$9.14 \times 10^5$	$2.11 \times 10^6$	$3.85 \times 10^5$	B
39/4	130				$2.19 \times 10^5$		$1.57 \times 10^5$	B
E18(R)	932	98		1050	$4.12 \times 10^5$	$7.5 \times 10^5$	$8.79 \times 10^5$	C
E18	400	42	10.7	450			$2.0 \times 10^7$	U
E1C	583	65		700	$3.32 \times 10^5$	$1.4 \times 10^6$	$2.32 \times 10^5$	C
E2B	380	136	2.7	372	$1.7 \times 10^5$	$4.79 \times 10^5$	$6.35 \times 10^5$	C
E2C	310	111	2.7	300	$2.5 \times 10^5$	$1.46 \times 10^7$	$1.53 \times 10^7$	C
F1A	146	77	4.1	318			$2.0 \times 10^7$	U
	552	292	4.1	1200	$1.05 \times 10^4$	$2.1 \times 10^5$	$2.4 \times 10^5$	C
F1C	48.6	857	1.4	1200	$1.05 \times 10^5$	$1.72 \times 10^5$	$2.45 \times 10^5$	C
F1D	15.7	285	1.4	400	$2.5 \times 10^5$	$7.5 \times 10^5$	$8.89 \times 10^5$	C
F2A	18.8	540		900	$8.36 \times 10^5$	$1.16 \times 10^6$	$2.13 \times 10^6$	B
F2B	14.25	419	1.67	700		$2.12 \times 10^6$	$7.32 \times 10^6$	B
F1B	166	85	4.1	350			$2.0 \times 10^7$	U
	284	146	4.1	600	$7.62 \times 10^4$	$2.4 \times 10^5$	$3.33 \times 10^5$	C
F2C	283	240		720	$3.0 \times 10^5$	$1.2 \times 10^6$	$2.75 \times 10^6$	B
F2D	191	166	3.0	500			$2.0 \times 10^7$	U
F2D(R)	573	500		1500	$8.0 \times 10^4$	$1.47 \times 10^5$	$2.3 \times 10^5$	B

表 2.26 ( 続き )  
Table 6 ( following ) - United Kingdom

SPECIMEN NUMBER	LOAD RANGE $K_n$	NOMINAL STRAIN RANGE	STRAIN CONCENTRATION FACTOR	EXTRAP. STRAIN RANGE	$\epsilon_2$ $\times 10^5$	$\epsilon_3$ $\times 10^5$	$\epsilon_4$ $\times 10^5$	FAILED MEMBER
K20	5800	264	3.2	845	0.19	0.64	0.74	Chord failure
K21	3600	164	3.75	617		0.627	4.34	' '
K22	280	1140	1.36	1550	0.053	0.093	0.11	Brace failure
K23(R)	270	895	1.36	1217	0.228	0.334	0.38	' '

B = Relegt  
U = Unbroken  
C = Chord failure  
D = Brace failure

表 2. 27

Table 7 - Holland (Review of tests results)

SPECIMEN NUMBER	LOAD RANGE Kt/M	NOMINAL STRAIN RANGE $10^{-6}$	SNCF EXTRA-POLATED 1)	HOT-SPOT STRAIN RANGE $10^{-6}$	FIRST CRACK OBSERVATION $t_1$	CRACK THROUGH CHORD WALL $t_2$	END OF TEST $t_3$
1	84	464	4.8	2739	-	$6.0 \times 10^4$	$6.3 \times 10^4$
2	28	155	4.8	745	$1.2 \times 10^7$	$1.2 \times 10^7$	$1.3 \times 10^7$
3	50	275	4.8	1325	$2.5 \times 10^6$	$3.0 \times 10^6$	$3.3 \times 10^6$
18	35	193	4.5	870	$2.8 \times 10^6$	$3.0 \times 10^6$	$3.6 \times 10^6$
19	80	442	4.5	1990	$3.0 \times 10^4$	$6.0 \times 10^4$	$7.4 \times 10^4$
22	45	249	4.3	1079	$1.5 \times 10^5$	$8.8 \times 10^5$	$9.5 \times 10^5$
23	32	177	4.3	750	$1.5 \times 10^6$	$2.0 \times 10^6$	$2.4 \times 10^6$
24	4000	1059	1.2	1285	$2.5 \times 10^5$	$3.3 \times 10^5$	$3.7 \times 10^5$
25	4500	1203	1.2	1445	$4.3 \times 10^5$	$4.7 \times 10^5$	$4.8 \times 10^5$
26	3450	841	1.2	1070	$8.3 \times 10^5$	$1.5 \times 10^6$	$1.7 \times 10^6$
4	85	75	5.8	435	$1.2 \times 10^6$	$2.2 \times 10^6$	$2.7 \times 10^6$
5	160	141	5.8	818	$3.3 \times 10^5$	$6.8 \times 10^5$	$7.8 \times 10^5$
6	144	127	5.8	737	$4.0 \times 10^5$	$1.1 \times 10^6$	$1.3 \times 10^6$
7	142	127	5.8	737	$3.5 \times 10^5$	$8.4 \times 10^5$	$1.1 \times 10^6$
8	85	75	5.8	435	$1.5 \times 10^6$	$7.5 \times 10^6$	$8.5 \times 10^6$
9	160	141	5.8	818	$2.8 \times 10^5$	$7.6 \times 10^5$	$1.0 \times 10^6$
10	85	75	5.8	435	$1.2 \times 10^6$	$2.3 \times 10^6$	$2.8 \times 10^6$
11	58	125	3.9	488	$8.0 \times 10^5$	$9.0 \times 10^5$	$1.1 \times 10^7$
12	110	245	3.9	956	$1.5 \times 10^5$	$7.0 \times 10^5$	$9.1 \times 10^5$
27	600	129	3.0	387	$1.2 \times 10^6$	-	$1.1 \times 10^7$ 2)
28	1300	279	3.0	837	$4.0 \times 10^5$	$6.6 \times 10^5$	$7.1 \times 10^5$
29	880	129	3.0	567	$9.0 \times 10^5$	$1.8 \times 10^6$	$2.2 \times 10^6$
30	880	338	2.7	913	$5.7 \times 10^5$	$1.0 \times 10^6$	$1.2 \times 10^6$
31	540	209	2.7	540	$3.5 \times 10^5$	$6.5 \times 10^5$	$8.4 \times 10^5$
32	660	254	2.7	686	$7.3 \times 10^5$	$2.0 \times 10^6$	$4.0 \times 10^6$
33	754	290	2.7	783	$1.4 \times 10^6$	$2.4 \times 10^6$	$2.9 \times 10^6$
36	520	199	2.7	537	$3.2 \times 10^5$	$1.0 \times 10^7$	$1.9 \times 10^7$
37	600	230	2.7	621	$3.9 \times 10^5$	$6.7 \times 10^5$	$8.1 \times 10^5$
38	574	220	2.7	594	$4.8 \times 10^5$	$7.8 \times 10^5$	$8.5 \times 10^5$
13	270	58	6.4	370	$2.1 \times 10^6$	$4.1 \times 10^6$	$5.0 \times 10^6$
14	770	165	6.4	1055	$5.0 \times 10^4$	$1.5 \times 10^5$	$1.7 \times 10^5$
15	450	95	6.4	615	$5.0 \times 10^5$	$9.5 \times 10^5$	$1.3 \times 10^6$
16	240	51	6.4	325	-	$3.9 \times 10^5$	$4.3 \times 10^5$
17	240	51	6.4	325	-	$3.7 \times 10^5$	$4.3 \times 10^5$
20	600	129	6.7	865	$2.5 \times 10^5$	$4.1 \times 10^5$	$6.8 \times 10^5$
21	220	47	6.7	315	$3.5 \times 10^6$	$8.1 \times 10^6$	$1.6 \times 10^7$
34	180	34	9.5	323	$4.0 \times 10^6$	$1.2 \times 10^7$	$1.4 \times 10^7$
35	400	85	9.5	817	$1.5 \times 10^5$	$7.0 \times 10^5$	$8.5 \times 10^5$
39	150	32	9.8	314	$3.0 \times 10^6$	$2.0 \times 10^7$	$2.6 \times 10^7$
40	390	84	9.8	823	$1.0 \times 10^5$	$5.0 \times 10^5$	$7.3 \times 10^5$

1) Average for each geometry

2) After  $4 \times 10^6$  cycles a very slow crack prop.

表 2.28

Table 8 b - Italy

FATIGUE TESTS

CODE	LOAD RANGE KN	NOMINAL STRESS IN BRACE $\sigma_{nom} \cdot 10^{-2}$	SMCF EXTRAP.	HOT SPOT STRAIN RANGE $\times 10^{-6}$	NUMBER OF CYCLES			
					$\Delta \epsilon - 15\%$ $N_1$	FIRST OBSERVATION $N_2$	FIRST THROUGH WALL CRACK $N_3$	END OF TEST $N_4$
II E	1177	53.8	13.5	3500	$5.5 \times 10^3$	$7.8 \times 10^3$	$1.7 \times 10^4$	$2.1 \times 10^4$
IV C	1177	53.8	10.9	2850	$5.5 \times 10^3$	$7.8 \times 10^3$	$1.9 \times 10^4$	$2.1 \times 10^4$
I D	785	35.9	14.1	2450	$1.7 \times 10^4$	$2.3 \times 10^4$	$5.0 \times 10^4$	$5.9 \times 10^4$
III D	785	35.9	14.4	2500	$1.3 \times 10^4$	$2.3 \times 10^4$	-	$5.9 \times 10^4$
II D	2650	120.0	2.5	1530	$3.3 \times 10^4$	$2.2 \times 10^4$	$6.2 \times 10^4$	$2.9 \times 10^5$
III C	2650	120.0	2.5	1475	$9.2 \times 10^4$	$7.5 \times 10^4$	-	$2.9 \times 10^5$
III E	3530	161.5	2.5	2080	-	$3.0 \times 10^4$	$6.0 \times 10^4$	$7.9 \times 10^4$
IV E	3530	161.5	2.5	1950	$1.9 \times 10^4$	$2.2 \times 10^4$	$4.8 \times 10^4$	$7.9 \times 10^4$

表 2.29

Table 9 - France

CODE	LOAD RANGE KN	HOT SPOT STRAIN RANGE EXTRAPOLATED $10^{-6}$	NUMBER OF CYCLES			
			$\Delta \epsilon - 15\%$ $N_1$	FIRST OBSERVATION $N_2$	FIRST THROUGH WALL CRACK $N_3$	END OF TEST $N_4$
A	390	960	$4.8 \times 10^4$	$1.4 \times 10^5$	$3.7 \times 10^5$	$7.5 \times 10^5$
			1340	$2.3 \times 10^5$	$3.5 \times 10^5$	
B	738	760	$2.1 \times 10^5$	-	-	$5.8 \times 10^5$
			1020	$5.5 \times 10^4$	$1.7 \times 10^5$	
D	1490	940	$6.0 \times 10^4$	$1.0 \times 10^5$	$4.3 \times 10^5$	$4.4 \times 10^5$
			1020	$6.0 \times 10^4$	$1.0 \times 10^5$	
C	1200	440	$3.9 \times 10^5$	$3.0 \times 10^5$	-	$1.3 \times 10^6$
			500	$1.3 \times 10^5$	$2.4 \times 10^5$	
E	2250	510	$7.8 \times 10^4$	$1.2 \times 10^5$	$6.6 \times 10^5$	$9.1 \times 10^5$
			1020	$2.6 \times 10^5$	$4.3 \times 10^5$	
A'	118	960	$5.5 \times 10^4$	$9.1 \times 10^4$	-	$1.9 \times 10^6$
			1020	$3.6 \times 10^4$	$8.2 \times 10^4$	
B'	193	580	$1.1 \times 10^5$	$1.3 \times 10^5$	$6.5 \times 10^5$	$7.8 \times 10^5$
			570	$3.4 \times 10^4$	$4.0 \times 10^4$	
D'	540	500	$1.3 \times 10^5$	$1.6 \times 10^5$	$4.7 \times 10^5$	$6.5 \times 10^5$
			500	$1.4 \times 10^5$	$1.8 \times 10^5$	
C'	199	660	$2.5 \times 10^4$	$1.6 \times 10^5$	$6.5 \times 10^5$	$7.2 \times 10^5$
			740	$1.7 \times 10^5$	$2.1 \times 10^5$	
E'	945	500	$3.5 \times 10^4$	$8.9 \times 10^4$	$4.7 \times 10^5$	$5.6 \times 10^5$
			500	$3.0 \times 10^4$	$8.9 \times 10^4$	

Etat: BS = as welded  
TT = heat treated

表 2. 3 0

Table 10 - Norway

NODE	LOAD RANGE KI	NOMINAL STRESS RANGE IN BRACE $\sigma \times 10^{-2}$	HOT-SPOT STRAIN $\epsilon \times 10^{-6}$	NUMBER OF CYCLES			
				$\Delta \epsilon = 15\%$	FIRST OBSERVATION	FIRST THROUGH WALL CRACK	END OF TEST
				$N_1$	$N_2$	$N_3$	$N_4$
1	140	19.0	980	-	-	-	$5.5 \times 10^6$
2	300	34.2	1740	-	$3 \times 10^4$	-	$2.1 \times 10^6$
3	200	27.1	1390	$5.6 \times 10^4$	$7.5 \times 10^4$	-	$5.8 \times 10^6$
4	185	21.1	1085	$1.2 \times 10^5$	$1.6 \times 10^5$	-	$8.7 \times 10^6$
5	196	26.6	1100	$4.5 \times 10^5$	$6.5 \times 10^5$	-	$1.6 \times 10^6$
8	150	20.4	960	$1.1 \times 10^5$	$2.0 \times 10^5$	-	$1.1 \times 10^6$
1/79	300	40.6	834	$2.9 \times 10^5$	$5.0 \times 10^5$	$8.1 \times 10^5$	$1.2 \times 10^6$
2/79	350	30.5	829	$9.8 \times 10^4$	$1.2 \times 10^5$	$4.6 \times 10^5$	$1.0 \times 10^6$
3/79	560	48.8	804	-	$3.0 \times 10^6$	$4.1 \times 10^6$	$4.6 \times 10^6$
A	192	28.1	1307	-	-	-	$5.9 \times 10^6$
B	108	14.7	715	$1.9 \times 10^5$	$2.3 \times 10^5$	-	$4.0 \times 10^6$

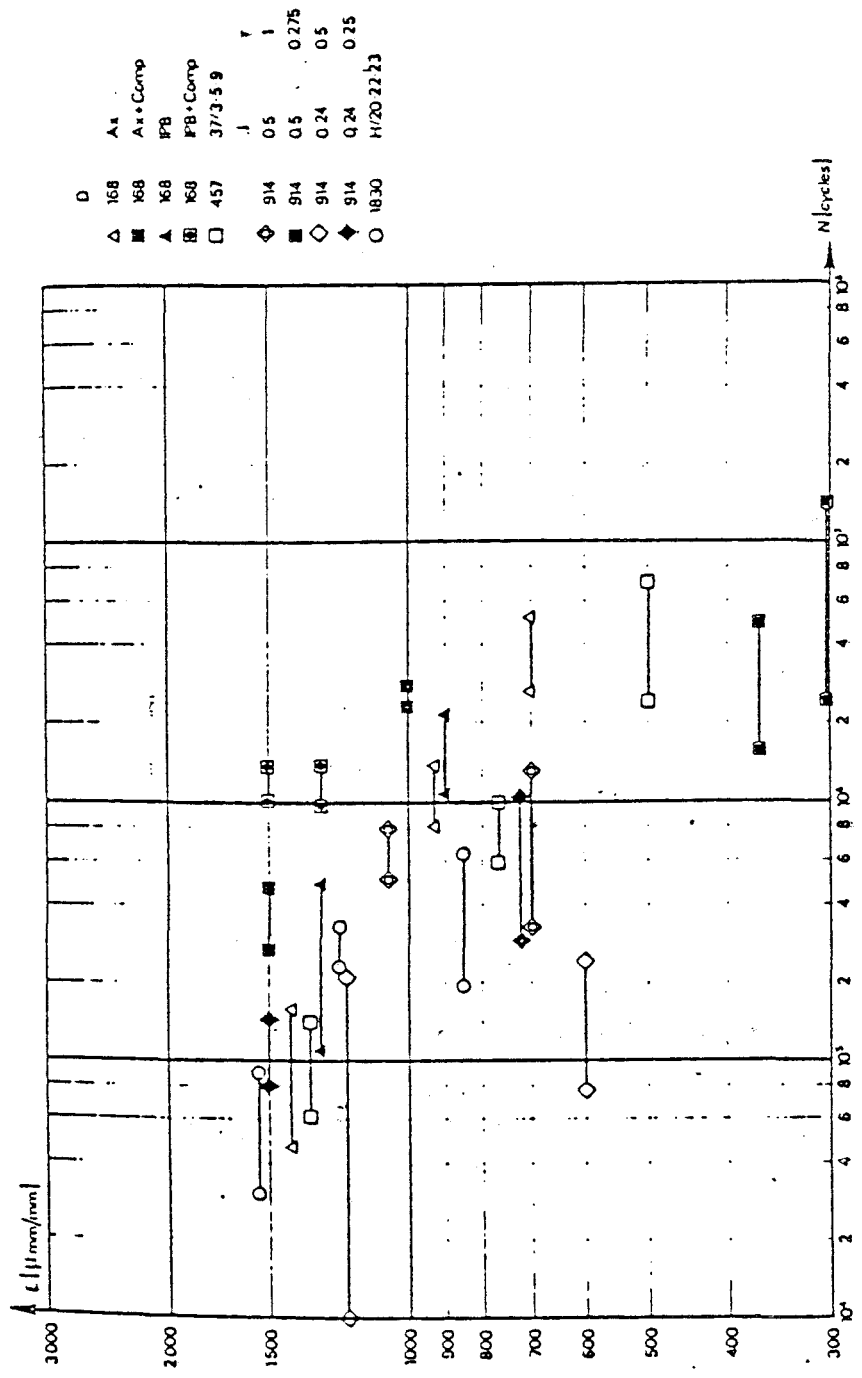


Fig. 3 - United Kingdom  
 T-Joints R = -1  
 Number of cycles from first observation to through wall crack

2.28

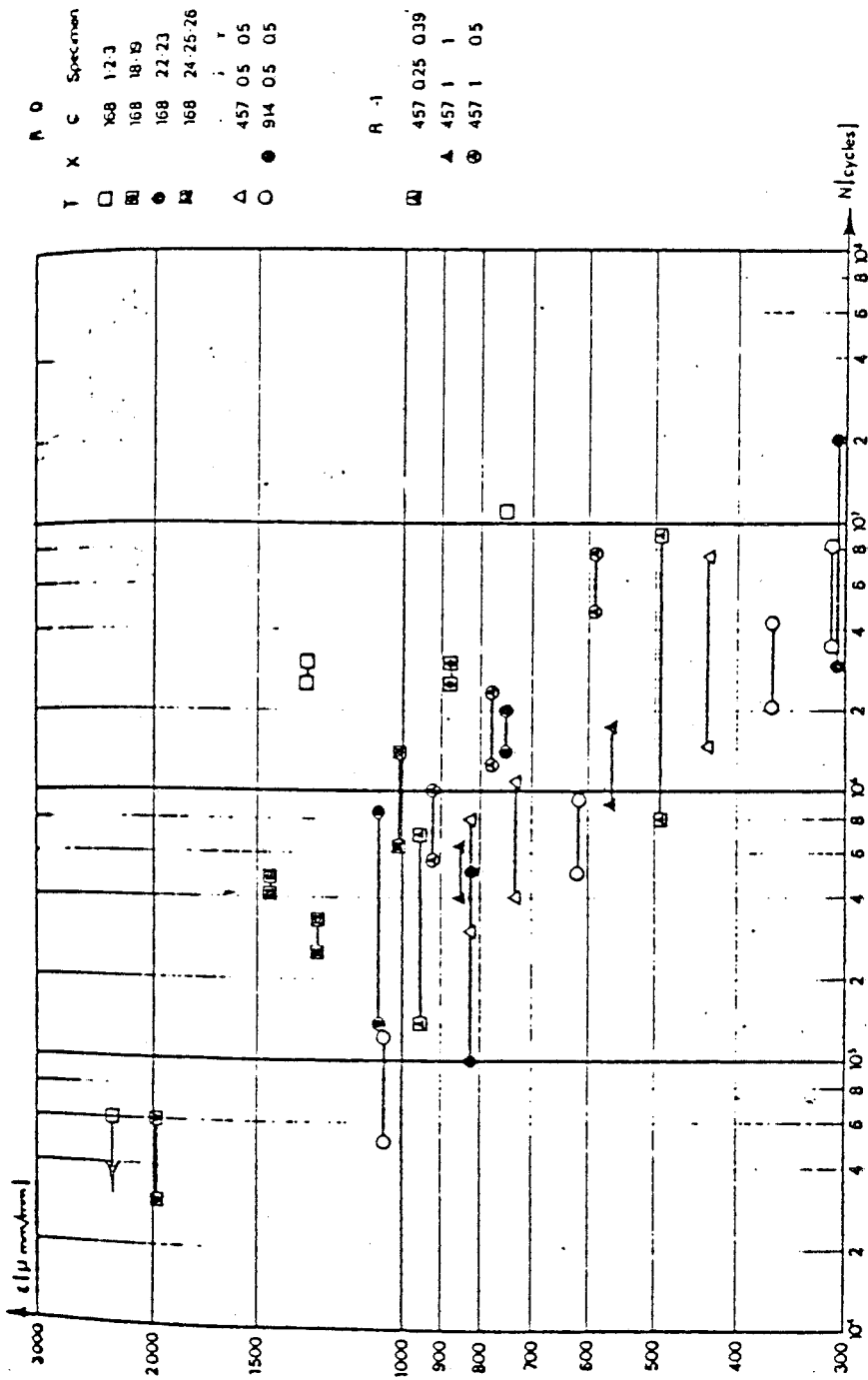


Fig. 4 - Holland  
Number of cycles from first observation to through wall crack

⊠ 2. 2 9

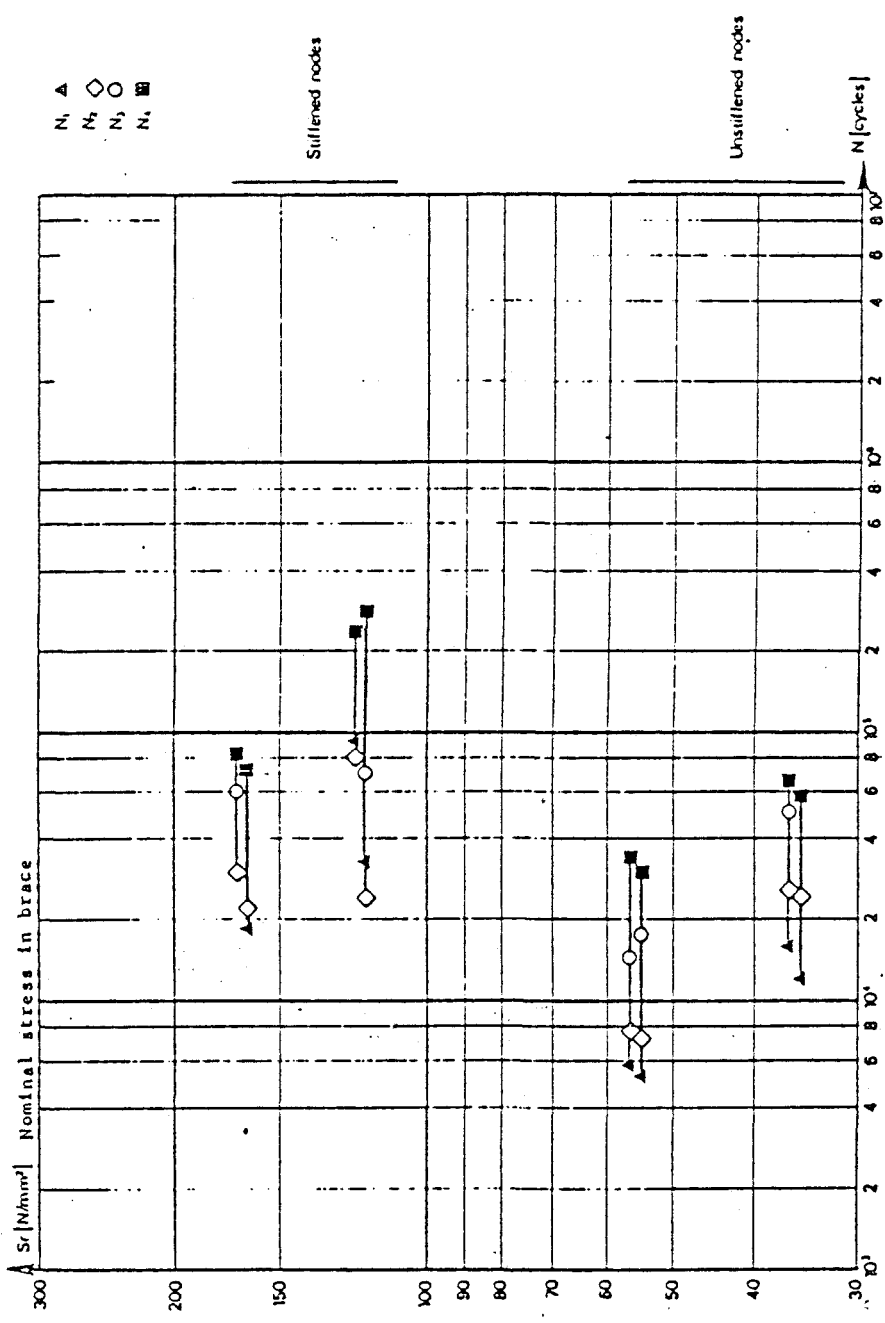


Fig. 5 - Italy  
Y-Joints R = -1

2.30

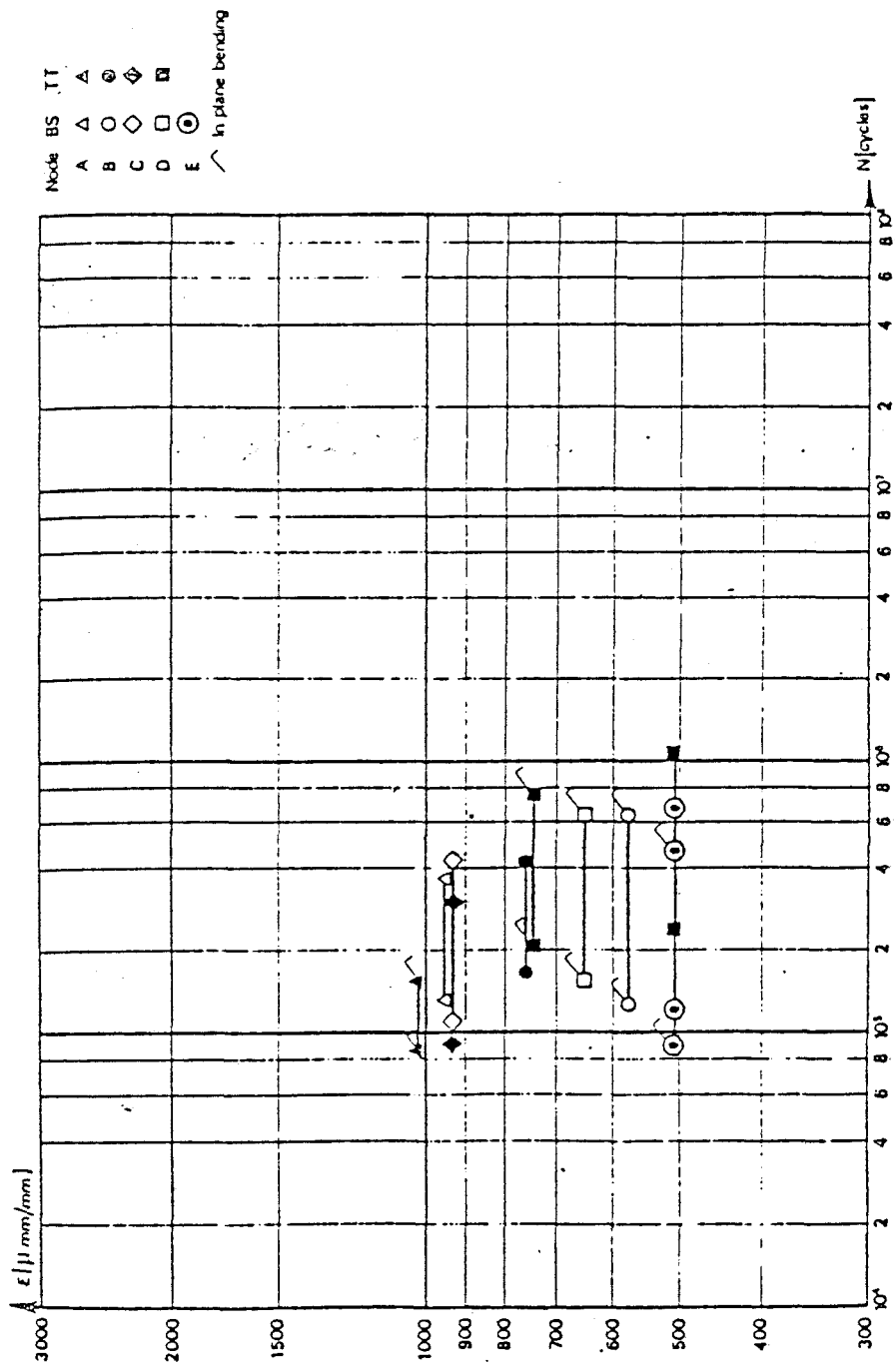
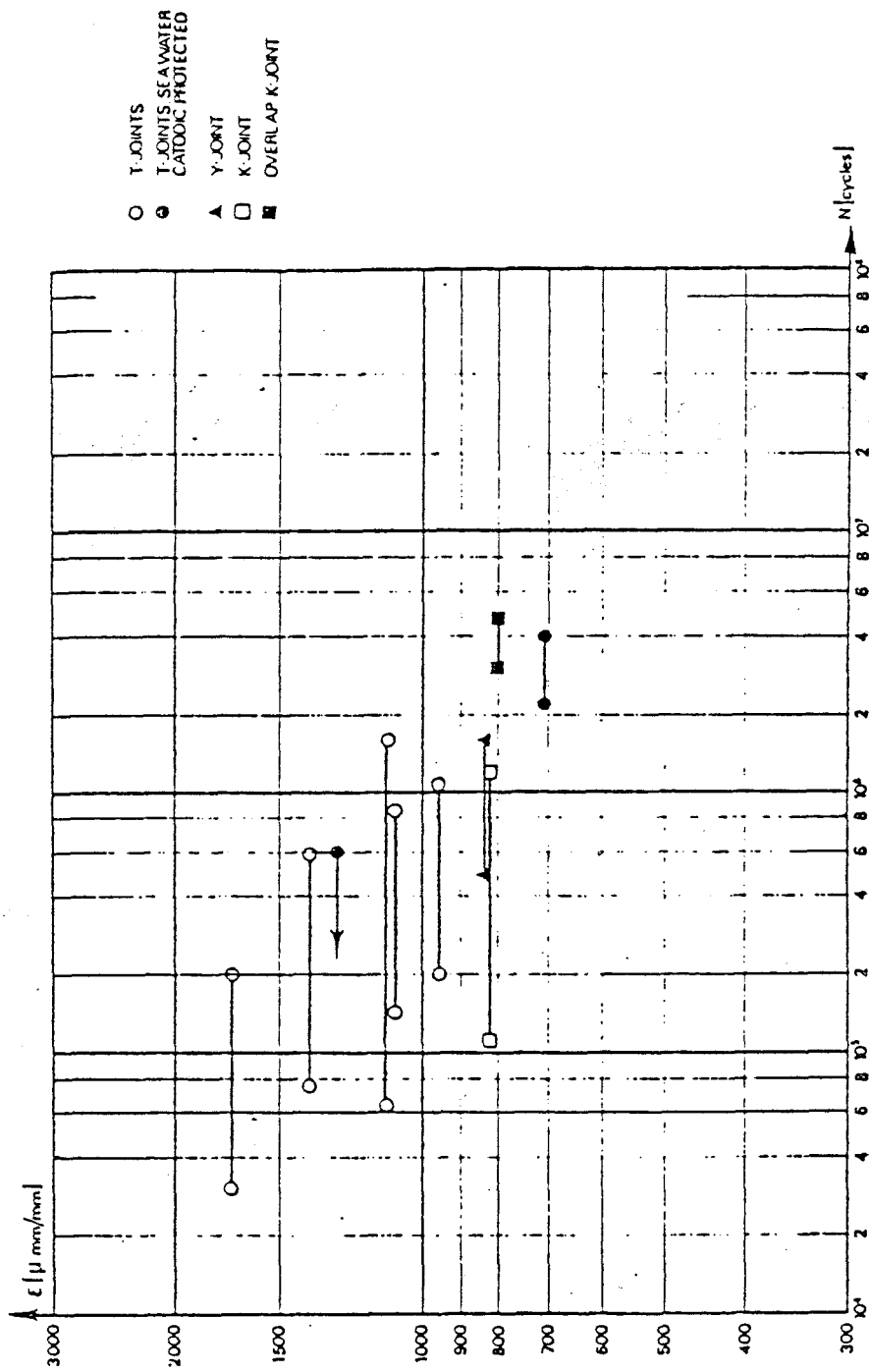


Fig. 6 - France X-Joints R = 0.10 Number of cycles from first observation to through wall crack





Number of cycles from first observation to end of test

Fig. 7 - Norway R = -1 Axial Load in brace

### (3) 試験結果の評価

#### 1) 破壊の定義

疲労試験を行う上で破壊をどう定義するかは重要な問題であり、実験要領等とともに試験結果にバラツキが出る原因の1つとされている。

ECSC の研究は協同研究と云う性格上、破壊の定義を統一する必要があり、 $N_1 \sim N_4$  の4段階に分け破壊の定義を行っている。

今後、疲労試験を計画する場合の参考として、ECSC での4段階の破壊の定義を以下に示す。

$N_1$  indicates a 15% drop in strain-gauges measurements, but gives no evidence that the node is already damaged.

Using Acoustic Emission techniques, which permit to locate very precisely where cracks start, Italians were able to discover cracks before to observe a 15% drop in strain gauges reading.

$N_2$  as no indication is given about the size of the observed crack, differences could arise among results of different laboratories. Only Norwegians associate  $N_2$  to a crack length of about 30 mm.

$N_3$  is very easily monitored, then is the best parameter to compare data from different laboratories. However it is necessary to remember that while for unstiffened nodes after the formation of a through thickness crack, the collapse of the node follows very shortly, for stiffened nodes internal rings act as crack arrestors.

A stiffened node in the Italian programme had a through chord wall crack at  $6.2 \times 10^4$  cycles and the test was stopped at  $2.9 \times 10^5$  for a rupture of the brace, when the chord was still in condition to stand additional fatigue cycles.

$N_4$  cannot be used to compare results as in some cases indicates a complete collapse of the model, while in other cases indicates that the test was stopped after the prescribed number of cycles but there was no indication of damage in the specimen.

また、破壊を定義する場合には、疲労試験上の問題のみではなく実構造との関連についても十分に考慮する必要がある。

## 2) スティフナーの効果

スティフナーの有効性については、図 2.30 より明らかである。

すべての他のパラメータを同じにしたイタリアの研究で内面のスティフナーリングによる静的耐荷力と疲労強度の向上が明らかになった。

また、実構造においても例えばセミサブドリリング等において内面のダイヤフラムで格点を補強することはすでに採り入れられている。

## 3) 寸法効果

供試体の寸法による影響は図 2.28, 29と31に示してある。

また、寸法効果については良く知られている。しかし、この効果を量的に把握するのが困難であり、実際問題として寸法効果と材質、载荷周期の影響を分離するのは不可能と述べている。

## 4) 設計パラメータの影響

図 2.28 において  $\beta$  と  $\tau$  を変化させた結果が示してある。

最も悪い結果は  $\beta = 0.24$  ,  $\tau = 0.5$  の場合である。

図 2.29 において  $\beta = 1$  の時は  $\tau = 0.5$  が  $\tau = 1.0$  より良い結果が得られている。

このパラメータに関して完全な議論をするのは困難であるが、パラメトリックな計算により SCF を求めることにより可能である。

## 5) 荷重モードの影響

英国、オランダ、フランスの試験でブレースに軸力を载荷した場合と面内曲げを载荷した場合について行った。その結果、若干のバラツキが認められた。

図 2.28 によれば 168mmの直径の供試体で軸力を载荷した場合に良い疲労耐力が得られている。

## 6) 海水の影響

図 2.32 にノールウェーの試験結果を示す。この図では電気防食をした海水中の疲労試験は大気中のそれと同じ結果となっている。

また、電気防食のしていない海水中の疲労試験もいくつか行っているが、特に新しい成果は得られていないようである。